

UNIVERSITY OF ZURICH  
DEPARTEMENT OF GEOGRAPHY  
PHYSICAL GEOGRAPHY  
GLACIOLOGY & GEOMORPHODYNAMICS GROUP (3G)

# The Glacier Inventory of the Antarctic Peninsula

## A Reassessment of Existing Datasets

---

GEO 511 Master's Thesis

**Student:**

Jacqueline Huber  
10-736-239

**Supervisors:**

PD Dr. Michael Zemp, 3G, Department of Geography, University of Zurich  
Dr. Frank Paul, 3G, Department of Geography, University of Zurich

**Faculty Member:**

Prof. Dr. Andreas Vieli

**29.01.2016**

Jacqueline Huber  
Grünhaldenstrasse 25  
8052 Zürich  
[jhuber@access.uzh.ch](mailto:jhuber@access.uzh.ch)

# Acknowledgements

The great support of the people I met, worked with or solely had around me made the realization of this Master's thesis possible. Whether I had content-related questions, technical issues or needed mental support; thank you all for caring and always giving me the support I needed.

First of all, I sincerely thank my supervisors Michael Zemp and Frank Paul for their enthusiastic engagement and their always warmly support they provided me at any time in the last year. The numerous hours of constructive comments, inputs, advices and encouraging words are very much appreciated.

Many thanks too go to Alison Cook for her generous gesture of providing the glacier basins outline dataset she and her colleagues compiled in meticulous work. This dataset was a major contribution for this thesis.

Also Matthias Huss and Daniel Farinotti deserve my gratitude for making their data available as well as for their practical input. This work and the inventory have benefited greatly from their provided bedrock and thickness dataset of the Antarctic Peninsula.

I want to thank Peter Fretwell und Adrian Fox for the detailed comments and statements about the development of the rock outcrops dataset of the Antarctic Digital Database (ADD).

I am grateful to Philipp Rastner for applying the sophisticated drainage basins algorithm to my data.

Special thanks go to my friends, fellow students and sufferers from the "Masterarbets-Rüümli" in room G10. The exchange of ideas, constructive discussions, pleasant and productive work environment as well as the fun activities helping to calm down from time to time are very much appreciated.

Additional thanks go to Andrea Walter, Annabelle Jaggi, Annette Ramp, Beat Bannwart and my mother, Patrizia Huber-Harteck, who all critically reviewed parts of this thesis.

Last but not least, I want to thank my parents and Beat for their unconditional support during this journey as well as throughout my entire life.



# Summary

In the context of a changing climate the knowledge about the amount of water stored in glaciers is important to determine the contribution of melting glaciers to sea level rise (SLR). The Antarctic Peninsula (AP) has shown exceptionally strong regional warming recently, associated with changing behavior and melting of the ice masses. However, most SLR estimations did not fully consider the glaciers of the AP, as no complete dataset was available so far delineating the glaciers as well as separating them from the ice sheet.

This thesis fills this gap and presents the first complete glacier inventory of the AP north of 70°S. The inventory was compiled by combining already existing data and geographic information system (GIS) techniques. To generate a vector layer of individual glacier outlines, rock outcrops have been removed from the glacier basin outlines of Cook *et al.* (2014) by using the corresponding layer of the Antarctic Digital Database (ADD; ADD Consortium, 2012). The glacier-specific parameters (i.e. area, min., max., median, mean elevation, mean slope and aspect) as well as the overall glacier hypsometry have been determined by applying the digital elevation model (DEM) of Cook *et al.* (2012). The glaciers have been assigned connectivity levels (CL) to the ice sheet based on the concept introduced by Rastner *et al.* (2012) and the Antarctic drainage systems of Zwally *et al.* (2012). Furthermore, the datasets of Huss and Farinotti (2014) enabled to determine ice thickness, ice volume and sea level equivalent (SLE) per glacier. The final dataset will be provided to the Global Land Ice Measurements from Space (GLIMS) database.

The final inventory consists of 1588 glaciers, covering an area of 94 743 km<sup>2</sup>, slightly more than the 90 000 km<sup>2</sup> covered by glaciers and ice caps surrounding the Greenland ice sheet Rastner *et al.* (2012). The AP is characterized by a few large glaciers in terms of area and a dominance of glaciers with an area between 1.0 and 50 km<sup>2</sup> in terms of number. Most of the area (63%) is drained by marine-terminating glaciers and 35% of the area is covered by ice shelf tributary glaciers. The total ice volume is 34 650 km<sup>3</sup>, of which one third lays below sea level, resulting in a SLE of 83.2 mm. The spatial pattern of median elevation, mean thickness and volume as well as the glacier hypsometry and the glacier (frontal) types are determined by the topography of the AP. No dependence on aspect or precipitation patterns is detectable. The overall hypsometric curve has a bimodal shape: The maximum of glacierized areas is located at about 200 – 500 m a.s.l. and a secondary maximum is found at about 1500 – 1900 m a.s.l.. This, and the fact that most glaciers have contact with ocean water, results in high sensitivities of the glaciers on climate change: First, at some point, rising equilibrium line altitudes (ELA) due to rising air temperatures would expose huge additional areas to ablation. Second, rising ocean temperatures increase melting and calving of glaciers with water contact. Ice shelf tributary glaciers reveal additional high sensitivities on changes of their frontal characteristics. Stable ice shelves have a buttressing effect on their feeding glaciers, but collapsing ice shelves result in the opposite effect and enhances ice loss.

This thesis is a contribution for more accurate SLE estimations, as well as it demonstrates the potential of such an inventory to improve the knowledge about glaciers of the AP.



# Zusammenfassung

Im Kontext des Klimawandels soll der Beitrag von Gletschern zum Meeresspiegelanstieg bestimmt werden. Dazu muss bekannt sein wieviel Wasser in diesen gespeichert ist. Die Antarktische Halbinsel hat in der letzten Zeit aussergewöhnlich starke regionale Erwärmungen gezeigt, verbunden mit schmelzenden und sich im Verhalten ändernde Eismassen. Allerdings sind die Gletscher der Antarktischen Halbinsel in Einschätzungen des Meeresspiegelanstiegs meist nicht berücksichtigt, da kein vollständiger Datensatz verfügbar war, welcher die einzelnen Gletscher voneinander als auch vom Antarktischen Eisschild trennt.

Die vorliegende Arbeit füllt diese Lücke durch das erste vollständige Inventar, bestehend aus Gletscherumrissen der Antarktischen Halbinsel nördlich von 70°S. Dieser entstand durch die Kombination bereits bestehender Datensätze in einem Geographischen Informationssystem. Um ein Vektorlayer der einzelnen Gletscher zu erstellen, wurden aus dem Eis ragende Felsen von den einzelnen Gletscher-Einzugsgebieten von Cook *et al.* (2014) entfernt. Dazu wurde ein entsprechender Datensatz der Antarctic Digital Database (ADD Consortium, 2012) verwendet. Gletscherspezifische Parameter (i.e. Fläche, min., max., durchschnittliche, mittlere Höhe, Exposition und Neigung) sowie die allumfassende Hypsometrie konnten mit Hilfe des Digitalen Höhenmodells von Cook *et al.* (2012) bestimmt werden. Des Weiteren wurden den Gletschern Konnektivitäts-Stufen mit dem Eisschild zugeordnet, basierend auf dem von Rastner *et al.* (2012) eingeführten Konzept und den Antarktischen Einzugsgebieten nach Zwally *et al.* (2012). Zudem wurden mit den Datensätzen von Huss und Farinotti (2014) Eisdicke, -volumen und Meeresspiegeläquivalent pro Gletscher bestimmt. Der erstellte Datensatz wird der Global Land Ice Measurements from Space Datenbank zur Verfügung gestellt.

Das Inventar besteht aus 1588 Gletschern mit einer Fläche von 94 743 km<sup>2</sup> und bedeckt somit etwas mehr als die 90 000 km<sup>2</sup> der Gletscher und Eiskappen um den Grönländischen Eisschild (Rastner *et al.* 2012). Die wenigen grossen Gletscher dominieren bezüglich Fläche, wobei die Gletscher mit einer Fläche zwischen 1 und 50 km<sup>2</sup> zahlenmässig dominieren. Im Meer endende Gletscher machen flächenmässig 63% und in Schelfeis endende Gletscher 35% aus. Das totale Eisvolumen beträgt 34 650 km<sup>3</sup>, wovon sich ein Drittel unter Meeresspiegelhöhe befindet. Das Meeresspiegeläquivalent beträgt somit 83.2 mm. Mittlere Höhe, mittlere Dicke, Volumen, Gletscherhypsometrie sowie der Gletschertyp sind durch die Topographie der Halbinsel bestimmt. Es ist kein Zusammenhang zu Exposition oder Niederschlag erkennbar. Die alle Gletscher umfassende Hypsometrie hat eine bimodale Form: Maximal vergletscherte Flächen befinden sich primär zwischen 200 – 500 m ü.M. und sekundär zwischen 1500 – 1900 m ü.M.. Daher, und der Wasserkontakt der meisten Gletscher, resultiert in einer hohen Sensitivität der Gletscher gegenüber Klimaänderungen, verbunden mit steigenden Gletscher-Gleichgewichtslinien und zunehmenden Wassertemperaturen. Die Sensitivität von in Schelfeis endenden Gletschern ist hoch gegenüber Veränderungen an der Front, denn nach dem Auseinanderbruch des Schelfeis ist deren Eisverlust erhöht.

Diese Arbeit trägt einerseits dazu bei, das Meeresspiegeläquivalent präziser zu bestimmen. Des Weiteren wird aufgezeigt, wie ein solches Inventar das Wissen über die Gletscher der Antarktischen Halbinsel verbessern kann.





# Contents

<b>ACKNOWLEDGEMENTS</b> .....	<b>I</b>
<b>SUMMARY</b> .....	<b>III</b>
<b>ZUSAMMENFASSUNG</b> .....	<b>V</b>
<b>CONTENTS</b> .....	<b>VII</b>
<b>LIST OF FIGURES</b> .....	<b>IX</b>
<b>LIST OF TABLES</b> .....	<b>XI</b>
<b>1 INTRODUCTION</b> .....	<b>1</b>
1.1 Motivation.....	1
1.2 Aim of the thesis, research tasks and questions.....	2
1.3 Organization of the thesis .....	3
<b>2 STUDY REGION</b> .....	<b>5</b>
2.1 Antarctic Peninsula.....	5
2.2 Glacier cover.....	6
2.3 Climatic setting.....	7
<b>3 BACKGROUND</b> .....	<b>9</b>
3.1 Glacier inventory and Global Land Ice Measurements from Space .....	9
3.2 Technical workflow to generate a glacier inventory .....	10
<b>4 REASSESSMENT</b> .....	<b>13</b>
4.1 Inventory data currently existing .....	13
4.2 Qualitative description and comparison .....	14
4.2.1 Datasets of the Global Land Ice Measurements from Space database.....	14
4.2.2 Glacier catchment outlines of Cook <i>et al.</i> (2014) .....	16
4.2.3 Glacier catchment outlines from the Antarctic Digital Database.....	21
4.3 Suitability examination and data selection .....	24
<b>5 METHODS APPLIED</b> .....	<b>27</b>
5.1 Excluding rock outcrops.....	27
5.2 Assignment of connectivity levels.....	28
5.3 Deriving glacier parameters.....	29
5.3.1 Topographic parameters.....	30
5.3.2 Ice thickness, volume and sea level equivalent.....	34
<b>6 RESULTS</b> .....	<b>37</b>
6.1 Area and size classes .....	38
6.2 Connectivity levels.....	38

<b>6.3</b>	<b>3D parameters.....</b>	<b>39</b>
<b>6.4</b>	<b>Glacier hypsometry .....</b>	<b>42</b>
<b>6.5</b>	<b>Thickness, volume and sea level equivalent .....</b>	<b>43</b>
<b>6.6</b>	<b>Nominal inventory parameters .....</b>	<b>47</b>
<b>7</b>	<b>DISCUSSION .....</b>	<b>49</b>
<b>7.1</b>	<b>Applications of the Antarctic Peninsula glacier inventory .....</b>	<b>49</b>
7.1.1	Identifying glacier tendencies based on median elevation and aspect .....	49
7.1.2	Identifying glacier sensitivity to climate based on glacier hypsometry .....	51
7.1.3	Comparison of inventory characteristics with those of other regions .....	53
7.1.4	Comparison of the sea level equivalent with that of other studies and regions .....	55
7.1.5	Representativeness of the mass balance glaciers of the World Glacier Monitoring Service	56
<b>7.2</b>	<b>Challenges and restrictions.....</b>	<b>59</b>
7.2.1	Challenges of the inventory compilation based on existing datasets .....	59
7.2.2	Restrictions of the inventory: origins, impacts and suggestions for improvements.....	60
<b>8</b>	<b>CONCLUSIONS AND PERSPECTIVES .....</b>	<b>63</b>
<b>8.1</b>	<b>Compilation of the glacier inventory .....</b>	<b>63</b>
<b>8.2</b>	<b>Major findings of the glacier inventory analysis .....</b>	<b>64</b>
<b>8.3</b>	<b>Outlook.....</b>	<b>65</b>
8.3.1	Suggested improvements .....	65
8.3.2	Possible further analysis and applications.....	66
<b>9</b>	<b>REFERENCES.....</b>	<b>67</b>
<b>10</b>	<b>APPENDIX.....</b>	<b>75</b>
<b>11</b>	<b>PERSONAL DECLARATION.....</b>	<b>77</b>

# List of Figures

Figure 2.1. A) Map of the AP from Davies <i>et al.</i> (2012), including 1000 m contours and SRTM marine bathymetry. Rock outcrops (brown), contours and ice margins are from the Antarctic Digital Database. B) Simplified ocean circulation from Bentley <i>et al.</i> (2009). The green box delineates Graham Land, on which this work focuses.....	5
Figure 2.2. Locations of important climate records of the AP from King <i>et al.</i> (2003).....	8
Figure 2.3. Corresponding annual variations of surface air temperature of the climate stations indicated Figure 2.2 and described in Table 2.1.....	8
Figure 3.1. General workflow of the generation of a glacier inventory from Rastner <i>et al.</i> (2012) as done for the glaciers on Greenland. Based on Cook <i>et al.</i> (2014), the processing step <i>Glacier Mapping</i> has not been applied for the generation of a glacier inventory for the AP as explained in the text. ....	12
Figure 4.1. Difference between the GLIMS outlines of 1988 and the LIMA, illustrating the glacier change.....	15
Figure 4.2. Existing GLIMS and RGI glacier outlines and the LIMA.....	17
Figure 4.3. The WGI consisting of point information for the individual glaciers and the LIMA.....	18
Figure 4.4. Glacier catchment outlines from Cook <i>et al.</i> (2014) and the LIMA.....	19
Figure 4.5. Close-up of all datasets considered so far.....	20
Figure 4.6. Overlay with the catchment outlines dataset of the Antarctic Digital Database (ADD).....	22
Figure 4.7. Catchment outlines of Cook <i>et al.</i> (2014) vs. the basin delineation resulting from the watershed analysis based on Bolch <i>et al.</i> (2010). The general patterns of the two datasets are coincident. ....	25
Figure 5.1. Close-up of the Trinity Peninsula and James Ross Island showing the rock outcrops which are excluded from the catchment outlines of Cook <i>et al.</i> (2014).....	28
Figure 5.2. Antarctic drainage systems developed by the Goddard Ice Altimetry Group from ICESat data from Zwally <i>et al.</i> (2012). The numbers on Antarctica are the drainage system id's. The portions of the drainage systems within the MODIS grounding line are filled with solid color. The portions between the MODIS grounding line and the coastline are hatched.....	29
Figure 5.3. a) Color-coded visualization of the DEM provided by Cook <i>et al.</i> (2012) with 500 m contours and b) corresponding hillshade. ....	31
Figure 5.4. Digital elevation model of Cook <i>et al.</i> (2012) overlaid by the glacier outlines illustrating that for some glaciers the elevation information is partly or entirely missing. This region of the Renaud and Biscoe Islands is representative for other regions. ....	32
Figure 5.5. Modeled a) ice thickness and b) bedrock elevation of the AP from Huss and Farinotti (2014).....	35
Figure 6.1. Percentage of glacier number (blue) and area (red) per size class. Values are given in Table 6.2. ....	38

## List of Figures

---

Figure 6.2. Assigned connectivity levels (color-coded) overlaid over the LIMA.....	39
Figure 6.3. a) mean and median elevation vs. area and b) minimum and maximum elevation vs. area of the 1540 glaciers involving elevation information. ....	40
Figure 6.4. Color-coded glacier areas for visualization of the median elevation for 1540 glaciers. ....	40
Figure 6.5. Percentage of glacier number (blue) and area (red) per aspect sector.....	41
Figure 6.6. Mean glacier elevation vs. mean glacier aspect of 1540 glaciers. ....	41
Figure 6.7. Mean glacier slope vs. glacier area of 1540 glaciers.....	41
Figure 6.8. Glacier hypsometry of 1540 glaciers of the AP. a) Total areal distribution (blue), the areal distribution without rock outcrops (red) and areal distribution for marine-terminating and ice shelf nourishing glaciers (green). b) Areal distribution of the glacier cover per sector. ....	43
Figure 6.9. Scatter plot of the 1539 glaciers involving thickness information. a) mean thickness vs. area and b) mean thickness vs. mean slope.....	44
Figure 6.10. Color-coded glacier areas for visualization of mean glacier thickness. ....	44
Figure 6.11. Boxplots of a) mean thickness per mean aspect and b) mean thickness per sector.....	45
Figure 6.12. Total ice volume per sector. ....	45
Figure 6.13. Total volume per total glacier area for each individual glacier.....	46
Figure 6.14. Negative elevation values representing the bedrock below sea level. ....	46
Figure 6.15. Volume grounded below sea level per sector relative to the total volume per sector. ....	47
Figure 6.16. Color-coded glacier areas for visualization of the nominal parameters a) primary classification (glacier type) and b) frontal characteristics of the 1588 glaciers. Values are given in Table 6.5. The classification was done by Cook <i>et al.</i> (2014). ....	48
Figure 7.1. Distribution of normalized glacier cover with elevation for the entire AP and for each sector. ....	53
Figure 7.2. Spatial distribution of a) absolute and b) relative (% of basin size) change in area of Cook <i>et al.</i> (2014). Earliest records, on average, from 1958 and latest, on average, 2004. ....	53
Figure 7.3. Location of the two WGMS mass balance glaciers indicated by the two yellow arrows. ...	57
Figure 7.4. Localization of the WGMS mass balance glaciers Montiel Glacier (red) and Glaciar Smit (green) in the scatterplots area vs. mean slope (a) and mean aspect vs. mean elevation (b), based on values of the introduced inventory. ....	58
Figure 7.5. Glacier hypsometries with normalized area for the entire AP (blue), the Montiel Glacier (red) and the Glaciar Smit (green). The calculations are based on the here provided outlines. ....	59
Figure 7.6. Examples of glacierized islands incorrectly classified as rock outcrops (a and b) and an example of a highly fragmented glacier outline after intersecting with the rock outcrops layer (c). In addition, georeferencing inaccuracies are detectible.....	61

# List of Tables

Table 2.1. Details of the climate stations of Figure 2.2 and 2.3 from King <i>et al.</i> (2003).....	8
Table 4.1. Comparison of existing glacier inventory datasets of the AP, regarding relevant characteristics to generate a complete glacier inventory of the AP. ....	32
Table 5.1. Definition of the size classes and the corresponding values. Only the upper boundary value per size class is given. ....	32
Table 5.2. Aspect sectors and the corresponding conversion from 360° .....	33
Table 6.1. Glacier parameters in the attribute table of the inventory of the AP.....	37
Table 6.2. Statistics of all glaciers of the inventory and the nine size classes. In the top row <i>size class</i> only the upper limit of each class is listed. ....	38
Table 6.3. Total glacier number and area as well as the percentage per sector.....	43
Table 6.4. Glacier number, area, volume, volume grounded below sea level, the corresponding percentages and SLE per sector. ....	47
Table 6.5. Primary classification (Class) and frontal characteristics (Front) of the 1588 glaciers.....	48
Table 7.1. Summary of selected inventory parameters of different regions.....	54
Table 7.2. Selection of glacier attributes as provided by the present inventory (left) and as provided by the WGMS (2015; right). The Montiel glacier and the Anvers Ice Cap refer to the same glacier (red). Same is true for the Glaciar Smit and the Bahia del Diabolo (green). ....	58



# 1 Introduction

## 1.1 Motivation

During the 20<sup>th</sup> century the extent of glacial and periglacial features all over the world experienced partially drastic changes due to the changing climate (Haeberli and Beniston 1998; Haeberli 2005; Vaughan *et al.* 2013). The knowledge about the amount of water stored in glaciers and ice caps is important to determine the influence of melting glaciers on rising sea level due to global warming. In this context, inventories such as the World Glacier Inventory (WGI; WGMS and NSIDC, 1999, updated 2012) and the Global Land Ice Measurements from Space Initiative (GLIMS; Raup *et al.* 2007) pursued the idea of a global glacier inventory.

Recently, the ice masses of the Antarctic Peninsula (AP) received more attention as exceptionally strong regional warming has been detected in this region accompanied with changing precipitation patterns (Rau *et al.* 2006; Hock *et al.* 2009). Rau *et al.* (2006) illustrate several direct consequences of these changes on the cryosphere of the AP, such as ice shelf disintegration and changing glacier front positions.

*“These small glaciers around the edge of the Antarctic Peninsula are likely to contribute most to rising sea levels over the coming decades, because they can respond quickly to climate change” said Dr. Davies from the Department of Geography at Royal Holloway*” (Royal Holloway University of London, 2014).

This statement demonstrates the crucial role of the glaciers of the AP regarding climate change and SLR. Therefore, the Intergovernmental Panel on Climate Change (IPCC) decided to adjudicate the region of the AP to be one out of eight regions for detailed investigation (Rau *et al.* 2006). The IPCC aims to consider all perennial surface land ice masses to describe the individual components of the cryosphere and their contribution to sea level rise (SLR). Hence, for the Fifth Assessment Report (AR5), released between September 2013 and November 2014, *“a new globally complete data set of glacier outlines was compiled”* (Vaughan *et al.* 2013: 335) based on outlines from different published and unpublished sources (including GLIMS): The Randolph Glacier Inventory (Arendt *et al.* 2012; Pfeffer *et al.* 2014).

However, neither GLIMS (GLIMS and NSIDC 2005, updated 2015) nor the newest version of the RGI (Arendt *et al.* 2015) entirely include the glaciers on the mainland of Antarctica, most of them probably located on the AP, due to missing separation of the glaciers from the Antarctic ice sheet (Vaughan *et al.* 2013). Therefore Vaughan *et al.* (2013: 335) admit:

*“[The] separation is still incomplete for Antarctica, and values discussed [in the IPCC] refer to the glaciers on the islands in the Antarctic and Sub-Antarctic (Bliss et al., 2013) but exclude glaciers on the mainland of Antarctica that are separate from the ice sheet.”*

The separation of the individual glaciers from one another, as well as from the ice sheet, is rather challenging and the method is not distinct (Rastner *et al.* 2012; Bliss *et al.* 2013). Depending on the aim of a study, the definitions and methods of this separation vary (Bliss *et al.* 2013). Several studies are challenging the lack of knowledge about the amount of ice stored in Antarctic (Hock *et al.* 2009; Radić and Hock 2010; Huss and Farinotti 2014). However, as no complete outline dataset separating the individual glaciers from each other and from the ice sheet is available, the glaciers on the mainland of the AP are not included in these studies. Hence, these glaciers are not separately taken into consideration for their estimation of the sea level equivalent (SLE). The separation of the local glaciers from the ice sheet is also necessary because, firstly, the glaciers of the AP have a distinctively different behavior regarding glacier sensitivities and time scales compared to the ice sheet (Rau *et al.* 2006; Hock *et al.* 2009). Secondly, it can help solving the problem of double-counting their sea level contribution, as the ice mask of the Antarctic ice sheet might (partially) include glaciers of the AP (Paul 2011; Pfeffer *et al.* 2014).

In general, previous available inventories of the AP, which consist of different dataset formats, are deficient in either spatial coverage or breadth of data (e.g. Rabassa *et al.* 1982; Braun *et al.* 2001; Davies *et al.* 2011; Bliss *et al.* 2013). The lack of a complete outline dataset has recently been approached by Cook *et al.* (2014) by generating dataset of all glacier catchment of the AP, which would have to be further processed to create glacier outlines. However, the full dataset is neither published nor provided by any database yet. Therefore, as no global-scale inventory includes a complete inventory of the AP, it is of urgent demand to acquire accurate and globally complete information about the location and extent of glaciers and to amalgamate these datasets into a glacier inventory.

In addition, to estimate the SLE, ice thickness and volume information are needed. However, the geometry of the AP's glaciers is distinct of other regions. The often applied volume-area scaling (e.g. Erasov 1968 (in Radić and Hock (2010)); Bahr *et al.* 1997; Radić *et al.* 2007, 2008; Radić and Hock 2010) is not appropriate for the very distinct glacier hypsographies of the AP. Hence, more physically based data are needed.

The two key open point are the missing delineation of the glaciers as well as their separation from the ice sheet. In addition, this lack of data lead to a limited knowledge about the AP's glaciers, their characteristics and their corresponding role in a changing climate.

## **1.2 Aim of the thesis, research tasks and questions**

To fill this gap, this Master's thesis aims at generating a complete glacier inventory of the AP consisting of glacier outlines, including a separation of the glaciers from the Antarctic ice sheet. To achieve this, already existing inventory data are reassessed and further processed. The description of the characteristics of the glaciers (i.e. size and aspect distribution, median elevation, glacier (frontal) types and glacier hypsometry) and the extension of the inventory with ice thickness, volume and SLE information demonstrate the potential of this dataset to identify the impacts of climate change on the AP's glaciers. Furthermore, the potential of this dataset is demonstrated by identifying glacier tendencies, glacier climate-sensitivities as well as by describing similarities and differences to other glacier regions.



Hence, the main research tasks of this thesis are:

- (1) The reassessment of currently existing inventories of the glaciers of the AP
- (2) The generation of a glacier inventory based on already existing, suitable data to integrate it into the GLIMS database
- (3) The separation of the glaciers from the ice sheet
- (4) Deriving the glacier parameters area, minimum, maximum, mean, median elevation, mean slope and aspect for each glacier
- (5) The extension of the inventory with ice thickness, volume and SLE information
- (6) Analyzing the topographic characteristics of the glaciers on the AP in terms of size and aspect distribution, slope, elevation, ice thickness and volume, glacier (frontal) types and overall glacier hypsometry

The realization of the above tasks should enable to answer the following research questions:

- (1) Can geo-spatial datasets of different origin and quality be merged to create a complete inventory for the AP?
- (2) What are the characteristics of the glaciers on the AP in terms of their topographic parameters?
- (3) What does the hypsometry reveal about the sensitivity of the glaciers on changes in air or water temperature?
- (4) What is the potential SL contribution of the AP?
- (5) What are similarities and differences to other glacierized regions, namely Greenland, Alaska/northwest Canada and Svalbard?

### **1.3 Organization of the thesis**

This Master's thesis is structured in seven sections, including this first section describing the motivation and the resulting aims, research tasks and questions. Section 2 introduces the AP as the study site. Some background information is given in Section 3 about the concept of a glacier inventory and GLIMS, as well as the technical workflow to generate a glacier inventory. The main part of this study consists of a reassessment of existing inventory datasets of the glaciers of the AP and the corresponding qualitative description and comparison (Section 4), followed by the description of the methods applied for the generation of the glacier inventory of the AP (Section 5), and finally the presentation of the results, regarding the current status and characteristics of the glaciers, including glacier size distribution, connectivity levels, 3D parameters, glacier hypsometry, ice thickness, volume, SLE as well as the nominal glacier parameters *glacier type* and *frontal characteristics* (Section 6). Further, a critical discussion of the noteworthy results is performed. This includes interpreting the findings with respect to the research questions as well as in a broader context. Also encountered challenges and limitations of the presented inventory are described (Section 7). The final section summarizes the main conclusions and answers the research questions. In addition, perspectives for future work are illustrated (Section 8). The thesis ends with the references and an appendix.



## 2 Study region

### 2.1 Antarctic Peninsula

The AP extends significantly northwards of the mainland of Antarctica stretching into the Southern Ocean (Figure 2.1). Following common definitions (Turner *et al.* 2009; Zwally *et al.*, 2012; Cook *et al.* 2014; Huss and Farinotti 2014) the AP spans from about 75°S for more than 1500 km north-easterly to 60°S, surrounded by a vast number of rugged islands. According to Cogley *et al.* (2010), the South Shetland Islands are not defined as being part of the AP, as these islands are not considered as *close* to the mainland and therefore belong to the Subantarctic Islands. The mainland is dominated by a narrow mountain chain with a mean height of 1500 m and an average width of 70 km. The high elevation plateau region and steep-sided valleys of the mainland are enclosed to the west by the Bellingshausen Sea and to the east by the Weddell Sea (Turner *et al.* 2009). The spatial focus of this work is on Graham Land and the peripheral islands (green box in Figure 2.1).

The Antarctic Treaty System governs Antarctica and the AP, regulates the international relations, promotes scientific work and prevents military activity on the continent. The sovereignty claims of Chile, Argentina and the United Kingdom are not internationally admitted (Fund and Hogan, 2013).

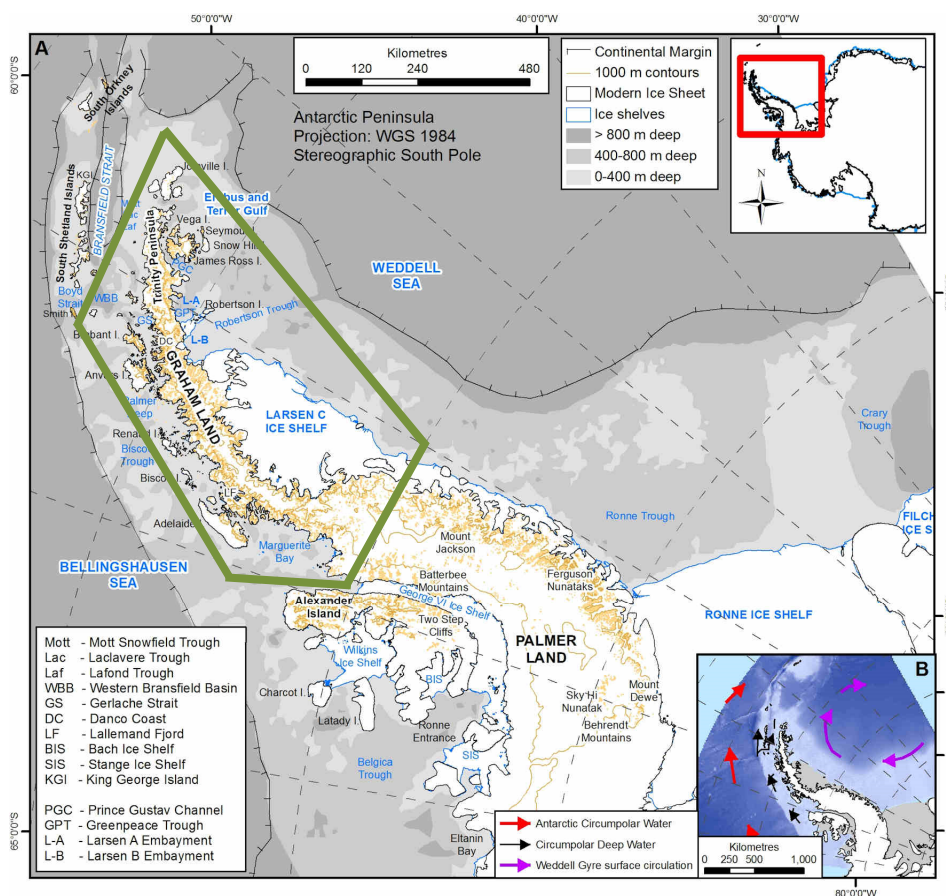


**Figure 2.1. A) Map of the AP from Davies *et al.* (2012), including 1000 m contours and SRTM marine bathymetry. Rock outcrops (brown), contours and ice margins are from the Antarctic Digital Database. B) Simplified ocean circulation from Bentley *et al.* (2009). The green box delineates Graham Land, on which this work focuses.**

## 2.2 Glacier cover

The mainland and islands are highly glacierized with several rock outcrops interrupting the ice cover (Figure 2.1). The topography causes a complex glacier system with often unclear topographic divides. The interior is dominated by ice masses flowing out of the plateau region, but the steep valleys cause these glaciers to be heavily crevassed. At the periphery the glaciers are low-sloping ice streams. These glaciers are much thinner compared to the ice sheet covering the rest of Antarctica. Most of the glaciers on the AP are marine-terminating glaciers, ending with a grounded ice cliff producing ice bergs (tidewater glaciers), have a floating terminus or are ice shelf nourishing (Cook *et al.* 2005; Cook *et al.* 2014). The glaciers along the AP's west coast north of the George VI Sound and along the east coast north of 66°S are mainly tidewater glaciers. Further south the glaciers are ice shelf nourishing. In the east they are flowing into the still existing Larsen C Ice Shelf (Cook *et al.* 2014). The bottoms of several valleys and channels underneath the ice are lying considerably below sea level (Huss and Farinotti 2014). In contrast to most of Antarctica, the polythermal glaciers in this maritime climate experience a distinct melting period in summer, particularly the glaciers in the north. Therefore runoff from surface melt is a significant component of these glaciers' mass budget (Turner *et al.* 2009; Arigony-Neto *et al.* 2014).

As mentioned before, there is no consistent separation of the glaciers and the Antarctic ice sheet. The separations vary depending on the technique or the application (Bliss *et al.* 2013; Cook *et al.* 2014). For this study the most recent Antarctic ice sheet drainage divides dataset provided by the Cryosphere Science Laboratory of NASA's Earth Sciences Divisions (Zwally *et al.* 2012) is considered for the separation of the Antarctic ice sheet and the AP with its glaciers (cf. Section 5.2). Accordingly, the ice masses south of 70°S are classified as Antarctic ice sheets and therefore are not taken into consideration in this study.

The climatic and oceanographic regime varies across the AP (cf. Section 2.3) causing varying glacier dynamics and glacial response times (Arigony-Neto *et al.* 2014). However, the relatively small glaciers of the northern AP (Graham Land), compared to the much larger ice masses towards the south (Palmer Land), are expected to react with rather short response times (years to decades (Rau *et al.* 2006)) to changes in their mass balance. Hence, these glaciers are major indicators of changes of the regional climate (Rau *et al.* 2006). Nevertheless, the knowledge about the mass balance of the glaciers of the AP is sparse (Rignot and Thomas 2002). Shepherd *et al.* (2012) estimated the mass balance of the ice sheet by combining of a variety of observations and models. Helm *et al.* (2014) derived elevation changes of Antarctica from CryoSat-2 data. These studies reveal change in mass of the AP between 1992 and 2011 by  $-20 \pm 14$  Gt per year (Shepherd *et al.* 2012) and even increased volume loss between 2011 and 2014 (Helm *et al.* 2014). However, they admit, that for the AP improved datasets are required, as the spatial and temporal sampling of mass fluctuations is currently inadequate (Shepherd *et al.* 2012) and large uncertainties occur (Helm *et al.* 2014).

Many ice shelves are surrounding the Antarctic continent and the AP. Atmospheric or oceanic warming is seen to have accounted for recent collapse events of ice shelves around the AP (Rott *et al.* 1996; Rott *et al.* 1998; Scambos *et al.* 2000; Rignot and Thomas 2002). Moreover, also

structural glaciological factors are influencing the stability of ice shelves, such as crevasse propagation by meltwater (Scambos *et al.* 2000; Glasser and Scambos 2008). However, several studies affirm that the existence of ice shelves around the AP is mainly determined by the  $-1.5\text{ }^{\circ}\text{C}$  January isotherm and  $-8\text{ }^{\circ}\text{C}$  mean annual isotherm, which have moved south in the last decades (Rott *et al.* 1996; Rott *et al.* 1998; Scambos *et al.* 2000).

## 2.3 Climatic setting

The AP has a polar to subpolar maritime climate. Even though it represents only about 1% of Antarctica's area, it receives about 10% of the precipitation (van Lipzig 2004). As about one third of the area is found close to the coast at rather low elevations, temperatures above  $0\text{ }^{\circ}\text{C}$  are frequent (Turner *et al.* 2009). Therefore, the AP is dominated by austral summer rainfall, austral winter snowfall and strong westerly winds (Arigony-Neto *et al.* 2014). In addition, the Amundsen-Bellinghshausen Sea low pressure system causes the advection of warm mid-latitude air masses from the northwest, resulting in a rather mild climate compared to the rest of Antarctica and other regions at similar latitude. The north-south oriented mountain chain in combination with the persistent Southern Ocean north-westerlies causes a strong orographic effect. The prevailing winds from the warm Bellingshausen Sea transport warm and humid air towards the AP. Hence, large spatial variations in precipitation and accumulation are found. Most of the precipitation (solid in winter, both liquid and solid in summer) and highest accumulation values are found in the northern and central regions of the AP, whereas the east and southeastern parts are affected by the precipitation shadow (King *et al.* 2003). In addition, on the eastern side of the AP cold continental air flows northwards, due to a climatological low east of the Weddell Sea, acting as a barrier for the warm air of the Bellingshausen Sea. As a result, the mean annual surface temperatures of the west coast are  $5 - 10\text{ }^{\circ}\text{C}$  higher than those of the east coast and monthly means can be positive for up to four months (King *et al.* 2003; Turner *et al.* 2009). Figure 2.2 and 2.3 show the locations of different climate stations and the corresponding annual variations of surface air temperature. Table 2.1 lists the details of these stations. Temperature gradients across the regions are strong in winter (June-August) and weak in summer (December-February). The west and northern coast of the AP show similar annual cycles of temperature as other maritime regions of Antarctica: Long summer maximum and minimum temperatures in July/August. The annual cycle of the southerly parts of the east coast conform to those of continental Antarctica: A short summer and a long winter season (King *et al.* 2003).

Since the early 1950s significant atmospheric warming trends (Turner *et al.* 2009) and changing ocean temperatures (Shepherd *et al.* 2003) have been observed across the AP. However, these trends are very complex as they are spatially and seasonally heterogeneous. Turner *et al.* (2009) showed that in winter the warming trend is most pronounced in the north and west (Faraday/Vernadsky Station:  $+1.03\text{ }^{\circ}\text{C}$  per decade from 1950 – 2006), whereas the eastern part of the AP experienced warming mainly during summer and fall (Esperanza Station:  $+0.41\text{ }^{\circ}\text{C}$  per decade from 1946 – 2006). Hence, the west coast of the AP is the region of fastest warming trends of the Southern Hemisphere. The increased emission of greenhouse gases and the formation of the Antarctic ozone hole caused the westerlies to strengthen. The resulting changes

in southern hemisphere atmospheric circulation (mainly in winter) bring warm, maritime air towards the AP (Turner *et al.* 2009). The increase in summer temperatures in the past 50 years is similar to other regions in the Southern Hemisphere and therefore not exceptional. However, these small temperature changes in summer cause the 0 °C isotherm to move further southward resulting in drastic increases in summer melt (King *et al.* 2003). As a consequence, ice shelves and glacier fronts are collapsing and retreating (Pritchard and Vaughan 2007; Cook *et al.* 2014).

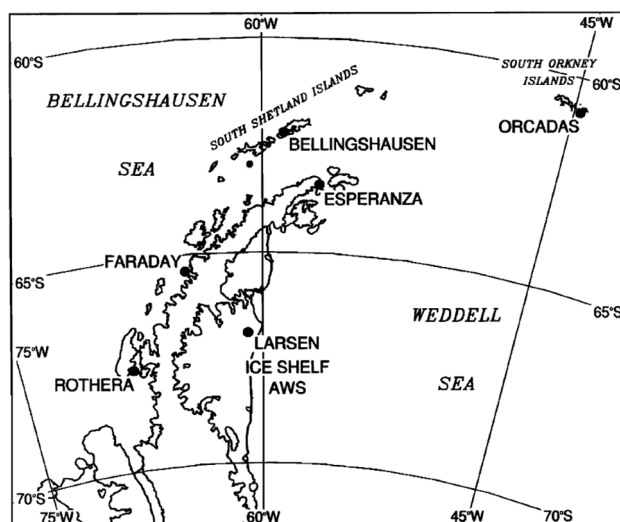


Figure 2.2. Locations of important climate records of the AP from King *et al.* (2003).

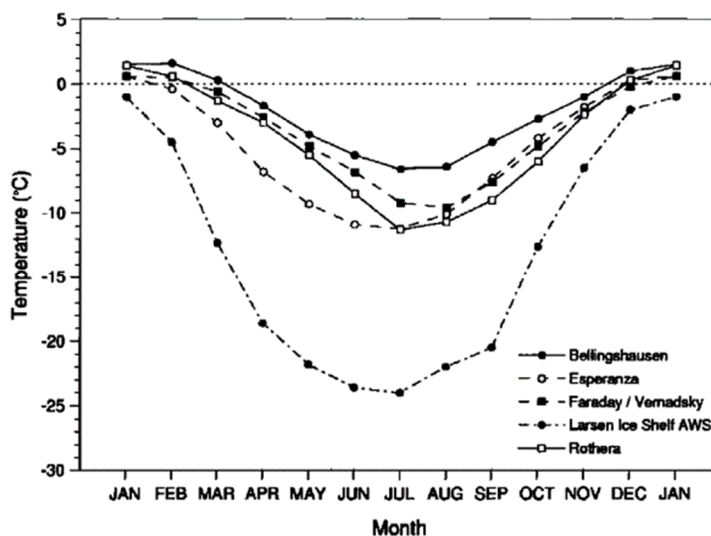


Figure 2.3. Corresponding annual variations of surface air temperature of the climate stations indicated Figure 2.2 and described in Table 2.1.

Station	Latitude [°S]	Longitude [°S]	Elevation [m a.s.l.]	Period in operation	Period analyzed
Bellingshausen	62.2	59.0	16	1968-	1968-2000
Esperanza	63.4	57.0	13	1945-8; 1952-	1952-2000
Faraday/Vernadsky	65.2	64.3	11	1947-	1951-2000
Larsen Ice Shelf (automatic weather station)	66.9	60.9	17	1985-	-
Orcadas	60.8	44.7	6	1903-	1903-2000
Rothera	67.6	68.1	16	1976-	1976-2000

Table 2.1. Details of the climate stations of Figure 2.2 and 2.3 from King *et al.* (2003).

## 3 Background

### 3.1 Glacier inventory and Global Land Ice Measurements from Space

The continued glacier-by-glacier studies, such as glacier-specific area and volume change assessments, as well as global-scale assessments, such as potential and future contribution of glaciers to SLR, request glacier inventories. These inventories need to include the definition of outlines for each individual glacier using a consistent technique and need to store this information comprehensively (Rastner *et al.* 2012; Cook *et al.* 2014; Pfeffer *et al.* 2014). During the International Hydrological Decade (1965 – 74) the need for a global glacier inventory arose, leading to the establishment of guidance material to create a detailed global inventory of existing perennial snow and ice masses (WGMS 1989). As a consequence, the World Glacier Inventory (WGI; WGMS and NSIDC, 1999, updated 2012) was established in the 1980s to determine the amount, distribution and variation of all snow and ice masses for a better understanding of their influence on the global water balance (Ohmura 2010). The internationally collected and standardized datasets of over 130 000 glaciers contain a set of glacier attributes and represent the glacier distribution in the second half of the 20<sup>th</sup> century, mainly based on maps and aerial photographs (WGMS and NSIDC, 1999, updated 2012). However, the information is only available as point data, which makes tracing changes of individual glaciers impossible (Racoviteanu *et al.* 2009; Pfeffer *et al.* 2014). The full inventory is available from the National Snow and Ice Data Center (NSIDC) in Boulder, Colorado, USA ([http://nsidc.org/data/glacier\\_inventory/index.html](http://nsidc.org/data/glacier_inventory/index.html)). As the enhancement of remote sensing techniques and automated computer processing accelerated inventory work, the multi-national Global Land Ice Measurements from Space initiative (GLIMS; Raup *et al.* 2007) was launched in 1995. This initiative aims at continuing the compilation of a global inventory of land ice masses and monitoring these, using data from mostly optical satellite instruments and digitized topographic maps (Kieffer *et al.* 2000; Ohmura 2010) to measure changes in the extent of glaciers (Braun *et al.* 2001; Ohmura 2010). The regularly extended GLIMS inventory (GLIMS and NSIDC 2005, updated 2015) also contains a set of glacier attributes, but additionally includes more recent digital glacier outlines in a digital vector format. The idea is to archive standardized and comparable results of glaciers and their analyses in the database along with corresponding meta-information of the analysis, such as analyst name, time of analysis, images used, description of processing and so on (Rau *et al.* 2006; Paul *et al.* 2009, Raup and Khalsa, 2010, 2010). The NSIDC designed, implemented and is maintaining the GLIMS Glacier Database (Rau *et al.* 2006; Paul *et al.* 2009). The RGI (Arendt *et al.* 2012) has been compiled in short time (1-2 years) and with limited sources in order to meet the needs of the Fifth Assessment of the IPCC for a globally complete dataset with accepted limitations in regional quality (Pfeffer *et al.* 2014). Hence, none of the RGI versions provide the same richness in meta-data and source information as GLIMS database, that is designed to store multi-temporal datasets (compared to the RGI being one snap shot in time). It is a supplement to GLIMS and currently merged into the GLIMS database to have the same spatial coverage (Raup *et al.* 2013;

Pfeffer *et al.* 2014). The newest RGI (v5.0; Arendt *et al.* 2015), the GLIMS, as well as the WGI data are provided by the GLIMS/NSIDC website and can be obtained for free through the web-based interfaces and map services (<http://glims.org/maps/glims>).

As this thesis aims, *inter alia*, at compiling a glacier inventory, which then can be implemented into the GLIMS database, the compilation bases on the recommendations and guidelines provided by the GLIMS community (Rau *et al.*, 2005; Paul *et al.* 2009; Racoviteanu *et al.* 2009; Raup and Khalsa, 2010).

### 3.2 Technical workflow to generate a glacier inventory

The remoteness and the scale of the AP requires a remote sensing approach for the generation of a glacier inventory. Remote sensing allows acquiring information of areas and objects without being in physical contact with it (Lillesand *et al.* 2015). Besides the availability of digital source material, modern data-generation and analysis techniques, such as Geographic Information Systems (GIS), are available (Paul *et al.* 2009). The applications as well as the definition of GIS are diversified. A general definition is given by Dueker and Kjerne (1989: 7- 8):

*“Geographic Information System - A system of hardware, software, data, people, organizations and institutional arrangements for collecting, storing, analyzing and disseminating information about areas of the earth.”*

The combination of remote sensing and a GIS enables generating a glacier inventory. The schematic flow chart in Figure 3.1 illustrates the general workflow of the generation of a glacier inventory as applied for the glaciers on Greenland by Rastner *et al.* (2012). By applying an automated mapping algorithm on satellite data within a GIS, glaciers can be delineated (Racoviteanu *et al.* 2009). In this context, the definition of a glacier is crucial. This is not further discussed here, but a comprehensive explanation is given by the GLIMS analysis tutorial (Raup and Khalsa, 2010) and GLIMS recommendations (Racoviteanu *et al.* 2009). Besides the satellite data, a digital elevation model (DEM) is needed as input data. The DEM enables to calculate drainage divides for glaciers, for which several algorithms exist (Racoviteanu *et al.* 2009; Bolch *et al.* 2010; Kienholz *et al.* 2013). The terms drainage basins, drainage divides, catchment outlines, glacier catchments and so on are often, and also here, used synonymously. The automated mapping algorithm as well as the drainage basin algorithm require subsequent manual corrections. The accuracy of the resulting drainage divides and hence the extent of the remaining manual corrections mainly depend on the quality of the DEM and the topography of the corresponding region. Good representations of steep ridges in a rough terrain lead to an accurate result. However, the delineation in smooth areas, such as the top of ice caps, is rather arbitrary (Rastner 2014). By intersecting the drainage basins and the glacierized area delineation in a GIS, a vector layer of individual glaciers is generated. The individual glaciers can be further analyzed, for instance, in terms of connectivity levels (cf. Section 5.2), area (cf. Section 5.3.1) and glacier (frontal) type. By digitally combining the outlines of individual glaciers (as vector format) with the DEM, topographic parameters such as minimum, maximum, mean and median elevation, mean slope and aspect can be automatically calculated



(cf. Section 5.3.1). Henceforth, these parameters can be statistically analyzed, for instance, to identify the characteristics of a glacierized region.

However, in the case of the AP not all of these processing steps of glacier mapping are implicitly needed as shown by Cook *et al.* (2014). The AP is highly glacierized without larger areas of rock, debris or frozen lakes. Hence, the band ratio method would basically delineate the entire region as glacierized area. In addition, as the ocean is extensively riddled with icebergs and sea ice, which also would be classified as glacierized areas by the algorithm, time-consuming manual exclusion would be needed. Hence, the processing step *Glacier Mapping* in Figure 3.1 has not been applied neither by Cook *et al.* (2014) nor for this thesis. However, as the drainage basins are solely based on the DEM, the coastline has to be digitized manually based on satellite images and the location of the grounding line. Further, also ice velocity data should be considered to revise the basin boundaries. This approach was applied by Cook *et al.* (2014) to generate the glacier catchment outlines of the AP. Unfortunately, as these *glacier catchment outlines* still include rock outcrops and hence are not *glacier outlines*, additional corrections are needed. These outcrops can either be excluded manually or the glacier catchments can be intersected with an already existing rock outcrops dataset to separate them from glaciers (cf. Section 5.1), assuming all areas not being rock outcrops to be glacierized. Glacier-specific parameters can be calculated subsequently and statistically analyzed.

The process of determining ice thickness and ice volume per glacier (needed to estimate the SLE) is an additional working step applied for the present inventory. The previously used volume-area scaling to estimate the volume of glaciers (e.g. Erasov 1968 (in Radić and Hock (2010)); Bahr *et al.* 1997; Radić *et al.* 2007, 2008; Radić and Hock 2010) is not appropriate for the glaciers of the AP, as it does not account for individual glacier characteristics, or more precisely, their geometry (Huss and Farinotti 2012). The geometry of the glaciers on AP is distinct from ice caps of other regions, to which this approach is appropriately applied. However, a new approach was adapted to glaciers on the AP by Huss and Farinotti (2014) using a physically based method. It individually considers the characteristics of each glacier (Huss and Farinotti 2012, 2014). The resulting bedrock and ice thickness datasets are used to estimate mean thickness, ice volume, ice volume grounded below sea level and SLE per glacier (cf. Section 5.3.2).

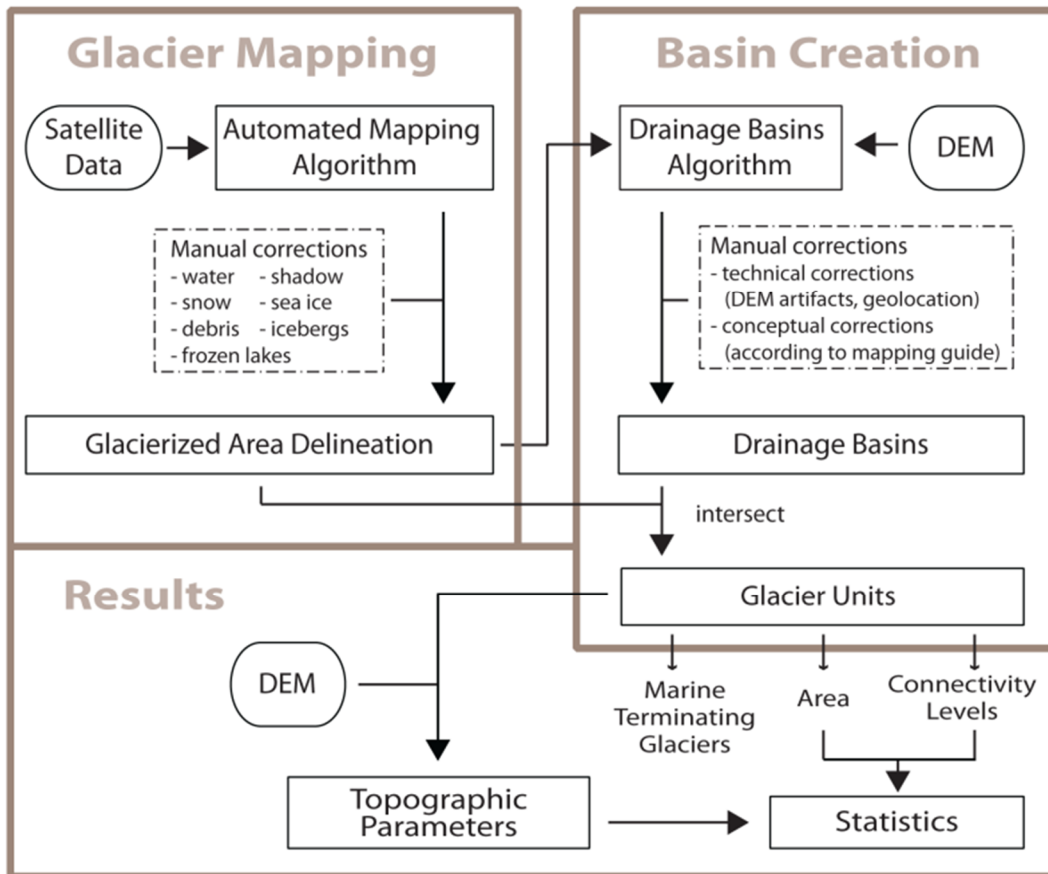


Figure 3.1. General workflow of the generation of a glacier inventory from Rastner *et al.* (2012) as done for the glaciers on Greenland. Based on Cook *et al.* (2014), the processing step *Glacier Mapping* has not been applied for the generation of a glacier inventory for the AP as explained in the text.

## 4 Reassessment

The reassessment of available inventory datasets of the AP is performed in two steps:

- (1) Qualitative description and comparison of the existing inventories of the AP glaciers, including an overview on the accessibility of the datasets
- (2) Examination of the suitability of the datasets based on (1) regarding their use as a basis for the generation of the inventory, resulting in a dataset selection

So far, there is no dataset available outlining all the glaciers on the AP in detail. The available datasets lack of different aspects needed for a complete glacier inventory and for the implementation into the GLIMS database (e.g. limitation in spatial scope and/or relevant data attributes). In addition, missing consistency in terms of definitions and methodologies for satellite data processing and glacier inventory generation does not allow simply merging the different datasets. Therefore, several recommendations and guidelines have been published by the GLIMS community to ensure some consistency of GLIMS database entries (Paul *et al.* 2009; Racoviteanu *et al.* 2009; Raup and Khalsa, 2010). Hence, the following reassessment, including the qualitative description and comparison as well as the suitability discussion of the individual datasets, is carried out with respect to these rules, guidelines and recommendations for the generation of a glacier inventory for the GLIMS database.

### 4.1 Inventory data currently existing

The following reassessment considers existing inventory datasets. For the purpose of this Master's thesis, requirements are defined for the datasets to control the amount of information and data for the reassessment. First, a spatial definition of the AP is introduced. The reassessment focuses on the AP north of 70°S, excluding islands not being close to the mainland such as the South Shetland Islands. Even though these islands belong to the same GLIMS regional center (Regional Center 18), for this work they are defined as Subantarctic Island (Cogley *et al.* 2010) and therefore not regarded as part of the AP. As the ice masses south of 70°S are classified as Antarctic ice sheet, these areas are not taken into consideration either (cf. Section 5.2). Second, the reassessment mainly focuses on datasets covering a large part of the AP (i.e. Graham Land), and not only small parts or single glaciers. Lastly, even though the final dataset will be a vector dataset of glacier outlines, point data about the glaciers on the AP are also considered in the reassessment.

Based on literature and database review, the reassessment is applied to the following datasets:

- Glacier data of the AP already existent in the GLIMS database
- Glacier catchment outlines of the AP from the Scientific Committee on Antarctic Research (SCAR) Antarctic Digital Database (ADD; ADD Consortium, 2012)
- Glacier catchment outlines of the AP from Cook *et al.* (2014)

## 4.2 Qualitative description and comparison

This section describes and compares the different already existing inventory datasets of the AP with respect to the suitability of a dataset for the processing and (re-)implementation into the GLIMS database. Hence, it focuses on a limited set of aspects of the datasets, which are crucial to determine their suitability, mainly on spatio-temporal coverage and availability of relevant parameters for individual glaciers. Hence, this description does not include all characteristics of the individual datasets. In terms of relevant parameters, the final inventory dataset will have to be accomplished with the following glacier parameters required by the GLIMS database as described in Paul *et al.* (2009): Identification (ID), coordinates, date, surface area, minimum, maximum, mean and median elevation as well as mean aspect and slope. The availability of additional attributes (e.g. the primary classification type, form and frontal characteristics, etc.) is not mandatory. However, if such additional useful information is available it should be included in the dataset. Hence, ideally these glacier parameters can be provided by an already existing dataset. In addition, the meta-information for clear identification of the dataset, including the acquisition dates of the satellite scenes used, is mandatory for the implementation of a dataset into a GLIMS database (Paul *et al.* 2009). As these meta-data can hardly be reconstructed, they have to be included in the dataset itself or, respectively, provided by the analyst.

The comparison of the relevant characteristics available in the attribute tables of all datasets discussed is summarized in Table 4.1.

### 4.2.1 Datasets of the Global Land Ice Measurements from Space database

The GLIMS database provides three datasets which are of relevance for this reassessment:

1. GLIMS glacier outlines (GLIMS and NSIDC 2005, updated 2015)
2. RGI version 5.0 glacier outlines (Arendt *et al.* 2015)
3. WGI point information (WGMS and NSIDC, 1999, updated 2012)

The outlines of GLIMS and the RGI (Figure 4.2), which are overlapping on James Ross Island but are not congruent, are available from the GLIMS Global Glacier Browser (<http://glims.org/maps/glims>). The extent of the currently existing GLIMS glacier outlines of the AP, shown in Figure 4.2 (yellow), illustrates that not all of the AP is covered by this dataset. The attribute table includes several parameters per individual glacier such as location, time stamp, primary classification length and width (incomplete) and so on. The 3D parameters as well as the glacier classification (form, type and front) of the glaciers are missing. The analysis of these outlines was carried out recently (2005 and 2011), however the as-of date for several outlines dates back several years or even decades. Therefore, these outlines are partly not representing the current state of glacier extent. For instance, the as-of date of the glacier outlines on and around Ross Island dates back to 1988. Since then the glacier recession, especially of those glaciers nourishing an ice shelf has been considerable. Also the Larsen B ice shelf, which almost entirely collapsed in 2002, is still included in this dataset. Figure 4.1 shows a close-up of the area around Ross Island. The Landsat Image Mosaic of Antarctica (LIMA; Bindshadler

*et al.* 2008; available for download at <http://lima.usgs.gov/>), consisting of Landsat-7 ETM<sup>+</sup> scenes from 2000-2002, is overlaid with the current GLIMS outlines illustrating the changed extent of these glaciers since 1988.

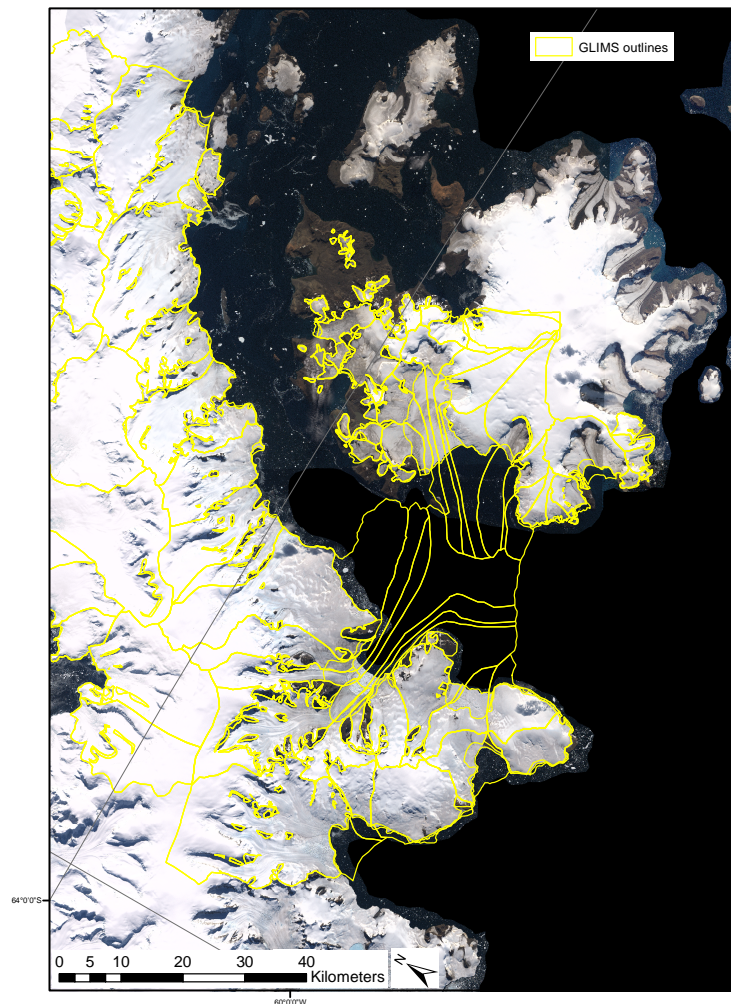


**Figure 4.1.** Difference between the GLIMS outlines of 1988 and the LIMA, illustrating the glacier change.

In general, the RGI does not provide the same richness in meta-data and source information as GLIMS does (Raup *et al.* 2013). The extent of the currently existing RGI (v5.0) glacier outlines of the AP, provided by Bliss *et al.* (2013), is shown in Figure 4.2. This inventory dataset excludes glacier on the mainland of the AP but also includes areas, which are not defined as being part of the AP for this work, such as the South Shetland Islands and Alexander Island. These areas are therefore not considered in the following description. Of the 851 glacier outlines, 232 glaciers are smaller than 0.05 km<sup>2</sup>. The attribute table includes parameters per individual glacier such as location, time stamp and area. Classification (type, form, front), 3D parameters, length and width are missing. Bliss *et al.* (2013) describe how they recorded feature type (glacier or ice cap), terminus characteristics (No significant calving, Terrestrial ("dry") calving, Marine calving, Lacustrine calving or Ice shelf), glacier type (Land- or lake-terminating, Marine-terminating, Lake-terminating, Shelf-terminating), volume estimates and so on. However, the classification of glacier type and form of Bliss *et al.* (2013) is not corresponding with the GLIMS/RGI classification system and therefore not included in the RGI dataset. Also here, the as-of dates lay back several years: About one third of the outlines

represents glacier extents between 1956 and 1990. The other outlines have an as-of date between 2000 and 2005. Furthermore, many islands (e.g. Ross Island, Joinville Island and surrounding islands) are represented as one glacier outline (Figure 4.2). Meaning, for those islands the division of individual glaciers based on drainage divides is missing.

Figure 4.3 illustrates the WGI point dataset (WGMS and NSIDC, 1999, updated 2012), which is also available from the GLIMS Global Glacier Browser (<http://glims.org/maps/glims>), including information about 816 glaciers of the AP. This dataset also includes areas not defined as AP, which are hence not included in the following description. Besides location, year of the photo, the nominal attributes glacier type, form, front and some additional classifications, time stamp, elevation (min., max., mean), total area, mean width, length (max.), orientation of accumulation and ablation area and so on are not available for the glaciers on the AP. In addition, the laying back of the available as-of years causes the inventory not to represent the current state of the glaciers of the AP.

#### **4.2.2 Glacier catchment outlines of Cook *et al.* (2014)**

The dataset of Cook *et al.* (2014), illustrated in Figure 4.4, consists of 1590 glacier catchment outlines of the AP with an area of 96 982 km<sup>2</sup>, covering the AP between 63°S-70°S. Islands smaller than 0.5 km<sup>2</sup> and ice shelves are excluded. However, the catchment outlines still include rock outcrops, which should be excluded in a glacier inventory. The glacier catchments are delineated automatically in ArcGIS applying hydrological tools based on the recently derived 100 m DEM of Cook *et al.* (2012). This is the common approach to divide contiguous ice mass into individual glaciers (Paul 2003; Rastner 2014). The ice velocity dataset of Rignot *et al.* (2011) was considered by Cook *et al.* (2014) to manually verify and adjust the side boundaries of glaciers. However, as the DEM does not include all islands around the AP, the coastline and some islands were digitized based on images between 2000 and 2002 of the Landsat Mosaic of Antarctica (LIMA; Bindschadler *et al.* 2008). Hence, for some islands, mainly in the southwestern part, the drainage divide analysis is missing. But the dataset ensures a consistent time period of all basins. It also includes several parameters per glacier such as location, time stamp, area, classification of type, form and front. The 3D parameters as well as length and width are missing. The definition of nominal parameters and category numbers conform to the GLIMS classification system as Cook *et al.* (2014) applied the GLIMS Classification Manual (Rau *et al.*, 2005) and the Glossary of Glacier Mass Balance (Cogley *et al.* 2011). The dataset provides some meta-information, but it is not complete. Furthermore, it has to be noted, this dataset is indeed available for download from the ADD (ADD Consortium, 2012), but does not include any of the above named attributes per glacier besides area and length. The dataset with the complete attribute table is not published and has been provided directly by Alison Cook for the purpose of this Master's thesis.

The close-up, combining and visualizing all the datasets described so far, reveals similarities and differences among the datasets regarding the location and delineation of the individual glaciers (Figure 4.5). For instance, in several cases one glacier/catchment outline of the RGI, GLIMS or Cook *et al.* (2014) includes several WGI points. Or for some outlines no WGI point is existent.

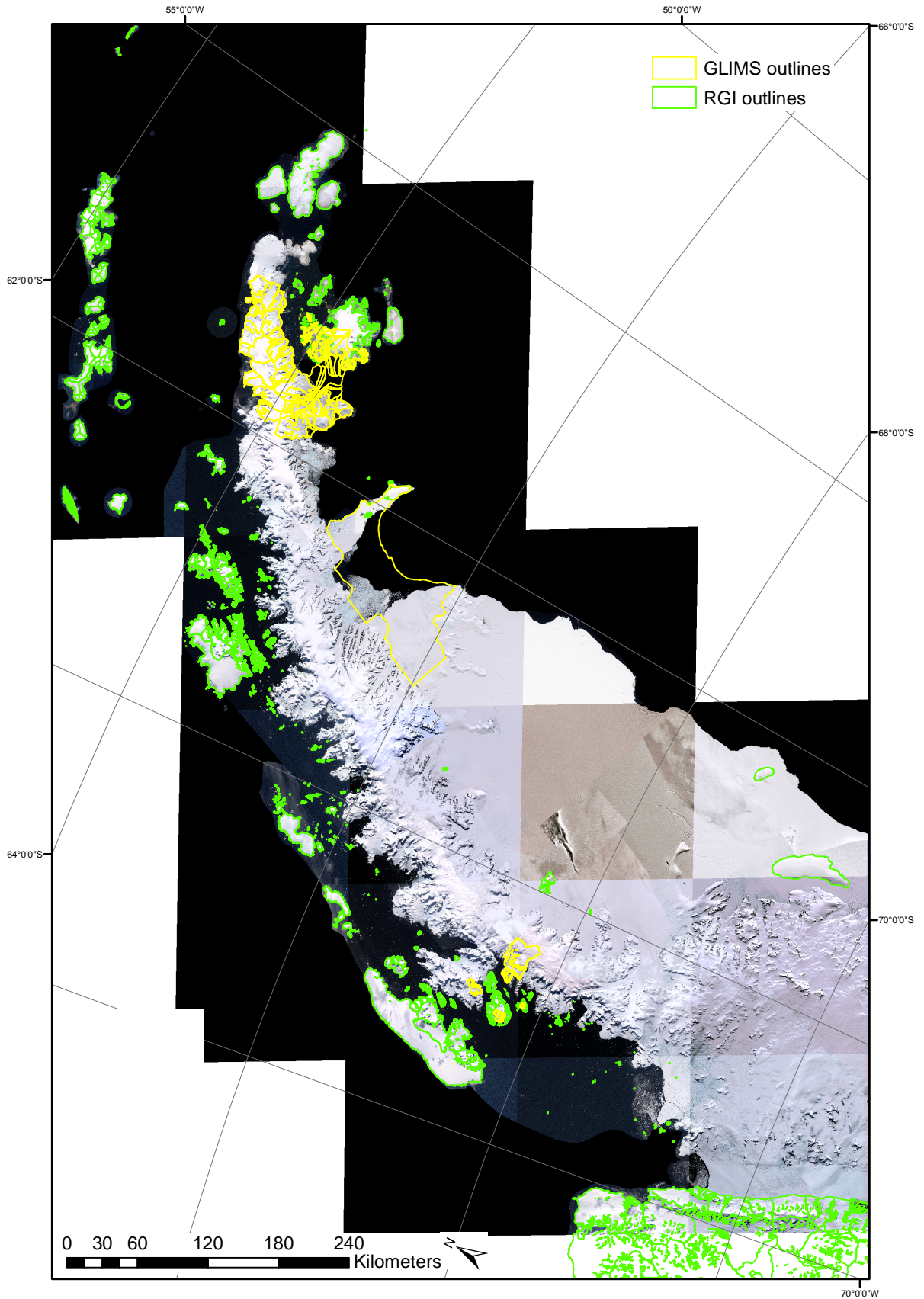


Figure 4.2. Existing GLIMS and RGI glacier outlines and the LIMA.

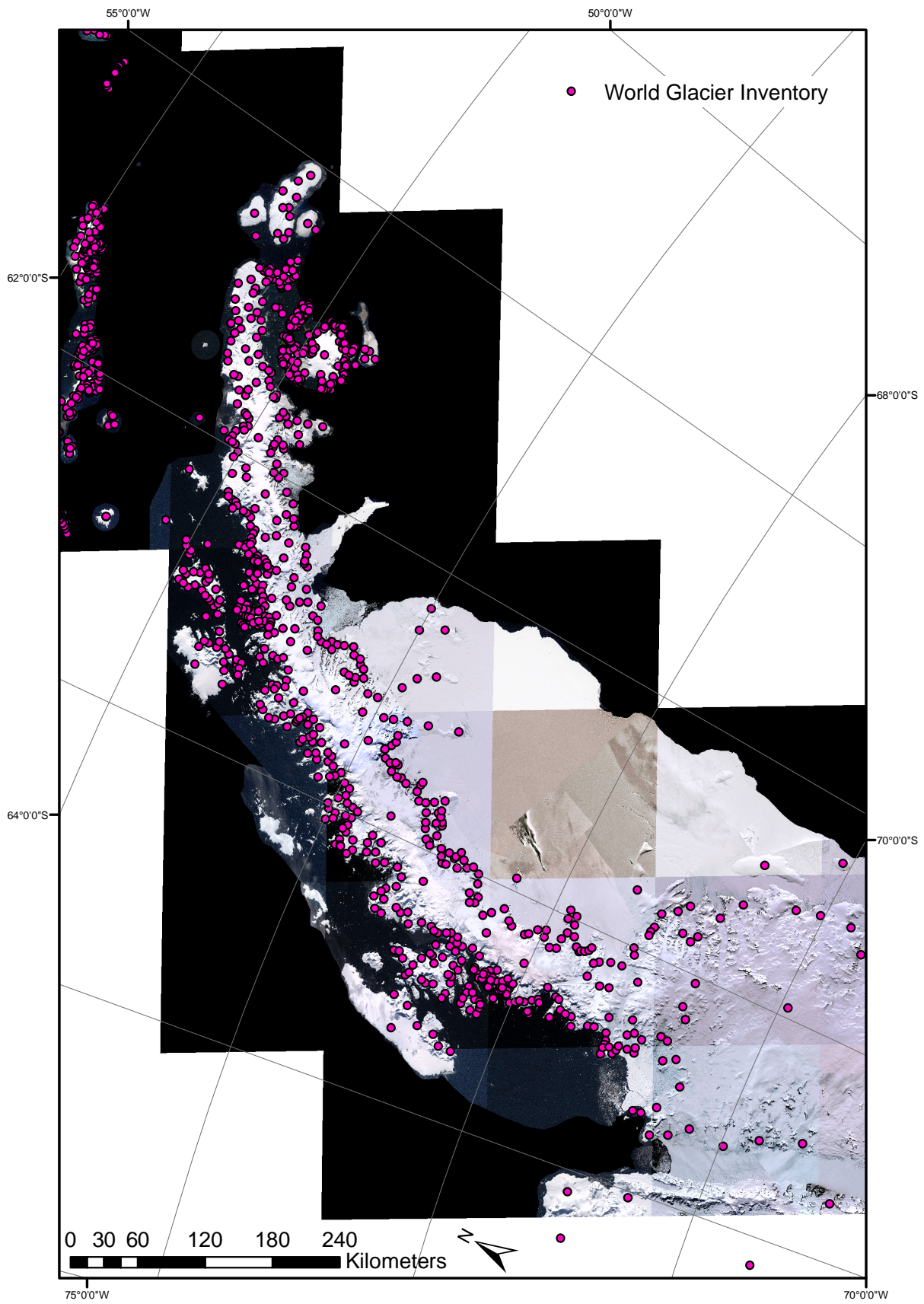


Figure 4.3. The WGI consisting of point information for the individual glaciers and the LIMA.



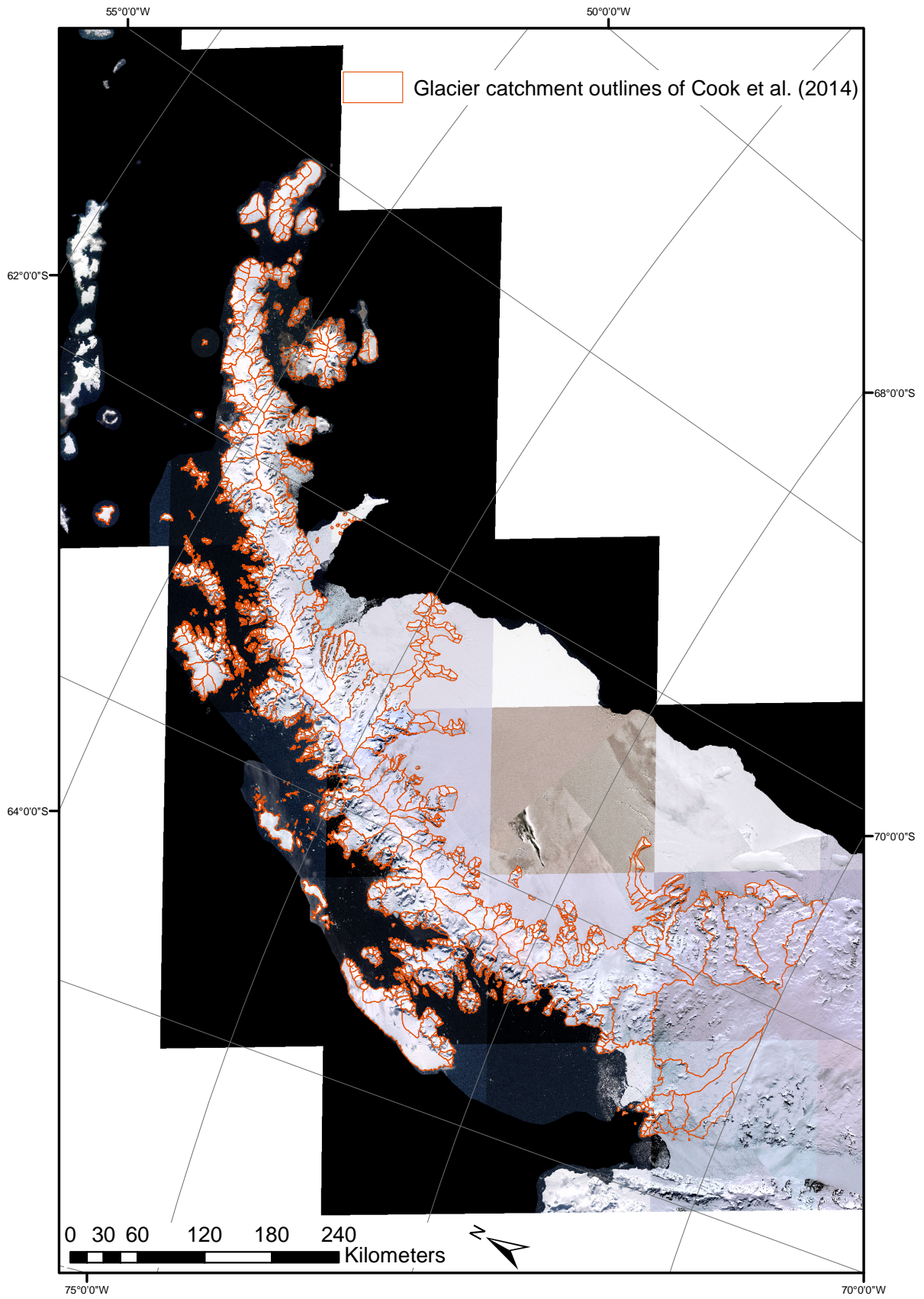


Figure 4.4. Glacier catchment outlines from Cook et al. (2014) and the LIMA.

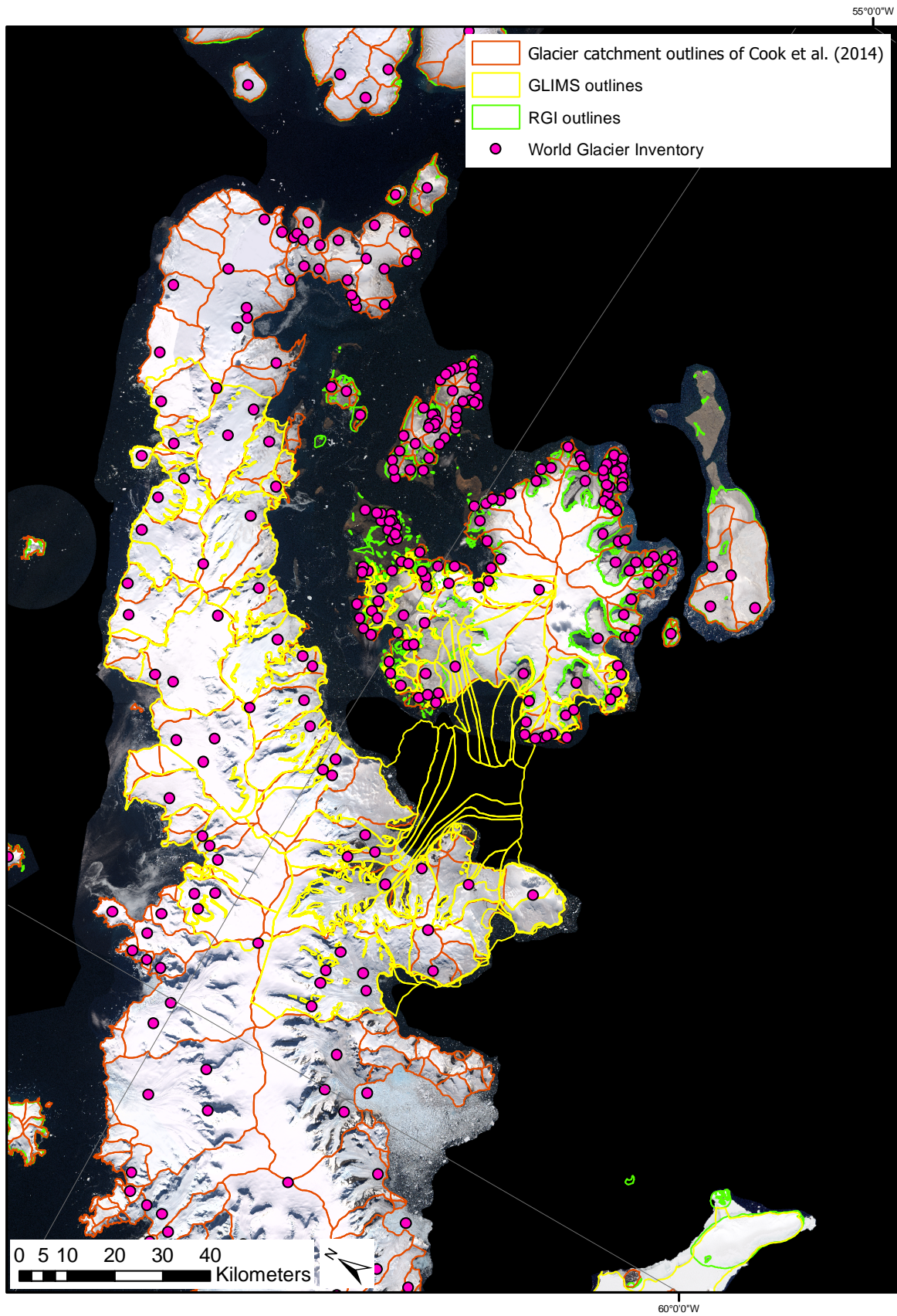


Figure 4.5. Close-up of all datasets considered so far.

### 4.2.3 Glacier catchment outlines from the Antarctic Digital Database

The SCAR ADD provides seamless topographic data for Antarctica to 60°S. Version 6 was released in 2012 and is updated regularly. The data is freely available for scientific and operational use through an easy to use web interface (<https://bas.ac.uk/project/add/>). The ADD provides a dataset of the AP, which merges the three following datasets (ADD Consortium, 2012):

1. A RGI file (Bliss *et al.* 2013), which covers most of the islands around Antarctica (see also Figure 4.2)
2. The glacier catchment outlines of Cook *et al.* (2014) of the northern part of the Peninsula (see also Figure 4.4)
3. An analysis of the catchments of the main Antarctic ice sheet and Palmer Land of Fretwell *et al.* (2013)

Figure 4.6 shows the area covered when merging the three datasets. The region covered by the Fretwell *et al.* (2013) dataset is not of relevance for the reassessment and generation of a glacier inventory of the AP, as the ice masses of this region are part of the Antarctic ice sheet as deliberated in Section 5.2. Therefore, this dataset is neither discussed nor is this region included in the glacier inventory.

According to Pfeffer *et al.* (2014), the ADD is an accurate source for investigations. With an area of 100 889 km<sup>2</sup> (excluding the dataset of Fretwell *et al.* (2013) and the Subantarctic Islands of the Bliss *et al.* (2013) dataset), this dataset covers the largest area of the AP (Table 4.1). The limitations of the RGI dataset are already described above. In addition, the combined dataset available for download from the ADD (ADD Consortium, 2012) only includes the glacier attributes glacier type, length and area, even though the original datasets of Bliss *et al.* (2013) and Cook *et al.* (2014) include more glacier attributes (Table 4.1). And what is more important, the dataset does not provide the mandatory meta-information.

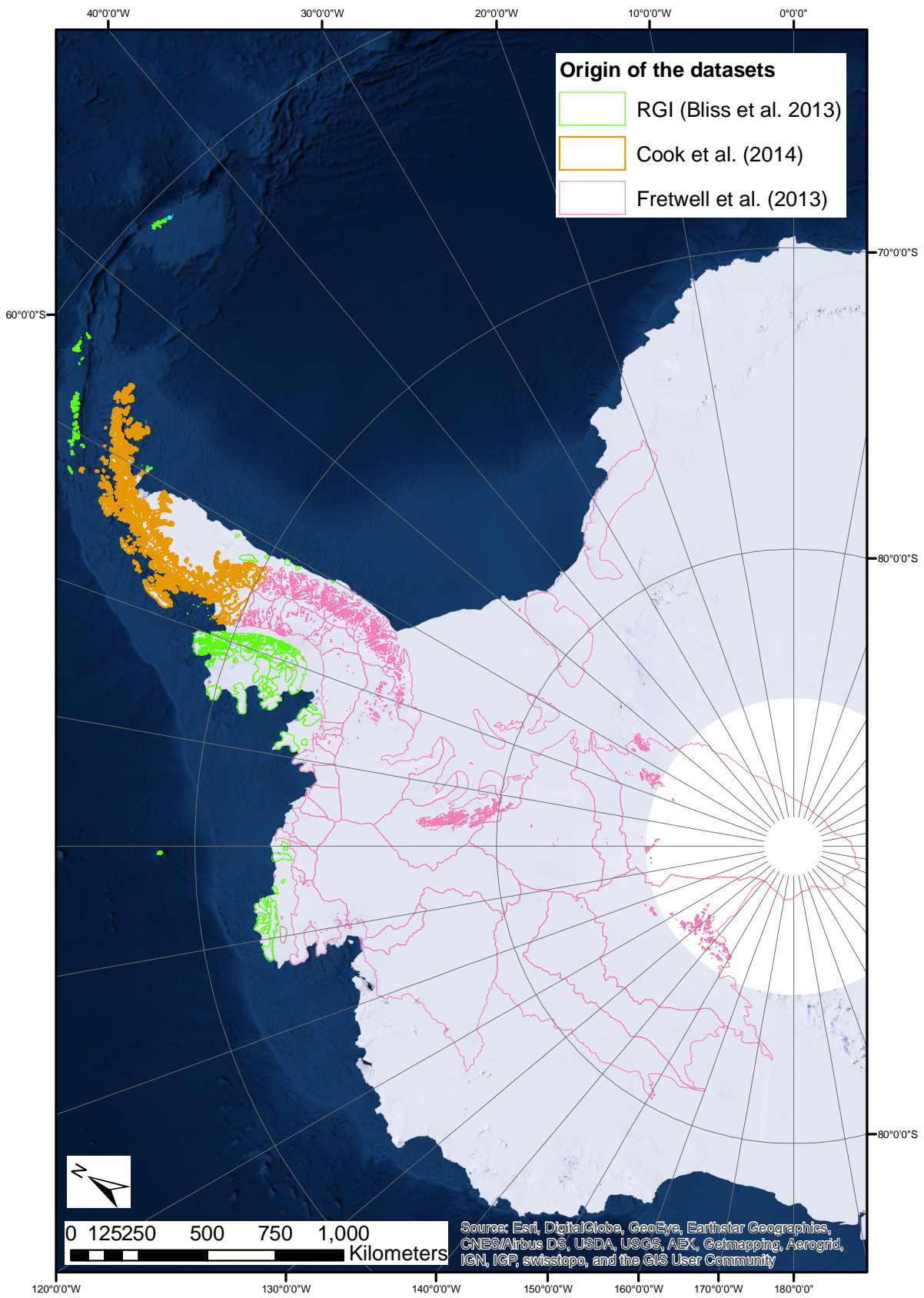


Figure 4.6. Overlay with the catchment outlines dataset of the Antarctic Digital Database (ADD).

Dataset characteristics	GLIMS	RGIV5.0	WGI	Cook <i>et al.</i> (2014)	ADD
Count	587	851	816	1590	1638
Vector outlines	Yes	Yes	No	Yes	Yes
Drainage divides	Yes	Mostly no	No	Mostly yes	Yes
Area covered	Mainland and James Ross Island (both partly)	Islands around AP <sup>1</sup>	Entire AP <sup>1</sup>	Entire AP	Entire AP <sup>1</sup>
Area [km <sup>2</sup> ]	26 450	15 961	Not available	96 983	100 089
Time stamp	Yes	Yes	Yes	Yes for 1274, no for 316 glaciers	No
Period (if available)	1988-2009	1956-2005	1957-2002	2000-2002	No
3D parameters (elevation, slope, aspect)	No	No	No	No	No
Length	Yes	No	No	No	Yes
Classification (type, form, front)	No	No	Yes	Yes	No
Source	ASTER and Landsat images	Mainly ADD Consortium (2000), Version 3.0	Aerial photographs	DEM of Cook <i>et al.</i> (2012), Landsat images	Bliss <i>et al.</i> (2013), Cook <i>et al.</i> (2014), Fretwell <i>et al.</i> (2013)
Accessibility	Free	Free	Free	Free only without complete attribute table	Free
References	GLIMS and NSIDC (2005, updated 2015)	Arendt <i>et al.</i> (2015) Bliss <i>et al.</i> (2013)	WGMS and NSIDC (1999, updated 2012)	ADD Consortium (2012); ADD Consortium; Cook <i>et al.</i> (2014)	ADD Consortium (2012)

Table 4.1. Comparison of existing glacier inventory datasets of the AP, regarding relevant characteristics to generate a complete glacier inventory of the AP.

<sup>1</sup> The RGIV5.0, WGI and the ADD also cover several islands, which are not defined as being part of the AP for this work, such as islands further north (e.g. the South Shetland Islands) and islands further south (e.g. Alexander Island). Hence, these areas are not taken into account in this compilation.

### 4.3 Suitability examination and data selection

Table 4.1 shows that the existing dataset of the WGI (WGMS and NSIDC, 1999, updated 2012) does not include any vector outlines and the vector datasets of GLIMS and the RGI cover the least areas of the AP. In addition, numerous glacier outlines are not up-to-date. Hence, a compilation of a new complete inventory for the AP using semi-automated glacier mapping techniques would be required. As explained in Section 3.2 this would include:

1. Glacier mapping by applying for example the recommended and well-established semi-automated band ratio (Paul *et al.* 2009) and manual corrections
2. Creation of drainage divides to separate glaciers from each other and manual corrections
3. Intersection of the glacierized area delineation with the drainage divides to obtain outlines of the individual glaciers

This workflow is very time-consuming for such a large and complex region as the AP: The first step would require extensive manual correction, mainly as a lot of ice on water exists around the AP which is difficult to distinguish from glacierized islands. In addition, to exclude ice shelves, further data would be needed (e.g. grounding line data). Also the second step is elaborate. Even though the drainage divides can be calculated automatically by a watershed algorithm (e.g. Bolch *et al.* 2010; Kienholz *et al.* 2013), adjustments are needed because an algorithm will divide the glacierized areas into a large number of individual divides that do not make sense (Rastner 2014). Laborious manual and to some part subjective merging of the vast number of separate small basins, which form one glacier, would be needed based on a set of rules to separate glacier-complexes (Rastner 2014). Hence, to do this for the entire AP would go beyond the scope of this Master's thesis. Fortunately, all glacier catchments are already included in the dataset of Cook *et al.* (2014), apart from a few peripheral islands, and existent in the composite dataset of the ADD (ADD Consortium, 2012). However, the enclosed attributes in the attribute table of the vector dataset available from the ADD is limited. The glacier parameters calculated by Bliss *et al.* (2013) and Cook *et al.* (2014) are not available in this dataset. Time-consuming and redundant self-elaboration or gathering and merging of the different attributes from different sources for each individual glacier would be required. Considering the relevant characteristics to determine a dataset's suitability (spatial coverage, being up-to-date and availability of relevant parameters for individual glaciers) as described in Section 4.2, the dataset of Cook *et al.* (2014) directly provided by A. Cook is the best suitable existing and available dataset to achieve the aim of this thesis. Besides the good spatial coverage of this dataset and the availability of relevant attributes for a GLIMS glacier inventory, another main advantage is that the criteria set out by GLIMS have been used for its compilation.

For additional qualitative assessment of the accuracy, drainage divides have been automatically derived as a reference based on the approach by Bolch *et al.* (2010), as done for the glaciers on Greenland by Rastner *et al.* (2012). As mentioned before, this watershed analysis gives a large number of separate basins with partially inappropriate divides (too small or too large divides) as shown in Figure 4.7 (blue). Especially the area close to the sea is separated in an inadequately large number of separate basins. Separation and merging of these outlines is not needed to be done here, as exclusively the general pattern and the main topographic divides are compared with the drainage basins of Cook *et al.* (2014) to assess their appropriateness. Comparing and

overlaying the output of the watershed analysis with the catchment outlines of Cook *et al.* (2014) shows that the general pattern and especially the main topographic divides along the mountain ridges of the AP are coincident (Figure 4.7). As a consequence, to generate the desired glacier inventory, the dataset of Cook *et al.* (2014) is further processed and analyzed as described in the following sections.

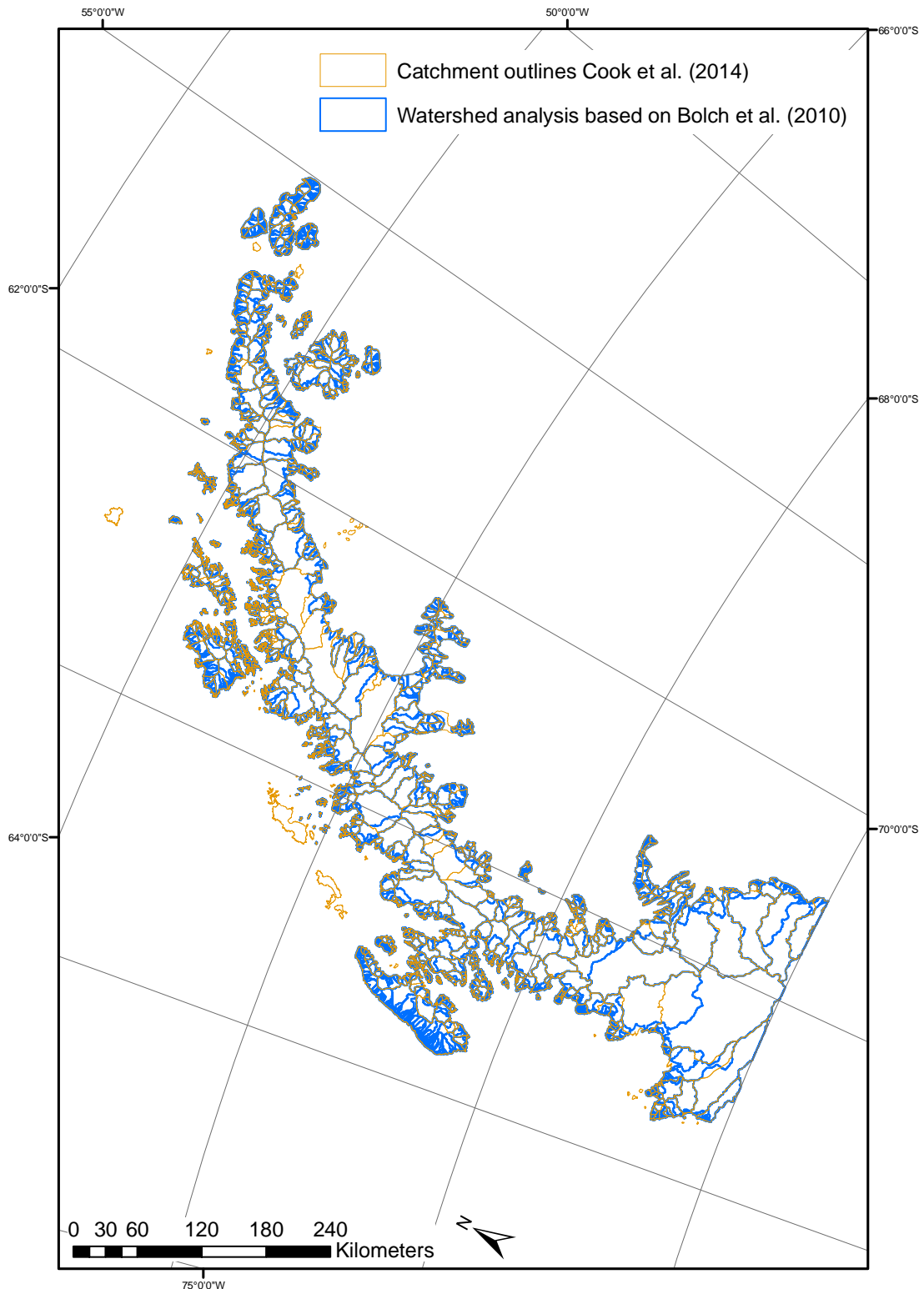


**Figure 4.7. Catchment outlines of Cook *et al.* (2014) vs. the basin delineation resulting from the watershed analysis based on Bolch *et al.* (2010). The general patterns of the two datasets are coincident.**





## 5 Methods applied

This chapter describes the specific methods applied to meet the research tasks described in Section 1.2. The following steps result from the outcome of the reassessment (Section 4). The already existing catchment outlines of Cook *et al.* (2014) are further processed (Section 5.1), the approach of separating the glaciers from the ice sheet is applied (Section 5.2) and the individual glacier parameters are derived (Section 5.3)

### 5.1 Excluding rock outcrops

The dataset of Cook *et al.* (2014) consists of 1590 glacier basins and hence not glacier outlines, meaning that rock outcrops are still included as if they were glacier covered. When generating an inventory based on the semi-automated band ratio method (Paul *et al.* 2009) such rock outcrops are mostly excluded. As this has not been done by Cook *et al.* (2014), these basins are intersected in ArcGIS with the detailed vector dataset of rock outcrop boundaries obtained from the ADD (ADD Consortium, 2012). The sources of the rock outcrops layer of the ADD are rather complex (a list of sources used in the ADD is available from <http://add.scar.org/manual/add3ch5.pdf>). The first rock outcrop data originate from the digitization of different maps with different accuracy and detail in the 1990s. Some areas have been updated by including Landsat imagery, but this update is not complete for the whole AP (Adrian J. Fox, British Antarctic Survey, written communication, 16.9.2015). The quality and possible improvements of the rock outcrop data are further discussed in Section 7.2.2. This rock outcrops dataset has already been used for instance by Bliss *et al.* (2013) to create the glacier inventory of glaciers of the Antarctic periphery. Rock outcrops can also be detected on the LIMA. The close-up of the very northern part of the AP (Trinity Peninsula and James Ross Island) exemplifies the rock outcrops layer (Figure 5.1). The LIMA is overlaid by the glacier basins of Cook *et al.* (2014) and the rock outcrops of the ADD. By excluding these rock outcrops from the catchment outlines of Cook *et al.* (2014) a vector layer of individual glaciers is generated, assuming that areas not identified as rock outcrops are ice covered.

Apart from removing the rock outcrops, no additional processing of this dataset has been done as the dataset of Cook *et al.* (2014) is generally in accordance with the procedures and guidelines for deriving GLIMS glacier information.

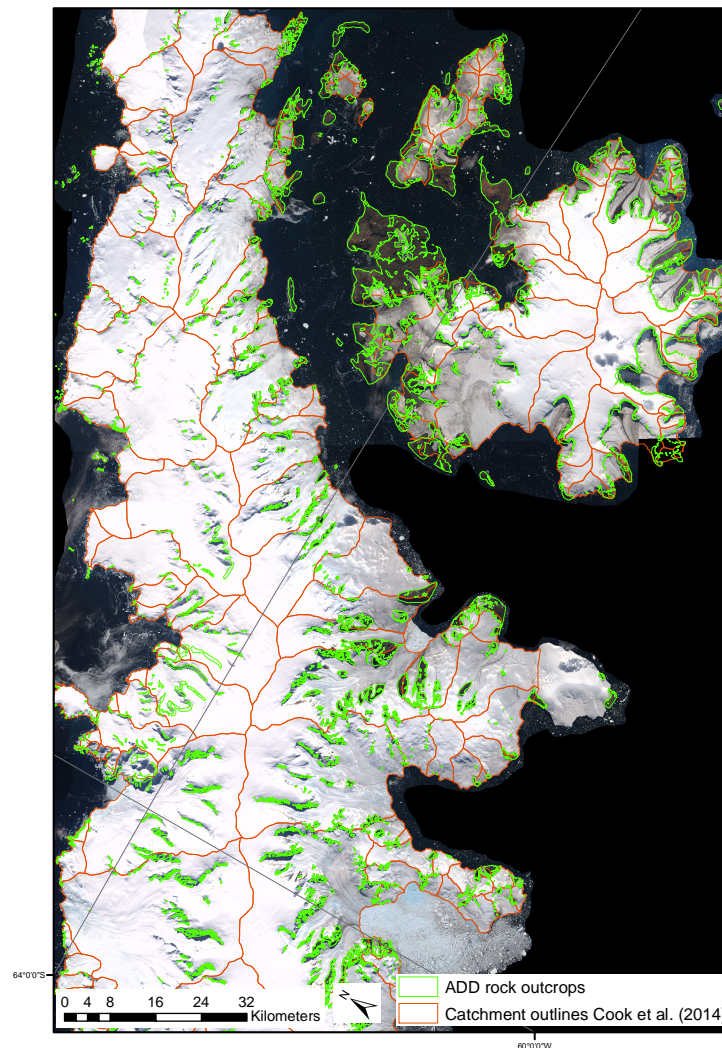


Figure 5.1. Close-up of the Trinity Peninsula and James Ross Island showing the rock outcrops which are excluded from the catchment outlines of Cook *et al.* (2014).

## 5.2 Assignment of connectivity levels

Glaciers connected with outlet glaciers of the ice sheet might experience a change in their flow behavior. Furthermore, the missing separation of ice sheet and glaciers leads to errors in estimating sea-level rise due to potential double counting (Rastner *et al.* 2012). Therefore, the concept of connectivity levels (CL) with a consistent automated classification method was introduced by Raster *et al.* (2012) for the glacier inventory of Greenland. The CL describe the connection of a glacier with the ice sheet. The assignment of three connectivity levels “*serve[s] the varying requirements of different communities (e.g. hydrological and glaciological modeling)*” Rastner *et al.* (2012: 1487). They defined the three CL as follows:

- CL0: no connection
- CL1: weak connection (clearly separable by drainage divides in the accumulation region, not connected or only in contact in the ablation region)
- CL2: strong connection (difficult to separate in the accumulation region and/or confluent flow in the ablation region)

The differentiation between CL1 and CL2 is based on the most recent Antarctic ice sheet drainage divides dataset provided by the Cryosphere Science Laboratory of NASA's Earth Sciences Divisions (Zwally *et al.* 2012) shown in Figure 5.2. This dataset defines 27 Antarctic drainage systems based on a 500 m resolution DEM derived from ICESat observations (cf. Zwally *et al.* 2012). Of the four systems defining the AP (systems 24 – 27), the systems 24 and 27 are connected to the East Antarctic ice sheet. Therefore, these glaciers would be assigned CL2. Rastner *et al.* (2012) suggested that the glaciers on Greenland with a strong connection to the Greenland ice sheet (CL2) should be regarded as part of the ice sheet. Accordingly, the CL2 glaciers of the AP are not included or further considered in the inventory introduced here. The assignment of the CL can be performed automatically within a GIS (cf. Rastner *et al.* 2012). However, the assignment of the CL0 and CL1 for the glaciers of the AP is rather straightforward and hence is made by hand: All glaciers on islands surrounding the AP are assigned CL0 and the glaciers on the mainland are assigned CL1.

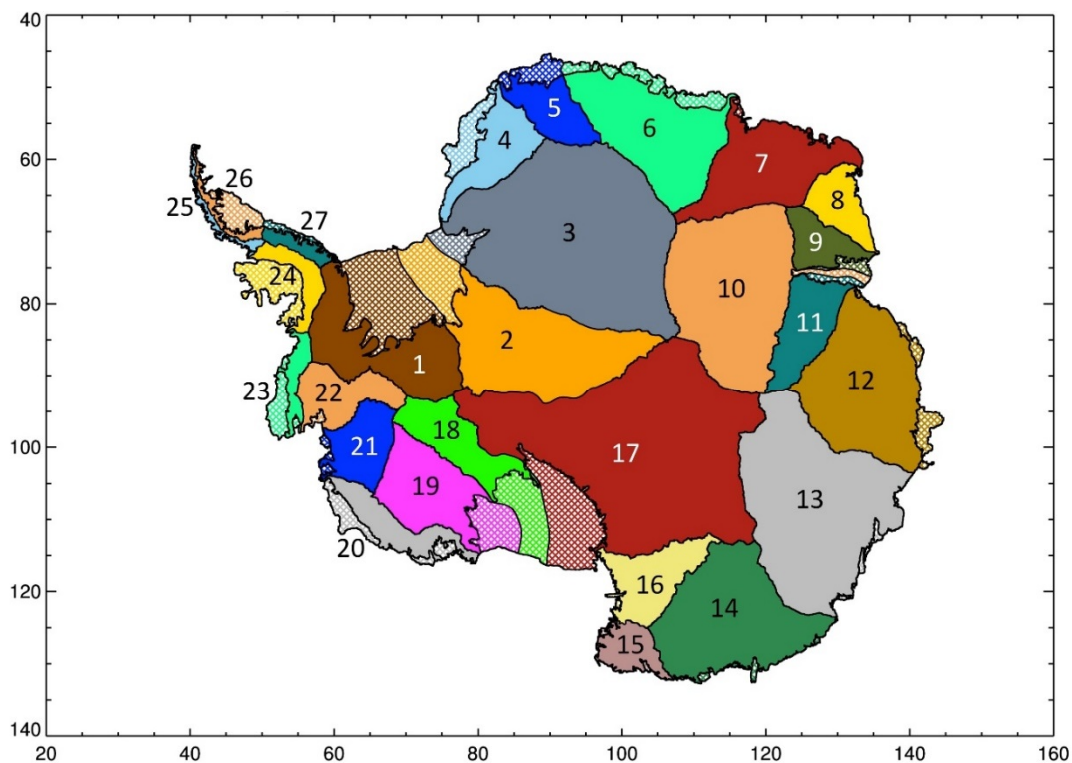


Figure 5.2. Antarctic drainage systems developed by the Goddard Ice Altimetry Group from ICESat data from Zwally *et al.* (2012). The numbers on Antarctica are the drainage system id's. The portions of the drainage systems within the MODIS grounding line are filled with solid color. The portions between the MODIS grounding line and the coastline are hatched.

### 5.3 Deriving glacier parameters

The final glacier inventory of the AP will be accompanied with several glacier parameters, which can be further analyzed (cf. Section 6), to determine the characteristics of this inventory. Furthermore, the inventory dataset is supplemented with information needed to accurately assess the impacts of climate change regionally and globally (Paul *et al.* 2009).

The calculations are conducted using GIS technology. Paul (2003) describes the advantages of this technique: It provides reproducible results, allows detecting geometry changes of the 2D glacier outlines in vector format and stores the glacier parameters in a relational database. In addition, by incorporating additional data, such as a DEM or ice thickness grids, and combining these with automated processing methods, further glacier-specific parameters can be calculated.

The derivation is divided in two sections, which are based on different datasets:

- (A) Using a digital elevation model (DEM) to derive the following set of topographic parameters guided by the recommendations for the compilation of a glacier inventory data from digital sources by Paul *et al.* (2009)
  - a. Area
  - b. Minimum, maximum, mean, median elevation
  - c. Mean slope
  - d. Mean aspect
  - e. Overall area-elevation distribution (hypsometry)
- (B) Using the bedrock and ice thickness datasets of Huss and Farinotti (2014) to extend the inventory with ice thickness, volume and SLE information

### 5.3.1 Topographic parameters

The processed dataset of Cook *et al.* (2014), meaning the two-dimensional glacier outlines (excluding the rock outcrops), is used to automatically calculate the two-dimensional parameter area for each glacier within ArcGIS. To calculate glacier-specific three-dimensional topographic parameters (minimum, maximum, mean, median elevation, mean slope and aspect) the glacier outlines dataset is digitally combined with a DEM and DEM-derived products such as slope and aspect (Paul *et al.* 2009). All parameters are derived using zone statistics (each glacier entity representing a zone) and are listed in the attribute table of the final inventory. In addition, the area-elevation distribution (hypsometry) for all glaciers on the AP is calculated in steps of 100 m by combining the glacier outlines with a DEM sliced into 100 m elevation bins. The DEM used and the calculations are shortly explained hereafter. All these parameters are calculated on the South Pole Lambert azimuthal equal area projection.

#### Digital elevation model

A 100 m resolution DEM of the AP (63 – 60°S) available from the National Snow and Ice Data Center (NSIDC; <http://nsidc.org/data/NSIDC-0516>) is provided by Cook *et al.* (2012) and shown in Figure 5.3. As the high-quality ASTER Global Digital Elevation Model (GDEM) still contains large errors and artifacts, Cook *et al.* (2012) developed a new correction method to create this DEM, which therefore is an improvement of the GDEM products (cf. Cook *et al.* 2012). Compared to former elevation data, such as the data acquired by ICESat, the original ASTER GDEM has a mean elevation difference of -13 m and an accuracy of  $\pm 97$  m (RMSE: root mean square error, a dimensional measure of scatter), whereas the new DEM has a mean elevation accuracy of -4 m ( $\pm 25$  m RMSE). However, the accuracies are reduced on mountain peaks and steep-sided slopes (Cook *et al.* 2012). In addition, small anomalies had to be removed, resulting in small inherent gaps along the coast and missing islands. Hence, the DEM

is spatially not perfectly congruent with the glacier outlines. Of the total 1588 glacier outlines, 48 do not have any elevation information. Therefore, the calculations including the DEM are applied only to 1540 glaciers, of which some only have partial elevation information. The problem is illustrated in Figure 5.4. The close-up of the region of Renaud and Biscoe Islands at the north-western coast of the AP exemplifies that some outlines do not have any elevation information, and others do have elevation information but not for the entire glacier extent.

To avoid ambiguity, unless otherwise stated, each time a DEM is addressed in the following, it refers to the DEM of Cook *et al.* (2012).

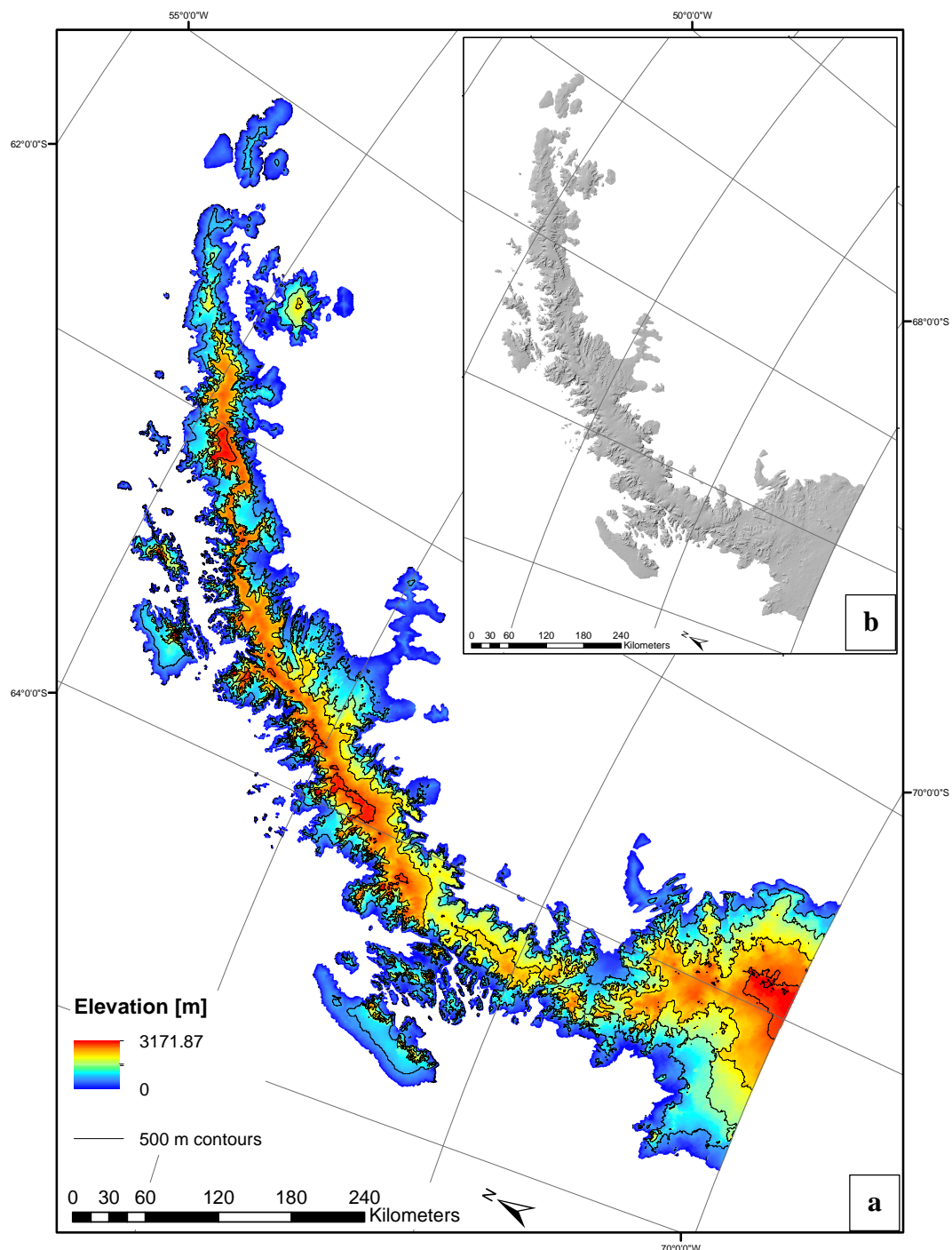


Figure 5.3. a) Color-coded visualization of the DEM provided by Cook *et al.* (2012) with 500 m contours and b) corresponding hillshade.

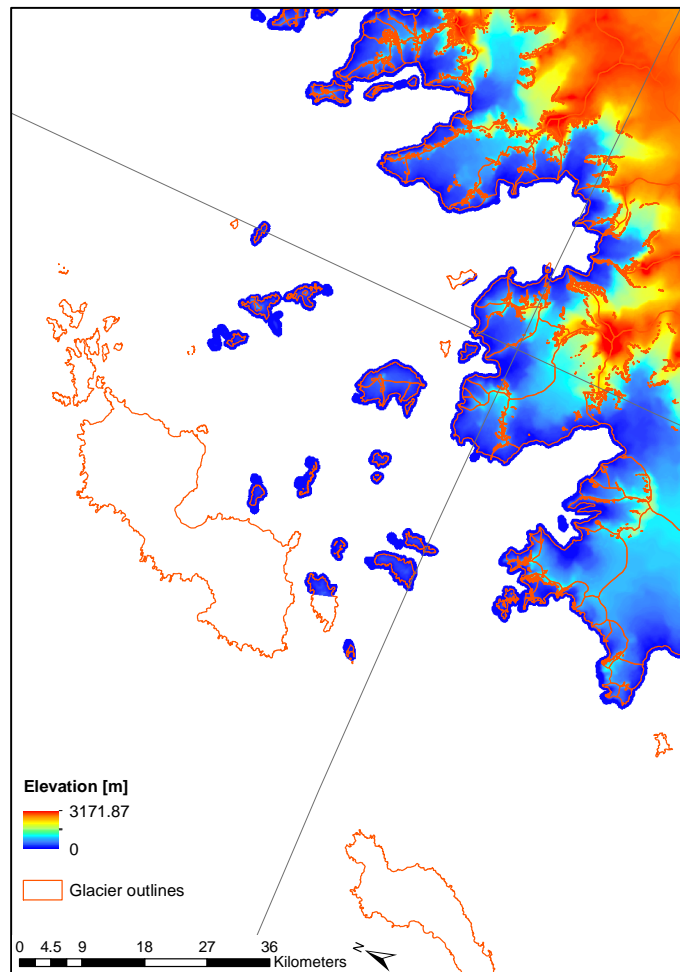


Figure 5.4. Digital elevation model of Cook *et al.* (2012) overlaid by the glacier outlines illustrating that for some glaciers the elevation information is partly or entirely missing. This region of the Renaud and Biscoe Islands is representative for other regions.

### Area

The glacier area is an important parameter for glacier change assessment and is easy to determine using the (horizontally projected) two-dimensional glacier outlines (Paul *et al.* 2009). The area of each individual polygon (glacier) is automatically calculated within ArcGIS using the *zonal statistics* tool and stored in the attribute table. As recommended by Paul *et al.* (2009) the values are stored in square kilometers with three digits after the decimal point. The glaciers are sorted into the same nine logarithmic size classes as the glaciers on Greenland (Table 5.1).

Value	1	2	3	4	5	6	7	8	9
Size Class [km <sup>2</sup> ]	-0.1	-0.5	-1.0	-5.0	-10.0	-50.0	-100.0	-500.0	>500

Table 5.1. Definition of the size classes and the corresponding values. Only the upper boundary value per size class is given.

### Elevation

Many parameters influencing the glacier mass balance are dependent on the elevation. In addition, elevation information helps understanding the general characteristics of a region's glaciers. By combining the DEM with the glacier outlines and applying the *zonal statistics* tool

the minimum, maximum and mean elevation is calculated for each glacier. The median elevation represents the elevation of the line dividing the glacier surface in half (Paul *et al.* 2009).

### Mean aspect (degree and sector)

Aspect is a glacier parameter necessary to approximate radiation impacts and valuable for modeling (Evans 2006). As the aspect values range from 0 – 360° the mean aspect cannot be determined by calculating the *zonal statistics* of the aspect grid. By doing so, for a glacier with expositions between 10° and 350°, the mean would be 180° instead of 0° (Paul 2003). Therefore, an aspect grid is generated in ArcGIS based on the DEM, of which a sine and cosine grid is calculated using the *raster calculator*. Then, the arctangent is calculated out of mean sine and the cosine values per glacier. The arctangent value allows calculating the correct mean aspect for each glacier after assigning the correct quadrant to the respective sine and cosine values. For the cardinal direction, the degree values are converted into the eight aspect sectors (Table 5.2) and stored in the attribute table (Paul 2003).

Grid Value	N	NE	E	SE	S	SW	W	NW
End of sector range [°]	22.5	67.5	112.5	157.5	202.5	247.5	292.5	337.5

Table 5.2. Aspect sectors and the corresponding conversion from 360°

### Mean slope

Slope can be used to approximate different parameters such as glacier thickness (Paterson 1994; Haeberli and Hoelzle 1995) and determines the climate-sensitivity of a glacier as it influences its response time (Oerlemans 2007). Therefore, it is recommended to include this topographic parameter in an inventory. The mean slope is determined by first generating a slope grid based on the DEM and the applying the *zonal statistics* tool to derive a mean slope value per glacier.

### Overall glacier hypsometry in 100 m bins

The areal distribution with elevation controls the glacier sensitivity to a rise in the Equilibrium Line Altitude (ELA). For instance, glaciers with a large, relatively flat accumulation area are more sensitive to a small increase in ELA than glaciers with a steeper accumulation area (Davies, 2014). Thus, this parameter provides essential information to improve the assessment of glacier response to climate change (Paul *et al.* 2009) by combining it with atmospheric data or model outputs (Pfeffer *et al.* 2014). The total area-elevation distribution (hypsometry) is calculated for the entire AP. First, the *extract by mask* tool has been used to extract the areas of the DEM being spatially congruent with the glacier outlines. Second, the resulting DEM is transformed from float to integer format using the *spatial analyst* tool. Third, the *reclassify* tool is used to create the 100 m elevation bins from the new integer DEM, by defining the intervals to be 100 m. A second glacier hypsometry is generated including the rock outcrops to show the effect of rock outcrops on the hypsometry. In addition, the area-elevation distribution is calculated for each of the sectors (NE, NW, SE and SW) to identify differences between the sectors. To compare different hypsometric curves, for instance with the curves of other regions or curves of single glaciers (cf. Section 7.1.3 and 7.1.5), the distribution of the normalized

glacierized area is calculated and plotted, by dividing the area of each elevation band by the total area represented by the corresponding curve.

### 5.3.2 Ice thickness, volume and sea level equivalent

Besides the thermal expansion of the ocean, glaciers are a major contributor to SLR. Therefore, global time series are needed to determine the contribution of glacier mass changes to SLR. However, the assessment of cumulative ice mass loss and the SLE of the IPCC (AR5) only include glaciers outside the mainland of Antarctica. Hence, the dataset introduced here provides mean ice thickness, volume and SLE values for the individual glaciers on the AP for more accurate future assessments.

As mentioned before, the often used volume-area scaling to estimate the volume of individual glaciers does not account for the distinct geometry of the glaciers on the AP (Huss and Farinotti 2012). In addition, the scaling approach does not provide any distributed ice thickness information, which is needed to model, for instance, future contributions to SLR (Huss and Farinotti 2012). A new approach by Huss and Farinotti (2012), which recently has been adapted for the AP (Huss and Farinotti 2014) counteracts this problem. Huss and Farinotti (2014) derived a bedrock and an ice thickness dataset on a 100 m grid (Figure 5.5a and b) based on surface topography and simple ice dynamic modeling. Compared to the ice bed, the surface and thickness dataset Bedmap2 of Fretwell *et al.* (2013) with a resolution of 1 km, the resolution of this dataset captures the rugged subglacial topography in great detail. The narrow and deep subglacial valleys, partially below sea level, and the high ice thickness variability are reflected much more accurately, which allows modeling of small-scale processes. Therefore, the bedrock and ice thickness dataset of Huss and Farinotti (2014) is used to compute mean thickness, total volume, volume grounded below sea level and SLE for each individual glacier of the inventory. As those datasets are based, *inter alia*, on the DEM of Cook *et al.* (2012) they are also not spatially congruent with the glacier outlines. Of the 1588 glacier outlines, the thickness, volume and SLE values can be determined only for 1539 glaciers of the inventory, of which some only have partial ice thickness and volume information. One glacier is only covered by one 100x100 m pixel of the DEM. This pixel does not have any bedrock/thickness information in the dataset of Huss and Farinotti (2014). Hence, 1540 glaciers have topographic information and only 1539 glaciers have thickness, volume and SLE information. These parameters are calculated on the WGS84 Antarctic Polar Stereographic projection.



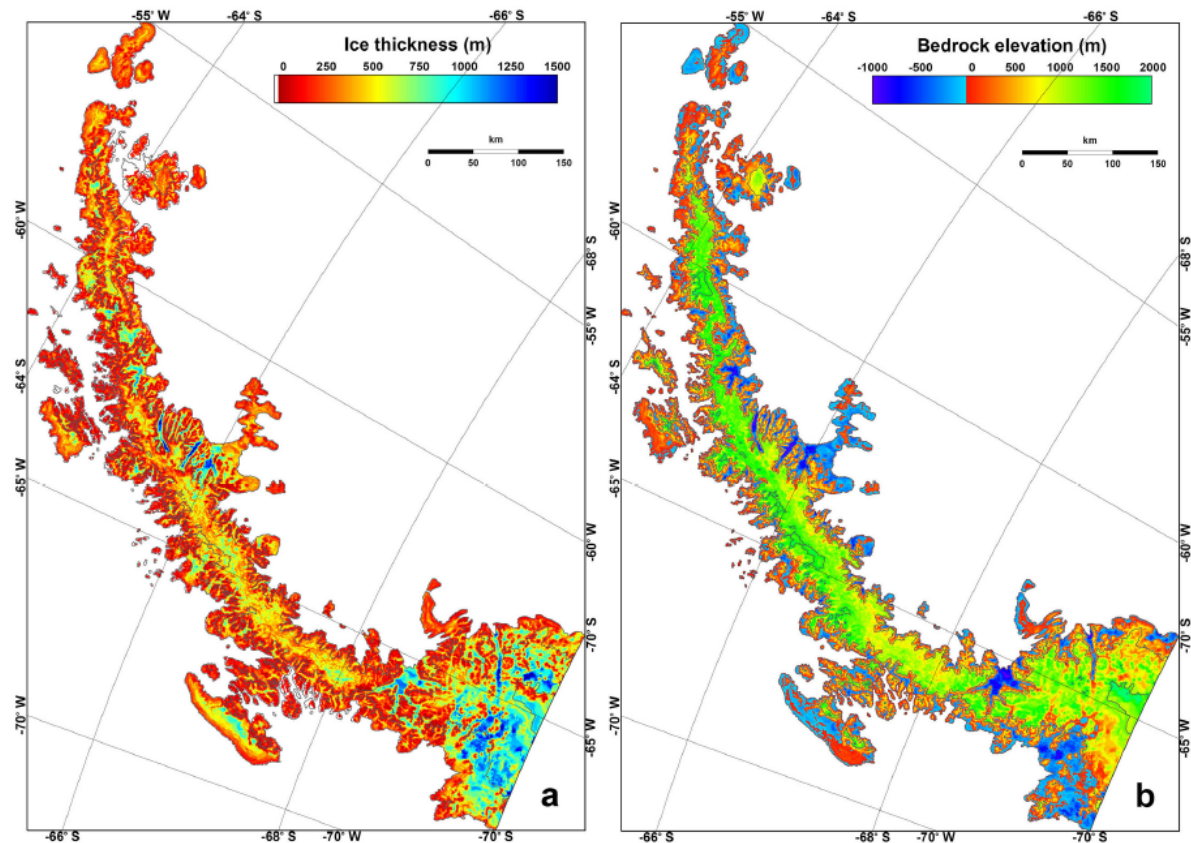


Figure 5.5. Modeled a) ice thickness and b) bedrock elevation of the AP from Huss and Farinotti (2014).

Mean thickness per glacier is determined by applying the *zonal statistics* tool to the thickness grid and the glacier outlines. A volume grid is calculated by multiplying the thickness grid (in meters) by 10 000 with the *raster calculator*. With this volume grid and the *zonal statistics* tool the total volume per glacier is determined. To estimate the volume grounded below sea level, first, the areas of the bedrock grid with negative values (areas below sea level) are extracted. This grid is converted to a vector dataset serving as layer to extract the volume values for the areas below sea level. The resulting grid represents the distribution of the volume grounded below sea level. Again the *zonal statistics* tool is used to determine the volume grounded below sea level for each glacier.

The SLE can be calculated by first multiplying the volume of ice by 0.9 (assuming a mean ice density of  $900 \text{ kg m}^{-3}$ ) to determine the corresponding volume of water. Dividing the volume of water by the ocean surface area ( $3.62 \times 10^8 \text{ km}^2$ ) gives the SL contribution of the volume in in m SLE, assuming all ice volume directly contributes to SL if melted. Nevertheless, the ice grounded below sea level has a negative (sea level lowering) effect as this volume will be replaced by water (with a higher density). This effect is considered in the presented SLE estimations. However, the mass of the ice grounded below sea level, which lies above the floatation level, still contributes to SLR (Fretwell *et al.* 2013). This and other effects, such as the cooling and dilution effect of ocean waters of floating ice (Jenkins and Holland 2007), are not taken into account here.



## 6 Results

After processing the dataset of Cook *et al.* (2014), as described in Section 5.1, the final inventory dataset covers the area between  $63^{\circ} - 70^{\circ}\text{S}$  and  $55^{\circ} - 70^{\circ}\text{W}$ , consists of 1588 glacier outlines in vector format and covers an area of  $94\,743\text{ km}^2$ . Rock outcrops, ice shelves and islands  $<0.05\text{ km}^2$  are excluded. The exclusion of the rock outcrops from the catchment outlines (Section 5.1) reduced the covered area by  $2239.7\text{ km}^2$  ( $96\,982.6\text{ km}^2$  to  $94\,742.9\text{ km}^2$ ). The smallest and largest glaciers have an area of  $0.06\text{ km}^2$  and  $7004.3\text{ km}^2$ , respectively.

This section presents some statistics of the glacier parameters in tabular and graphical form. The following parameter combinations and visualizations should help identifying glaciological characteristics of the glaciers of the AP. In Table 6.1 all parameters of the attribute table are listed. Several parameters, such as the nominal glacier parameters *primary classification*, *form* and *front*, and several meta-data about the satellite images used have been determined and provided by Cook *et al.* (2014). The others are the result of the methods described in Section 5.2 and 5.3. The AP is additionally divided into four sectors (NW, NE, SW and SE) to reveal latitude and exposition related differences among the glaciers on the AP. The division west/east is based on the main topographic divide, and north/south is based on the  $66^{\circ}\text{S}$  latitude.

Name	Item	Description
Name	Name	String, partially available
Satellite Image Date	SI_DATE	Date of the satellite image used for digitizing
Year	YEAR	Year the outline is representing
Satellite Image Type	SI_TYPE	Instrument name e.g. Landsat 7
Satellite Image ID	SI_ID	Original ID of image
Coordinates	lat, long	
Primary classification	class	cf. Appendix
Form	form	cf. Appendix
Front	front	cf. Appendix
Confidence	confidence	cf. Appendix
Mainland/island	mainl_Isl	cf. Appendix
Area	area	$\text{km}^2$ , cf. Section 5.3.1
Connectivity level	CL	cf. Section 5.2
Sector	sector	NW, NE, SW or SE
Size class	size_class	1 – 9, cf. Section 5.3.1
Minimum elevation	min_elev	m a.s.l., cf. Section 5.3.1
Maximum elevation	max_elevation	m a.s.l., cf. Section 5.3.1
Mean elevation	mean_elev	m a.s.l., cf. Section 5.3.1
Median elevation	med_elev	m a.s.l., cf. Section 5.3.1
Mean aspect in degree	mean_asp_d	$^{\circ}$ , cf. Section 5.3.1
Mean aspect nominal	mean_aspect	8 cardinal directions, cf. Section 5.3.1
Mean slope	mean_slope	$^{\circ}$ , cf. Section 5.3.1
Mean thickness	mean_thick	m, cf. Section 5.3.2
Total volume	tot_vol	$\text{km}^3$ , cf. Section 5.3.2
Mean volume	mean_vol	$\text{km}^3$ , cf. Section 5.3.2
Volume grounded below sea level	vol_below	$\text{km}^3$ , cf. Section 5.3.2
SLE	SLE	mm, cf. Section 5.3.2

**Table 6.1. Glacier parameters in the attribute table of the inventory of the AP.**

## 6.1 Area and size classes

Table 6.2 gives the total number, area and corresponding percentage of the nine size classes, into which the 1588 glaciers are divided. Figure 6.1 portrays the percentages per size class in terms of number and area. The mean area (59.7 km<sup>2</sup>) is considerably higher than the median area (8.2 km<sup>2</sup>), reflecting the areal dominance of the rather few larger glaciers as shown in Figure 6.1. Most of the glaciers can be found in size classes 4–6 (1.0–50 km<sup>2</sup>). These glaciers account for 75% of the total number but only for 14% of the total area. The glaciers larger than 100km<sup>2</sup> are representing most of the area (77%) with only 11% of the total number. With an area of 7004km<sup>2</sup> the Seller Glacier is the largest one, accounting for 7% of the total area and is twice as big as the second largest glacier (Mercator Ice Piedmont, 3483 km<sup>2</sup>).

Size class [km <sup>2</sup> ]	-0.1	-0.5	-1.0	-5	-10	-50	-100	-500	>500	Total
Count	3	26	65	510	258	436	113	148	29	1588
%	0.19	1.64	4.09	32.12	16.25	27.46	7.12	9.32	1.83	100
Area [km <sup>2</sup> ]	0.23	7.99	51.61	1389.81	1818.42	10295.15	8049.7	32362.59	40767.44	94742.93
%	0.0002	0.008	0.055	1.47	1.92	10.87	8.5	34.16	43.03	100
Mean Size	0.08	0.31	0.79	2.73	7.05	23.61	71.24	218.67	1405.77	59.66

Table 6.2. Statistics of all glaciers of the inventory and the nine size classes. In the top row size class only the upper limit of each class is listed.

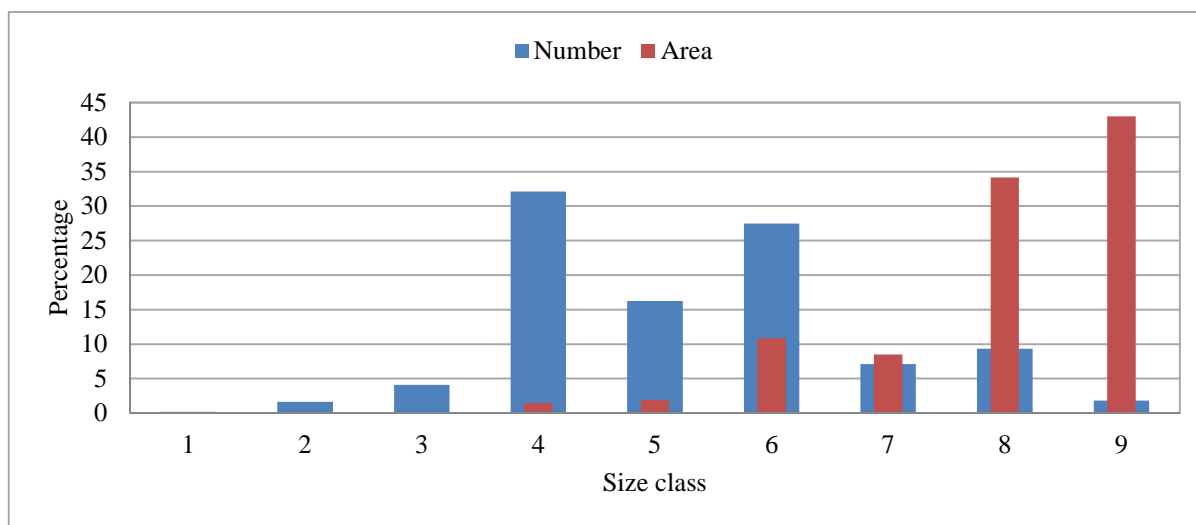


Figure 6.1. Percentage of glacier number (blue) and area (red) per size class. Values are given in Table 6.2.

## 6.2 Connectivity levels

Figure 6.2 illustrates the assigned connectivity levels CL0 and CL1 as a color-coded map. As explained in Section 5.2, the glaciers on islands are assigned CL0 (no connection) and the glaciers on the mainland are assigned CL1 (weak connection). As the glaciers further south are in connection with the ice sheet, they would be assigned CL2 (strong connection) and should be regarded as part of the ice sheet (Rastner *et al.* 2012). Hence, they are not included in this dataset. The 617 glaciers located on islands (CL0) cover an area of 14 240 km<sup>2</sup> representing 15% of the total glacierized area. The remaining 971 glaciers are located on the mainland (CL1) covering 80 503 km<sup>2</sup> and 85% of the total area

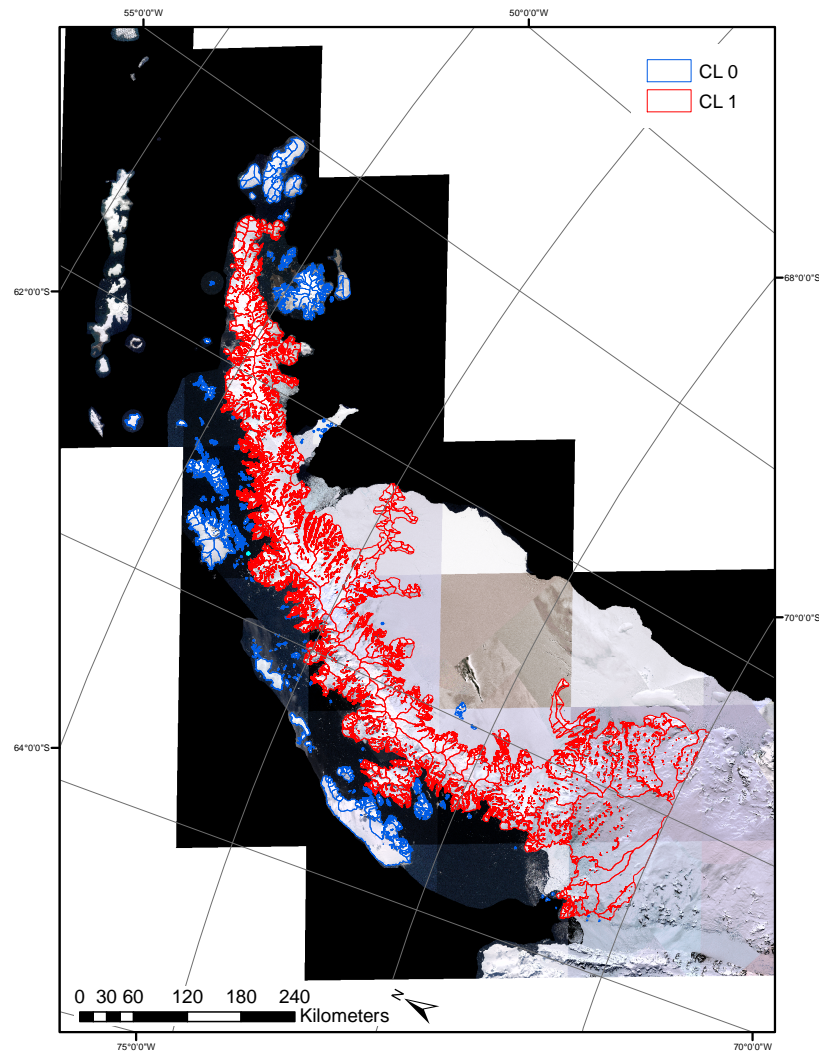


Figure 6.2. Assigned connectivity levels (color-coded) overlaid over the LIMA.

### 6.3 3D parameters

Figure 6.3a and b, plotting area against mean/median and area against minimum/maximum elevation, indicate that the mean, median and maximum elevation is increasing for larger glaciers. Three glaciers have a maximum elevation above 3100 m a.s.l., being 300 or more m higher than the others. The highest maximum elevation is 3158 m. Many glaciers have a minimum elevation of (close to) 0 m a.s.l. as most of the glaciers are marine-terminating glaciers. The average mean elevation of the 1540 glaciers involving elevation information is 406 m and the average median elevation is 390 m a.s.l. Figure 6.4, illustrating the spatial distribution of the median elevation as a color-coded visualization, reveals an increase of the median elevation from the coast and islands (0 – 500 m a.s.l.) to the interior of the AP (up to about 1800 m a.s.l.).

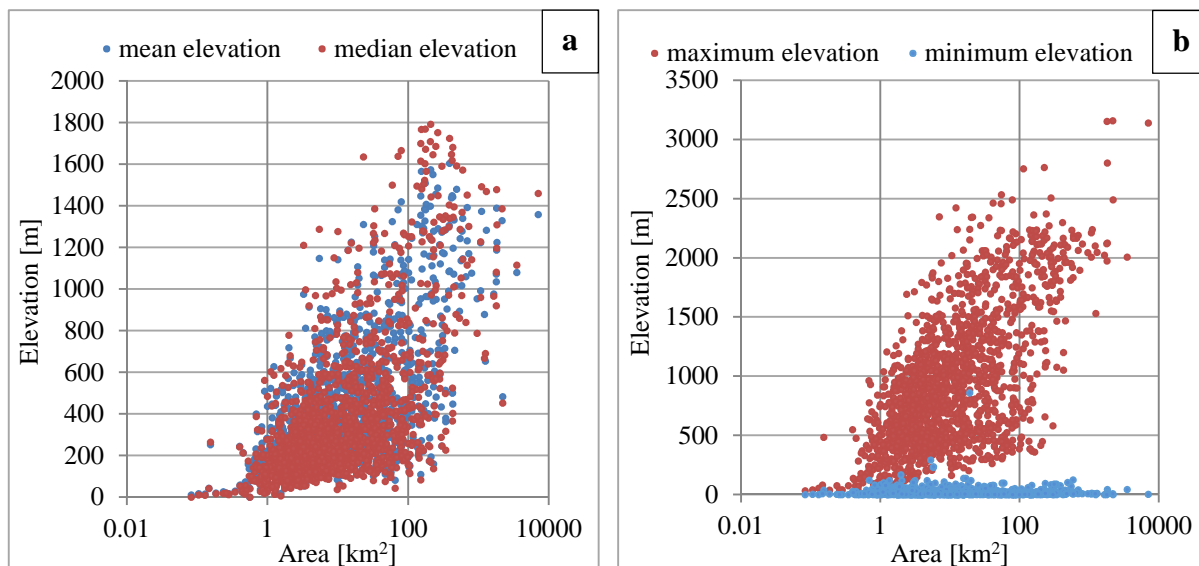


Figure 6.3. a) mean and median elevation vs. area and b) minimum and maximum elevation vs. area of the 1540 glaciers involving elevation information.

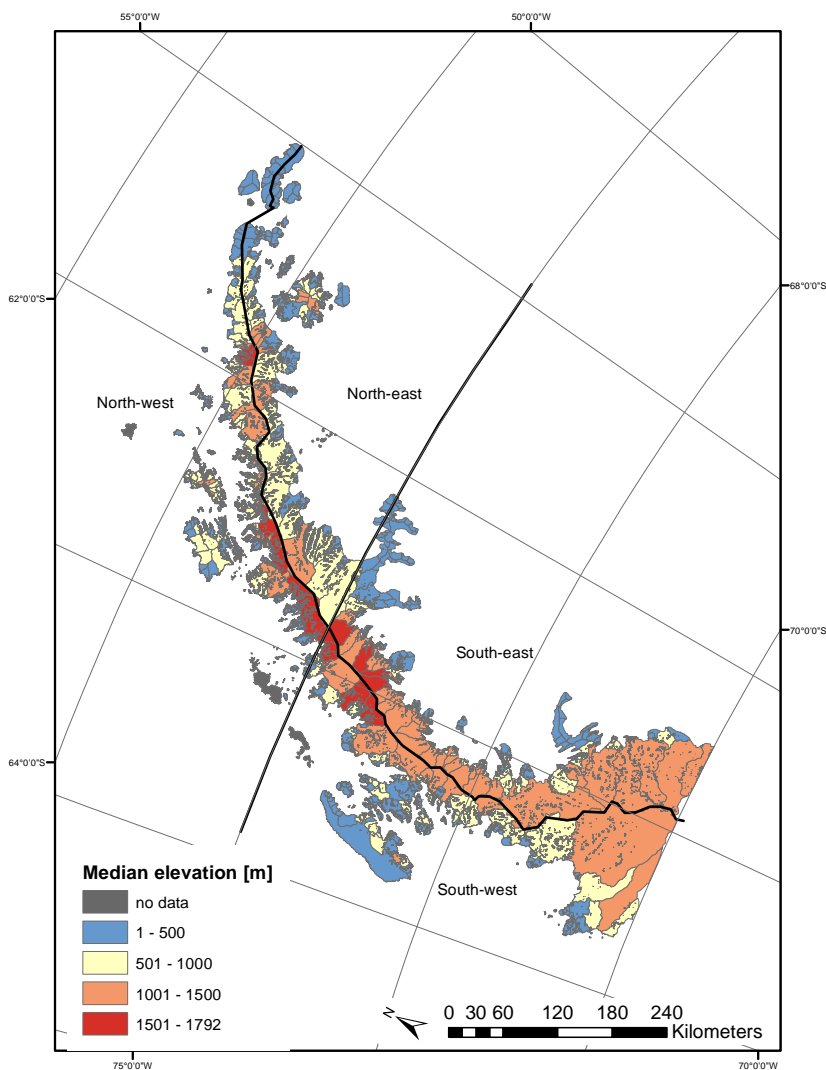


Figure 6.4. Color-coded glacier areas for visualization of the median elevation for 1540 glaciers.

Figure 6.5 shows the distribution of glacier number and area as percentages of the total for each aspect sector. The distribution is rather balanced and is not revealing any trends. Somewhat fewer glaciers and areas present aspects from south to south-east. The large value in the area of the south-western sector derives from the contribution of the largest glacier of the AP (Seller Glacier). Figure 6.6, plotting mean aspect against mean elevation, does not reveal any significant trends either. However, the highest mean elevation values are lower in the south-eastern sector.

The scatter plot of mean slope against area (Figure 6.7) reveals the dependence of mean slope on glacier size: the larger the glacier, the smaller the mean slope. Additionally, the scatter is smaller the larger the glacier, indicating that small glaciers exhibit a larger range of slope inclination.

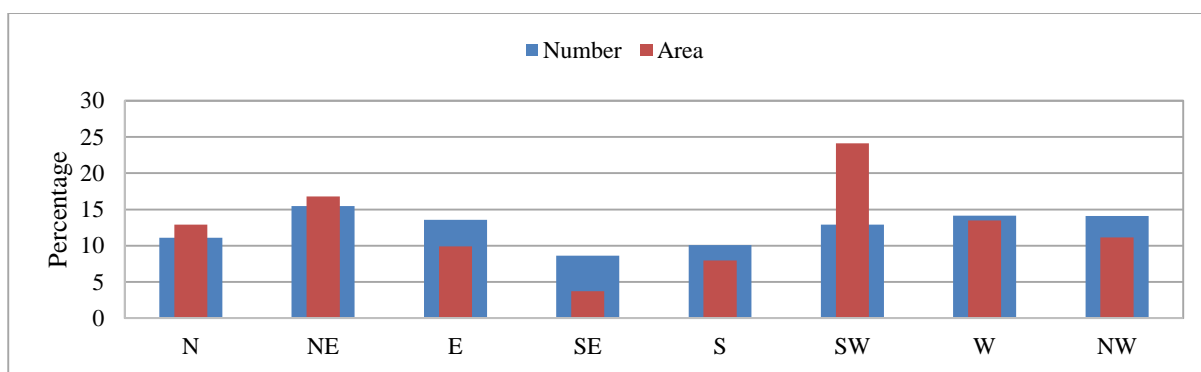


Figure 6.5. Percentage of glacier number (blue) and area (red) per aspect sector.

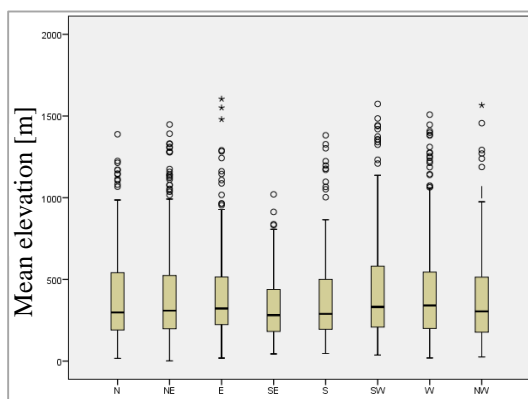


Figure 6.6. Mean glacier elevation vs. mean glacier aspect of 1540 glaciers.

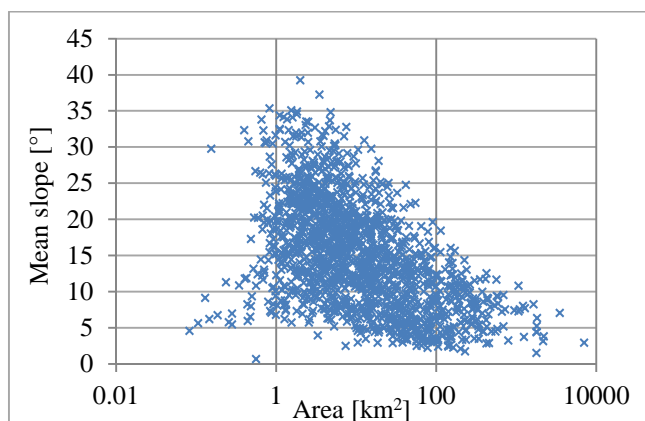


Figure 6.7. Mean glacier slope vs. glacier area of 1540 glaciers.

## 6.4 Glacier hypsometry

Figure 6.8 depicts the glacier hypsometry (area-altitude distribution) for (a) the entire AP as well as for (b) each sector, revealing a bimodal shape of the hypsometry. Figure 6.8a additionally displays the effect of excluding the rock outcrops as well as the hypsometry only for marine-terminating and ice shelf nourishing glaciers. Hence, excluding the rock outcrops does not change the general shape of the hypsometry. However, it slightly reduces the glacier cover below 1500 m a.s.l. with a maximum areal reduction at 200 – 600 m and 1000 – 1200 m a.s.l.. The total areal reduction amounts to 2239.7 km<sup>2</sup>. The creation of a hypsometry only for marine-terminating and ice shelf nourishing glaciers confirms that most of the glacierized area is covered by these two glacier types. Additionally, it demonstrates that these prevalent glacier types are extending over the entire elevation range. Hence, this bimodal shape of the glacier hypsometry does not arise from different glacier (types) at lower and higher elevations. It is rather determined by and reflects the topography of the AP: The low-sloping and low-lying coast regions covered by ice streams account for the maximum of the glacierized area at about 200 – 500 m a.s.l.. The glacierized plateau region accounts for a secondary maximum at about 1500 – 1900 m a.s.l.. The steep valley walls connecting the plateau with the coastal region cause the minimum at about 800 – 1400 m a.s.l.. In addition, the hypsometry reveals that 6000 km<sup>2</sup> of the 93 250 km<sup>2</sup> glacierized area covered by the DEM are found in the lowest elevation band (0 – 100 m). These areas are in direct or in close contact with water or ice shelves, which is crucial regarding the sensitivity on changes of the ice shelves and ocean temperatures, respectively (cf. Section 7.1.2). Additionally, it has to be noted that the area in the lowest elevation band, and therefore in contact with water or ice shelves, is expected to be somewhat higher as the DEM has several gaps along the coast.

The hypsometry per sector (Figure 6.8b; all exclusive rock outcrops), the glacier number and the glacier cover per sector (Table 6.3) show that the largest ice-covered areas can be found in the southerly sectors and most of the glaciers are found in the northerly sectors. Both maxima of the hypsometric curve are reduced for the northerly sectors compared to the southerly sectors. The elevation of the maxima is about the same for NW, NE and SW, whereas both maxima of the SE sector are somewhat lower. The glacier cover per sector reflects the bedrock topography of each sector (cf. Figure 5.5a). The bedrock of the northern sectors has less area in the high plateau regions and therefore, most of the glacierized areas are at lower elevations. The southern sectors have a more dominant plateau region favoring more glacierized areas at higher elevations. However, the north-eastern sector has the largest fraction of area in the lowest 100 m and therefore in direct or in close water or ice shelf contact.



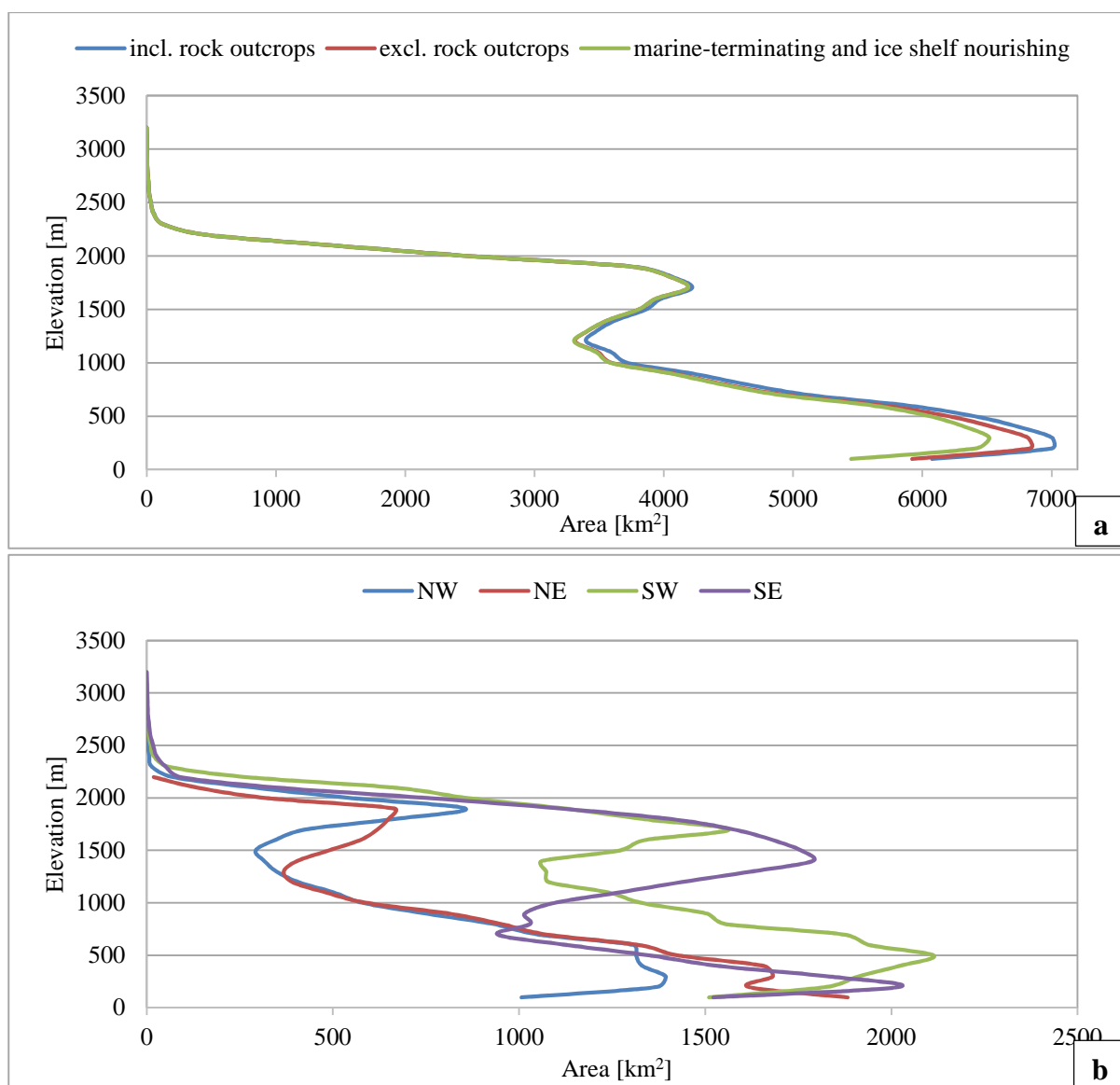


Figure 6.8. Glacier hypsometry of 1540 glaciers of the AP. a) Total areal distribution (blue), the areal distribution without rock outcrops (red) and areal distribution for marine-terminating and ice shelf nourishing glaciers (green). b) Areal distribution of the glacier cover per sector.

Sector	Count	Area [km <sup>2</sup> ]	Count [%]	Area [%]
NW	703	16864.67	44.3	17.8
NE	246	18296.75	15.5	19.3
SW	378	30984.51	23.8	32.7
SE	261	28597	16.4	30.2
<b>Total</b>	<b>1588</b>	<b>94742.93</b>	<b>100</b>	<b>100</b>

Table 6.3. Total glacier number and area as well as the percentage per sector.

## 6.5 Thickness, volume and sea level equivalent

The average mean thickness of all 1539 glaciers involving thickness information is 237 m. The Eureka glacier, located in the south, has the largest mean thickness with 853 m. The dependence of mean thickness on area and slope, indicating that the steeper/smaller the glacier, the thinner

the ice (Figure 6.9), is not surprising, as the thickness is neither entirely observed nor measured but modeled based on, inter alia, surface topography (Huss and Farinotti 2012, 2014). However, low-sloping glaciers reveal a large range of mean thicknesses. As visible in Figure 6.10, the large but low-sloping glaciers of the high plateau and in the very south towards the Antarctic ice sheet construct a cluster of glaciers with higher mean thicknesses. The mean thicknesses per sector and per mean aspect (Figure 6.11 a and b) do not reveal any significant spatial patterns.

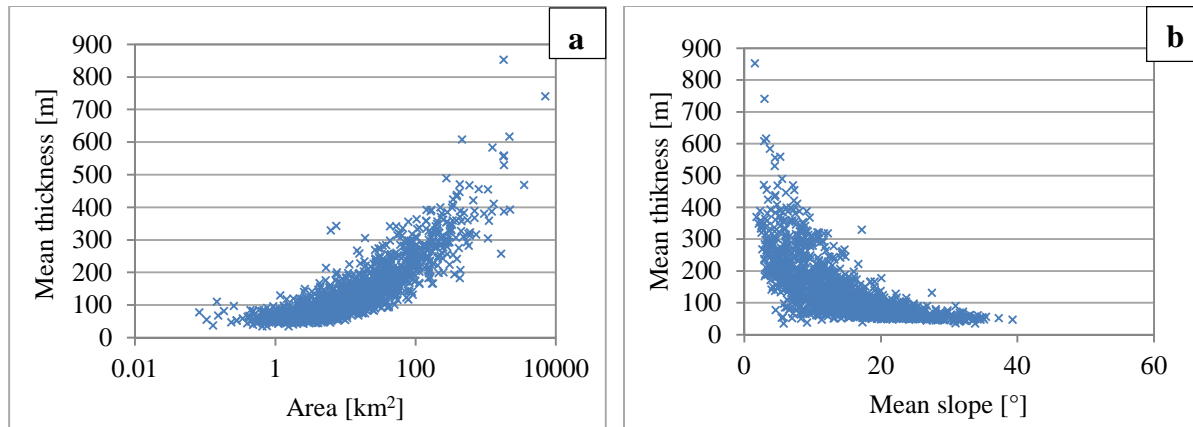


Figure 6.9. Scatter plot of the 1539 glaciers involving thickness information. a) mean thickness vs. area and b) mean thickness vs. mean slope.

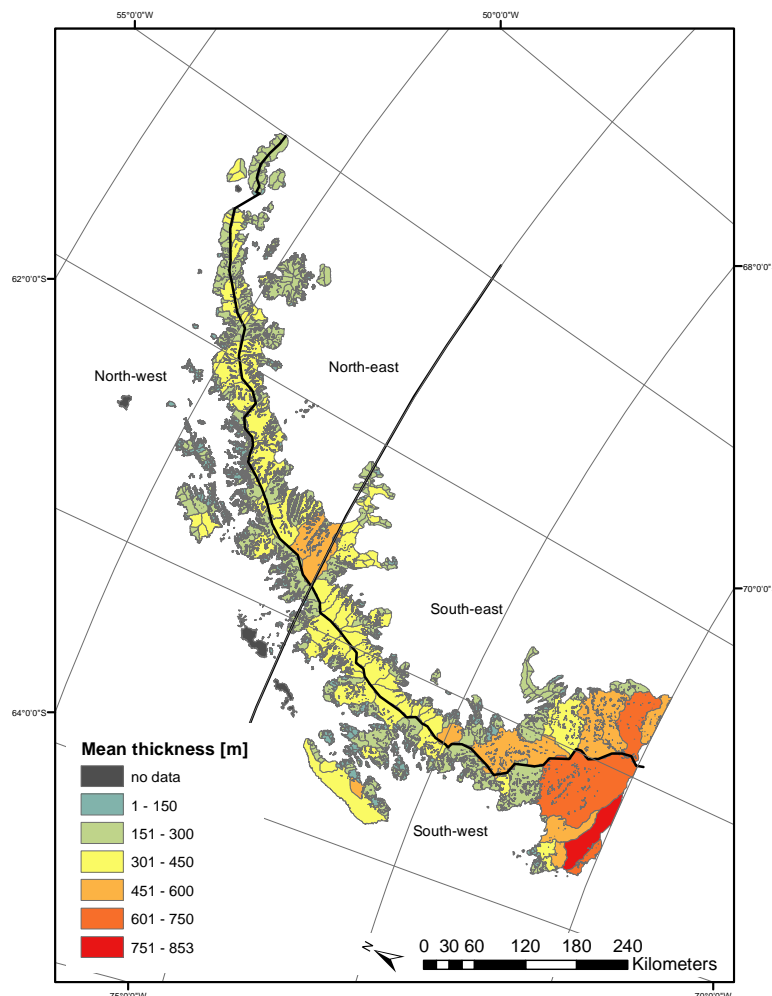


Figure 6.10. Color-coded glacier areas for visualization of mean glacier thickness.

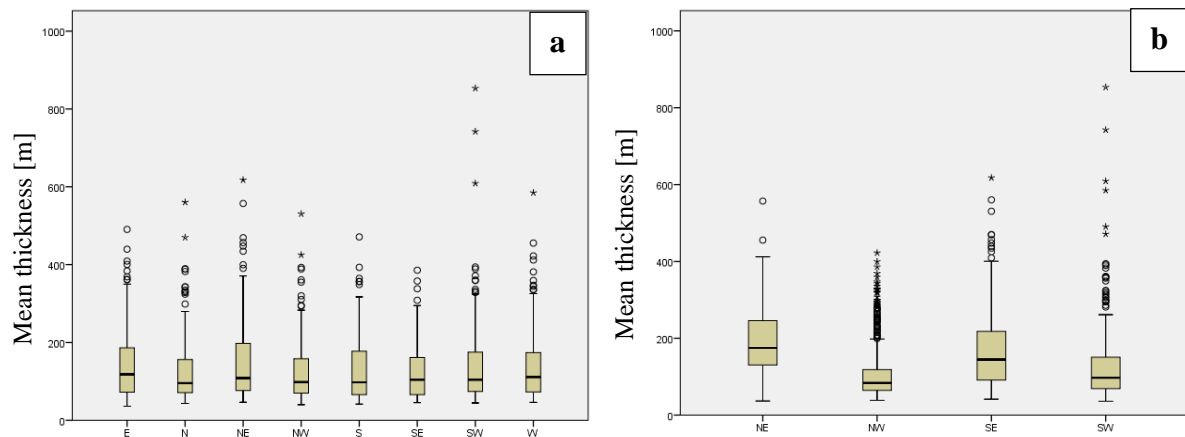


Figure 6.11. Boxplots of a) mean thickness per mean aspect and b) mean thickness per sector.

The total ice volume of the AP is  $34\,650\text{ km}^3$ . As the volume is calculated based on the thickness dataset, the volume distribution is basically a reflection of the thickness distribution. Figure 6.12 and Table 6.4, showing the total volume per sector, exhibit that most of the ice volume can be found in the south-west and south-east sector (38.6% and 32% of the total volume). This is not surprising as these two sectors make up 63% of the total glacier covered area. Regarding the total glacier volume per total glacier area for every individual glacier, visualized in Figure 6.13, the highest values are nevertheless prevalent in the very south of the AP, adjacent to the ice masses regarded as being part of the Antarctic ice sheet.

Figure 6.14 visualizes the areas of the bedrock below sea level, revealing numerous, partly very pronounced valleys below sea level especially in the north-eastern sector. As a consequence, about one third of the total volume is grounded below sea level (Table 6.4), which has a negative effect on SLR. Even about 50% of the volume of the north-eastern sector is grounded below sea level (Figure 6.15). Nevertheless, this negative effect on SLR is very small. Therefore, the southern sectors, holding most of the volume and hence revealing a SLE of 32 and 26.8 mm, contribute most to SLR. All in all, these calculations reveal that the glaciers of the AP could potentially raise the global sea level by 83.2 mm.

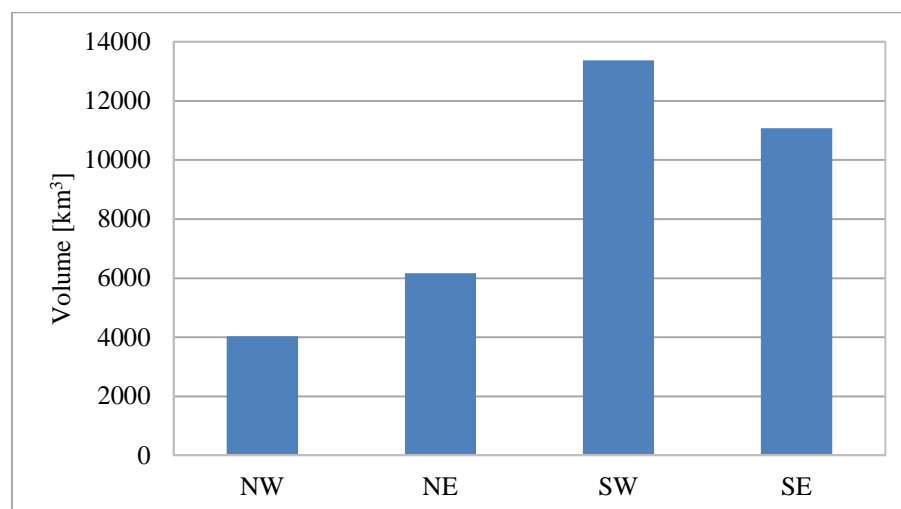


Figure 6.12. Total ice volume per sector.

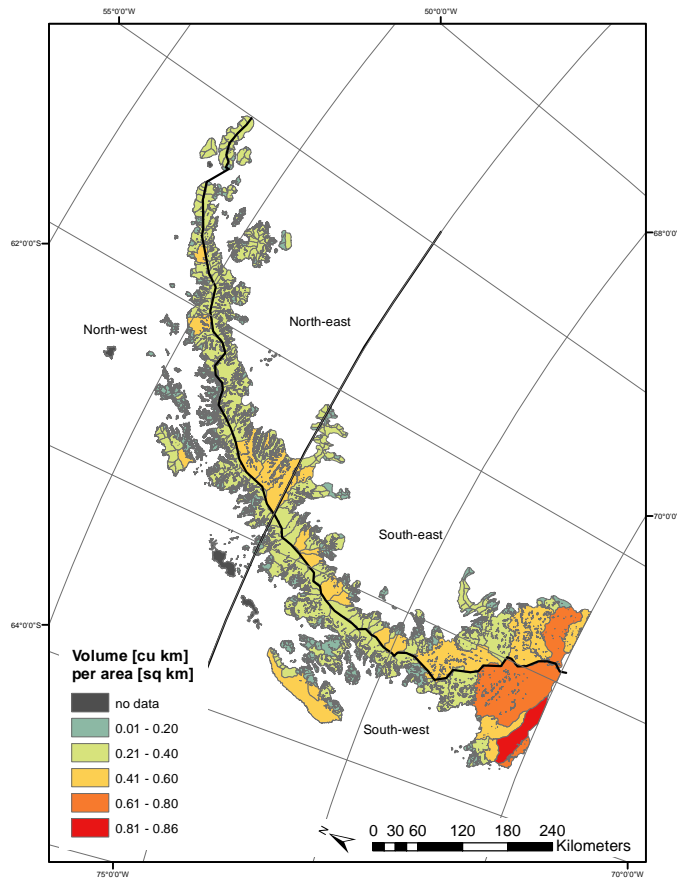


Figure 6.13. Total volume per total glacier area for each individual glacier.

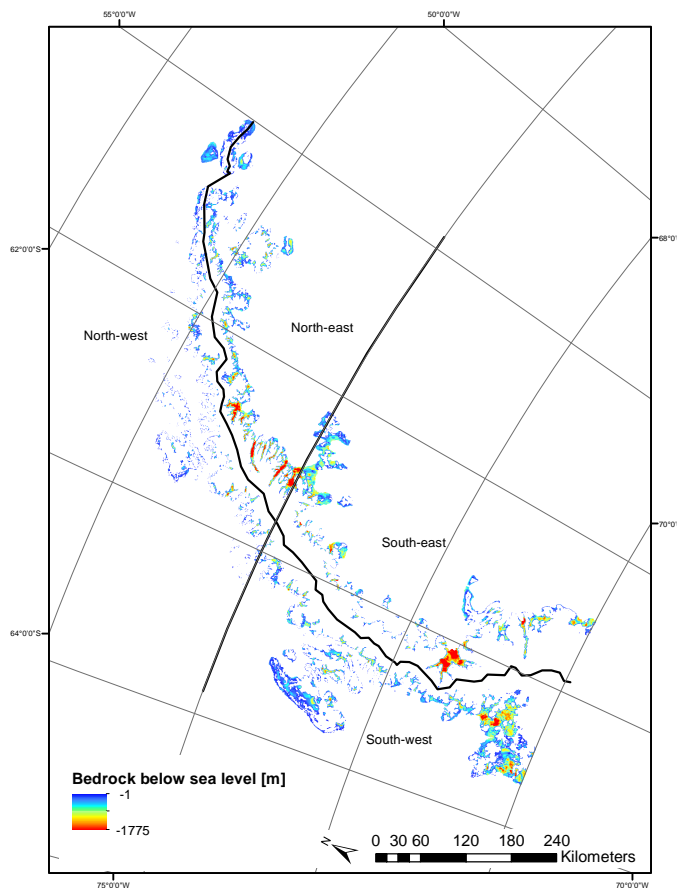


Figure 6.14. Negative elevation values representing the bedrock below sea level.

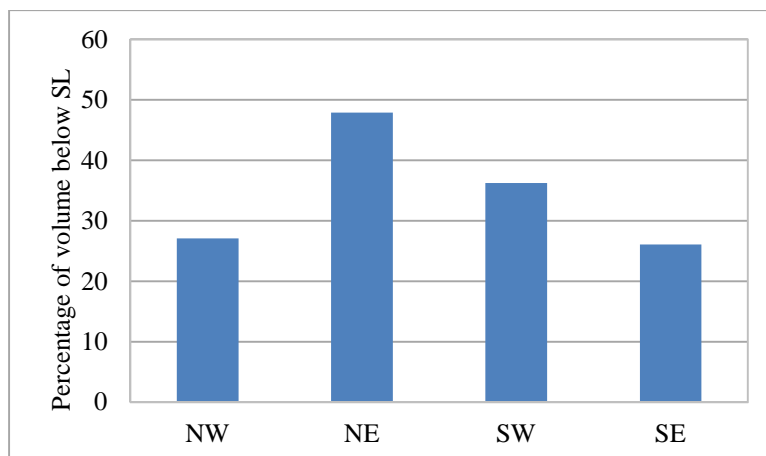


Figure 6.15. Volume grounded below sea level per sector relative to the total volume per sector.

Sector	Count	Area [km <sup>2</sup> ]	Count [%]	Area [%]	Volume [km <sup>3</sup> ]	Volume [%]	Volume <sub>&lt;0</sub> [km <sup>3</sup> ]	Volume <sub>&lt;0</sub> [%]	SLE [mm]
NW	703	16864.67	44.3	17.8	4029.7	11.6	1092.7	27.1	9.7
NE	246	18296.75	15.5	19.3	6172.7	17.8	2955.7	47.9	14.6
SW	378	30984.51	23.8	32.7	13375.1	38.6	4848.9	36.3	32.0
SE	261	28597	16.4	30.2	11072.24	32	2889.7	26.1	26.8
<b>Total</b>	<b>1588</b>	<b>94742.93</b>	<b>100</b>	<b>100</b>	<b>34649.9</b>	<b>100</b>	<b>11787</b>	<b>-</b>	<b>83.2</b>

Table 6.4. Glacier number, area, volume, volume grounded below sea level, the corresponding percentages and SLE per sector.

## 6.6 Nominal inventory parameters

The attributes *primary classification* (glacier type), *form* and *frontal characteristics* are rather subjective and dependent on the point of time when the classification was made, as changes in short time are possible. However, these attributes are still useful as they characterize the glacier in terms of inner dynamics, present state of development and surrounding climatic conditions. Therefore they should be included in an inventory if available (Rau *et al.*, 2005; Paul *et al.* 2009). Table 6.5 summarizes the count (total and percentage) as well as the area (total and percentage) of each glacier (frontal) type. Figure 6.16a and b visualize the spatial distribution of the glaciers according to their primary and frontal type classification. The classification was performed by Cook *et al.* (2014) and is based on the GLIMS Glacier Classification Manual of Rau *et al.* (2005). Most of the glaciers are mountain glaciers ( $n = 550$ ). However, outlet glaciers account for most of the area ( $n = 240$ , 67 565 km<sup>2</sup>, 71% of the total area). The glacier type *small ice-covered island* ( $n = 102$ , 387 km<sup>2</sup>), which is not a GLIMS glacier type, was added as such features are prevalent close to the AP. The frontal characteristics are useful to determine the climate-sensitivity and vulnerability of glaciers. Most of the glaciers (by area and number) of the AP are marine-terminating glaciers ( $n = 872$ , 59 406 km<sup>2</sup>), draining about 63% of the total glacierized area. These glaciers are highly vulnerable to changes in ocean circulation and temperatures (cf. Section 7.1.2). The ice shelf nourishing glaciers ( $n = 264$ , 33 260 km<sup>2</sup>, 35% of the total area) are exclusively located in the south-eastern sector. Only 9 glaciers are land terminating (113 km<sup>2</sup>, 0.1 % of the total area). However, 443 glaciers (1964 km<sup>2</sup>, 2% of the total area) have not been clearly classifiable in terms of frontal characteristics.

As the nominal categorization is rather subjective, Cook *et al.* (2014) introduced a degree of confidence in their classification decisions, which was assigned to each glacier as the *confidence* attribute. One value was assigned to summarise the overall confidence in allocation of *class*, *form* and *front* attributes. For further specification on how the dataset was compiled and how the nominal attributes are defined see Appendix and Cook *et al.* (2014).

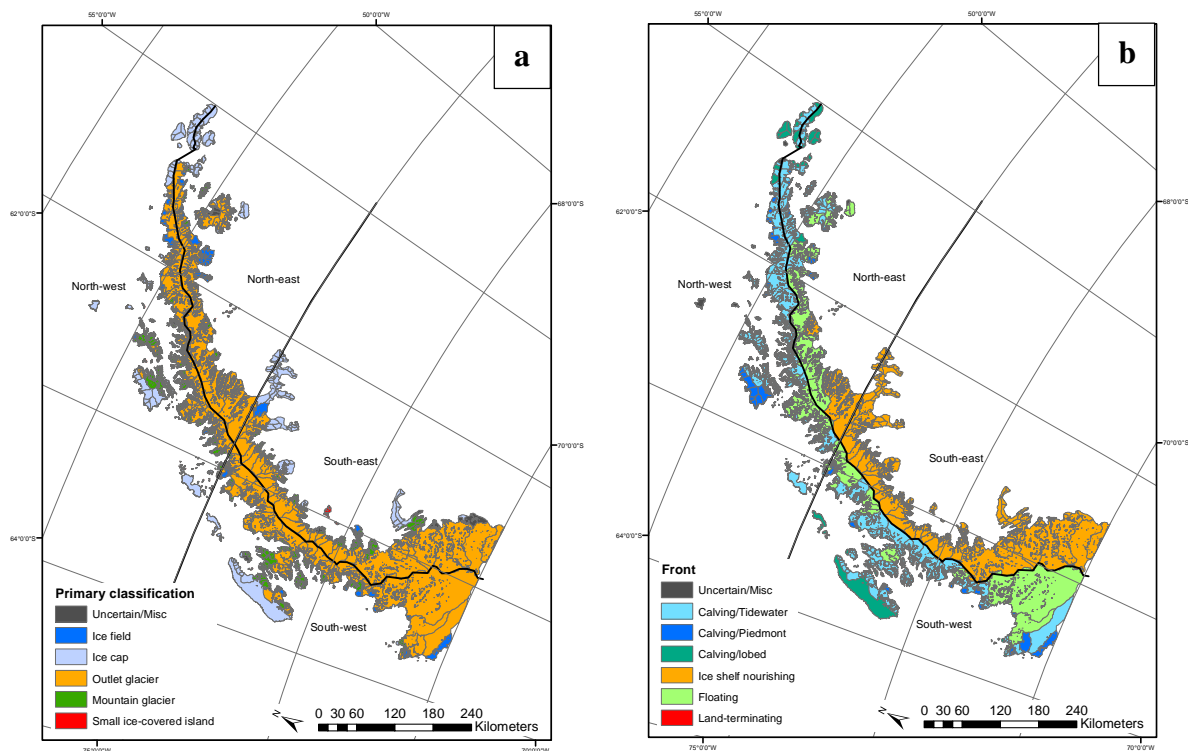


Figure 6.16. Color-coded glacier areas for visualization of the nominal parameters a) primary classification (glacier type) and b) frontal characteristics of the 1588 glaciers. Values are given in Table 6.5. The classification was done by Cook *et al.* (2014).

		Count	Count [%]	Area [km2]	Area [%]
<b>Class</b>	<b>Ice field</b>	77	4.8	3305.5	3.5
	<b>Ice cap</b>	234	14.7	12697.8	13.4
	<b>Outlet glacier</b>	240	15.1	67564.9	71.3
	<b>Mountain glacier</b>	550	34.6	8185.8	8.6
	<b>Small ice-covered island</b>	102	6.4	387	0.4
	<b>Uncertain/Miscellaneous</b>	385	24.2	2602	2.7
<b>Front</b>	<b>Calving (tidewater)</b>	671	42.3	27053.1	28.6
	<b>Calving/Piedmont</b>	78	4.9	3826.2	4.0
	<b>Calving/lobed</b>	41	2.6	4530.5	4.8
	<b>Ice shelf nourishing</b>	264	16.6	33259.7	35.1
	<b>Floating</b>	82	5.2	23996.4	25.3
	<b>Land-terminating</b>	9	0.6	113.3	0.1
	<b>Uncertain/Miscellaneous</b>	443	27.9	1963.8	2.1
<b>Total</b>		<b>1588</b>	<b>100</b>	<b>94742.9</b>	<b>100</b>

Table 6.5. Primary classification (Class) and frontal characteristics (Front) of the 1588 glaciers.

## 7 Discussion

So far, it was possible to compile a complete inventory dataset of the AP based on existing data (Section 5.1), separate all glaciers from the ice sheet (Section 5.2), derive glacier-specific parameters (Section 5.3), and further analyze these parameters (Section 6). The following paragraphs evaluate and discuss the results with respect to the research questions of this thesis (Section 1.2). Thereby, the potential regarding possible applications of the compiled inventory is demonstrated (Section 7.1). Moreover, difficulties faced and restrictions of the inventory are illustrated as well (Section 7.2).

### 7.1 Applications of the Antarctic Peninsula glacier inventory

Applications of a glacier inventory are shown, for instance, by Rastner (2014) exemplified on the Greenland glacier inventory. The following potentials of the compiled inventory are only a selection and exemplifies the wide range of possible applications of such an inventory.

#### 7.1.1 Identifying glacier tendencies based on median elevation and aspect

##### **Influence of the digital elevation model**

The accuracy, hence the total number of glaciers, the number of glaciers per size class, the aspect distribution and other topographic parameters are directly related to the location, quality and accuracy of the glacier outlines. The accuracy is therefore highly dependent on the quality of the DEM (Paul *et al.* 2009; Frey and Paul 2012) and the automated drainage basin delineation algorithm. According to Cook *et al.* (2014), the applied 100 m DEM is suitable for the delineation of the steep glacierized areas. Nevertheless, the delineation is rather arbitrary for the gentle and smooth high plateau (Figure 4.7). The manual division and merging of basins by considering additional datasets, such as grounding line data and ice velocity data, as done by Cook *et al.* (2014), is recommended but introduces subjective interpretation. However, objectivity regarding the calculation of glacier parameters is maintained, as they are calculated within a GIS. Frey and Paul (2012) investigated the influence on topographic glacier parameters for Swiss glaciers when applying two different DEMs (i.e. ASTER GDEM versus SRTM DEM). The analysis revealed that the influence depends on the parameter, on the sample size as well as on different acquisition dates and techniques of the DEM. First, the parameters based on a single DEM value (e.g. minimum and maximum elevation) are more prone to variability than parameters calculated for the entire glacier (e.g. mean elevation and slope). Second, the values can vary largely for individual glaciers, but these differences are evened out if a large number of glaciers is considered. However, both DEMs in the study by Frey and Paul (2012) are appropriate to be used for the calculation of topographic glacier parameters. Based on this outcome and as the new DEM of Cook *et al.* (2012) is a major step forward in terms of accuracy compared to the former ASTER GDEM, the application of this DEM is regarded as being appropriate for the calculations within the present glacier inventory. Nevertheless, the DEM still has limitations, which reduce the quality of the inventory (cf. Section 7.2.2).

### **Median elevation**

As shown in Figure 6.4, there is an increase of the median elevation from the islands and the coast towards the interior. The same has been detected in other regions with maritime climate such as for the glaciers around Greenland (Rastner *et al.* 2012), glaciers in Alaska (Le Bris *et al.* 2011) and in Norway (Paul *et al.* 2011). As proposed by Braithwaite and Raper (2009), the median elevation, which is the elevation of the line dividing the glacier surface in half, can be used as proxy for the equilibrium line altitude (ELA), which in turn divides per definition the glacier into an accumulation and ablation area. Hence, for Greenland (Rastner *et al.* 2012), Alaska (Le Bris *et al.* 2011) and Norway (Paul *et al.* 2011) a strong decrease of precipitation from the coast towards the interior is interpreted to account for the increasing median elevation towards the interior. However, as the glaciers of the AP, similar to the glaciers of Svalbard (Evans 2007), are mainly marine-terminating glaciers, the lower limit of the glacier is predefined. Therefore, for these regions, including the AP, the median, mean, mid-point or other elevation ratios proposed (cf. Paul *et al.* 2009) do not act as an appropriate approximation of the ELA. Because, if the lower limit is set to zero, the variability of the elevation ratios is only determined by the topography (i.e. maximum elevation). But the maximum elevation does not have any influence on the ablation. Hence, the usual concept and use of the ELA-proxy is not appropriate in this case. Therefore, the ELA-proxy is neither calculated, nor interpreted based on such an elevation ratio, nor on any other approximation. There is no technique proposed by the GLIMS community, which seems reliable to approximate the ELA of marine-terminating glaciers. Nevertheless, the increasing median elevation towards the interior does not come from decreasing precipitation towards the interior. It is rather an artefact of glacier delineation and depends on whether the glacier reaches sea level or not.

### **Glacier aspect**

Regarding the aspect of glaciers, several studies of Evans and others (Evans and Cox 2005; Evans 2006, 2007; Evans and Cox 2010) give rise to the expectation of poleward tendencies in numbers and lower glacier altitudes, and hence a strong north-south contrast of the AP's glaciers due to radiation differences. The studies did not consider Antarctic glaciers but reveal that these effects are reduced towards the poles as other factors such as wind, diurnal cycles and (lineated) topography can superimpose the effect of radiation and aspect (Evans and Cox 2005; Evans 2006). In addition, anomalies have already been discovered for regions also mainly consisting of marine-terminating glaciers, such as Svalbard (Evans 2007). As seen in Figure 6.5 and 6.6, the glaciers of the AP do not show the effect of poleward tendencies, as the number of glaciers and the mean elevation per aspect sector is rather balanced, with somewhat less glaciers facing to the south(-east). Three factors are seen to mask the effect of aspect: First, the elongated extension of the AP to the north causes glaciers to flow out of the mountain ridge towards the ocean in the north, east and west. Second, the surrounding ocean as a barrier causes to terminate the glaciers at the same elevation (about 0 m a.s.l.). And third, as a result of the glacier favorable climate the entire AP is glacierized anyway. Hence, a possible effect of poleward tendencies cannot evolve. However, the analysis of the glaciers' aspects might come to a different outcome in the future, as with further glacier recession the AP will not be entirely glacierized anymore and the ocean might not be reached by some glaciers. Furthermore, the



analysis of the aspect distribution of the glaciers located in the Antarctic Dry Valleys, lying between the East Antarctic ice sheet and the Ross Sea, might reveal a different pattern.

Mean thickness and volume also do not appear to depend on aspect. Moreover, a dependence on precipitation patterns cannot be interpreted as mentioned before. These parameters rather seem to be dependent on the topography and hypsometry of the AP: Increasing median elevation towards the (higher) interior (Figure 6.4), increasing mean thicknesses (Figure 6.10) and volumes (absolute and relative (Figure 6.13)) in regions where the bedrock lies below sea level, and towards the low-sloping interior and the Antarctic ice sheet in the south. Also the ice volume grounded below sea level reflects the bedrock hypsometry of the individual sectors. For instance, a large fraction of the bedrock of the north-eastern sector lies below sea level, hence almost 50% of its ice volume can be found grounded below sea level.

### 7.1.2 Identifying glacier sensitivity to climate based on glacier hypsometry

As the term *sensitivity* is not used consistently in glaciology, Rastner (2014) gives an overview on different understandings of climate and mass-balance sensitivity. In this thesis, glacier sensitivity is used to qualitatively describe how (strongly) the glaciers are expected to be influenced by and react on changes in air or water temperatures as well as on changes of their frontal characteristics.

As explained in Section 7.1.1, there is no significant trend in any glacier parameter, which could be explained through the climate pattern of the AP. Therefore, it is not possible to give a clear statement about climate-sensitivity based on these parameters. However, considering the glacier hypsometry (Figure 7.1; with normalized area) allows giving a statement on the sensitivity of the glaciers if changes in air or water temperatures occur. As mentioned before and explained by Jiskoot *et al.* (2009) the glacier elevational distribution determines its sensitivity for instance to a rise in the ELA. As the topography of the AP is reflected in the bimodal shape of the glacier hypsometry, as seen before in Section 6.4, all the many (marine-terminating) glaciers have large areal fractions both at lower and higher elevations. Therefore, both, changes in atmospheric, associated with ELA changes, as well as changes in ocean temperatures give rise to the expectation of high sensitivities. In tangible terms, on the one hand, top-heavy glaciers and regions, meaning those with a lot of glacierized area at higher elevations, are at some point expected to be very sensitive to rising air temperatures associated with a rising ELA. As long as the ELA lays between about 1000 – 1500 m a.s.l., not that many areas are additionally exposed to ablation. But as soon as the ELA reaches the elevations with a lot of glacierized areas (above 1000 – 1500 m a.s.l.), small rises in the ELA expose huge additional areas to ablation. Based on this, the south-eastern sector, having most glacierized areas at higher elevations with the maximum being somewhat lower, is expected to react soonest and most sensitively to changes in air temperature. But localizing the current ELA would be needed, which has not been done here, to determine the imminent migration of the ELA and the corresponding effects on the glaciers in more detail.

On the other hand, as most of the glaciers are also in direct water contact, they are not only influenced by atmospheric forces but are also subject to oceanographic forcing and subglacial topography. Even though, the response of these glaciers on changes in their mass balance is complex (Vieli *et al.* 2002; Pfeffer 2003), all the many marine-terminating glaciers of the AP

are very sensitive to climate change and associated ocean temperature changes. Hence, glaciers and regions with a high areal fraction in direct water contact (i.e. the north-eastern sector) are highly sensitive to water temperature changes. However, some of these glaciers are ice shelf tributary glaciers, most of them located in the south-eastern sector, meaning that they are rather sensitive to changes of their frontal characteristics because the retreat and collapsing of ice shelves is known to accelerate their nourishing glaciers (Cook *et al.* 2005).

Accordingly, all glaciers of the AP are affected by and sensitive on both: Changes in air temperature associated with ELA rise and changes in water temperature. Ice shelf nourishing glaciers are additionally highly sensitive in case of collapsing of their ice shelf.

These assumptions about the glacier sensitivity concord with the findings of recent studies of the AP illustrating glacier changes (Cook *et al.* 2005; Cook *et al.* 2014) and widespread acceleration of marine-terminating glaciers (Pritchard and Vaughan 2007). The latter showed that the flow rates of 300 marine-terminating glaciers on the AP north-west coast increased by 12% on average from 1992 to 2005 as a response of retreat and thinning glacier fronts due to the observed warming and corresponding increased summer melt. Cook *et al.* (2014) calculated the area changes of 860 marine-terminating glaciers from 1945 to 2010, showed the spatio-temporal differences in change in (a) absolute and (b) relative area (Figure 7.2) and discussed correlations between glacier characteristics and the area lost. What is really noticeable is, that ice shelves or rather their collapsing plays a crucial role for the spatial patterns of ice loss and the differences between east and west. As shown in Figure 7.2, the glaciers which once fed an ice shelf showed highest absolute and relative area losses. These findings confirm former studies, which already display the buttressing effect of stable ice shelves and the devastating effect of collapsing ice shelves on their nourishing glaciers of the AP (e.g. Scambos 2004; Wendt *et al.* 2010; Rott *et al.* 2011; Berthier *et al.* 2012).

All in all, the marine-terminating glaciers of the south-western, north-western and north-eastern sector of the AP are expected to react most sensitively to climate changes, at least currently. Especially those who fed an ice shelf until recently. The glaciers in the south-eastern sector seem to be less affected at the moment by such changes, as described for former ice shelf tributary glaciers. This is because almost all of the glaciers in this sector are currently nourishing the Larsen C ice shelf and hence benefit from the buttressing effect. This most southern ice shelf of the AP seems to be stable at the moment, based on flow modelling and analysis of surface morphological features (Glasser *et al.* 2009; Jansen *et al.* 2010). However, as the  $-5\text{ }^{\circ}\text{C}$  mean annual isotherm, to which ice shelves disintegration is linked, is approaching the Larsen C ice shelf, it might change its stability (Rott *et al.* 1996; Rott *et al.* 1998; Jansen *et al.* 2010) and lead to its break up in the future. This would affect about 250 glaciers with an area of  $32\,726\text{ km}^2$  currently nourishing this ice shelf. Additional extensive ice volumes of these ice shelf tributary glaciers are then potentially prone to the devastating effect of collapsing ice shelves. Besides this devastating effect, there is an additional effect if the bedrock is below sea level and deepens towards the inland as seen for many regions of the AP: Wouters *et al.* (2015) describe how retrograde slopes influence (i.e. reduce) the stability of glaciers and that glaciers laying on bedrock below sea level reveal increased thinning. Hence, not only the development of precipitation, air and water temperature, but also the behavior of the remaining ice shelves and the glaciers' bedrock topography have to be taken into account to identify the response of glaciers in terms of future changes.

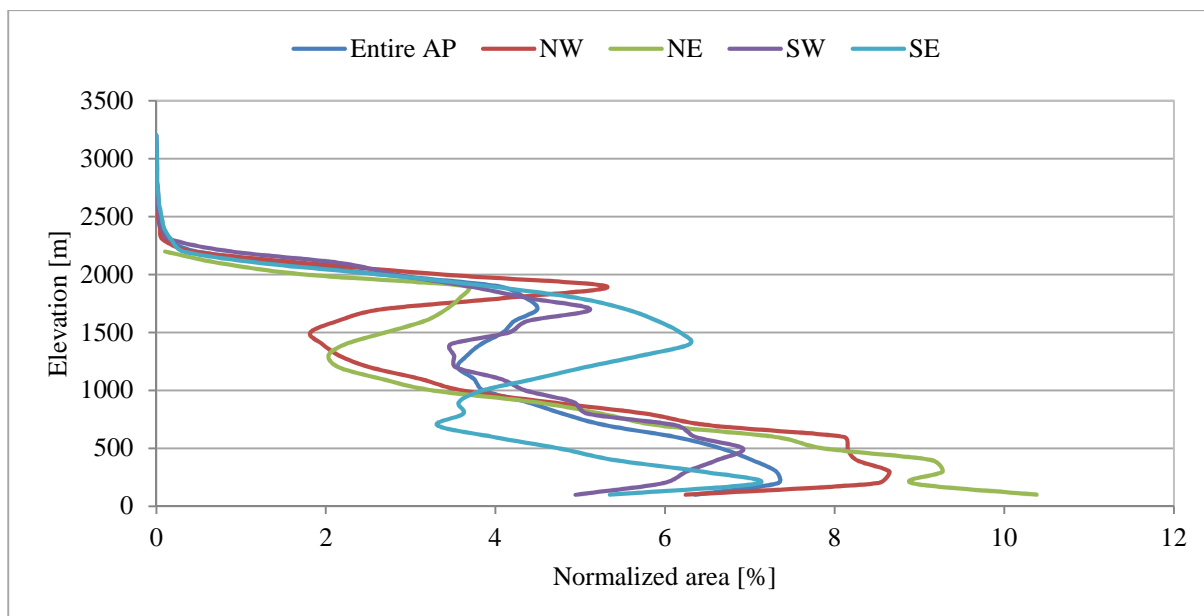


Figure 7.1. Distribution of normalized glacier cover with elevation for the entire AP and for each sector.

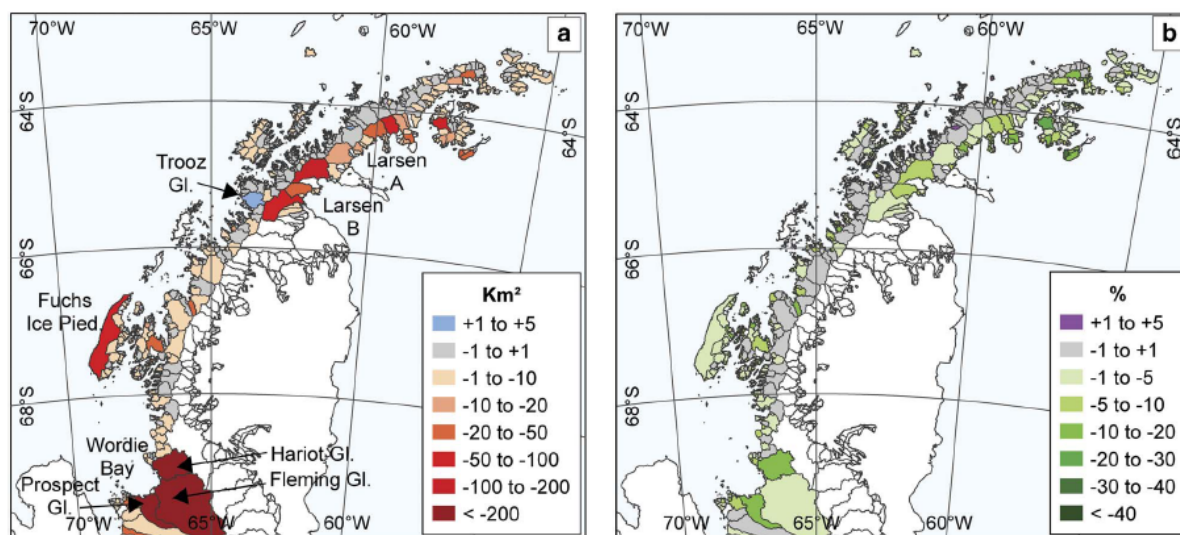


Figure 7.2. Spatial distribution of a) absolute and b) relative (% of basin size) change in area of Cook *et al.* (2014). Earliest records, on average, from 1958 and latest, on average, 2004.

### 7.1.3 Comparison of inventory characteristics with those of other regions

In this section, a selection of inventory characteristics (i.e. total number of glaciers, glacierized area, area covered by marine-terminating glaciers, median elevation and hypsometry) of the AP is compared with inventory characteristics of regions in similar environments (mountainous coastal regions with maritime climate). Therefore, the glacier inventories of Alaska (including northwest Canada) derived by Kienholz *et al.* (2015), Greenland (CL0 and CL1) derived by Rastner *et al.* (2012) and Svalbard derived by Nuth *et al.* (2013) are considered. Table 7.1 reproduces the total number of glaciers, which is largely influenced by the minimum-area threshold, the glacierized area and the area covered by marine-terminating glaciers for each region. Accordingly, the AP has the largest glacierized area, followed by Greenland and Alaska/northwest Canada. Least glacierized areas are found in Svalbard. However, the AP has the largest absolute and the second largest relative area covered by marine-terminating glaciers,

which are expected to be very sensitive on climate change and associated ocean temperature changes, as mentioned before. The glacier number and area distributions presented in the corresponding studies of Alaska/northwest Canada, Greenland, Svalbard and the AP reveal that the few larger glaciers make up for most of the area. This areal dominance of the rather few larger glaciers in all regions is reflected in the median area, which is considerably smaller than the mean area (Rastner *et al.* 2012; Nuth *et al.* 2013; Kienholz *et al.* 2015).

Though, in Alaska/northwest Canada, Greenland and Svalbard the number of glaciers is distinctively higher for smaller glaciers, with a maximum number between 0.25 and 1 km<sup>2</sup> (Rastner *et al.* 2012; Nuth *et al.* 2013; Pfeffer *et al.* 2014; Kienholz *et al.* 2015). The glaciers of the AP do not exhibit this pattern, which confirms the findings of Pfeffer *et al.* (2014) showing that Antarctic and Subantarctic glaciers do not display this common pattern.

The median elevation, shown for Alaska by Le Bris *et al.* (2011) and Kienholz *et al.* (2015), for Greenland by Rastner *et al.* (2012) and for the AP by this work, seems to depend on the distance from the coast, rather than on aspect. However, as these regions are dominated by marine-terminating glaciers, the appropriateness to use the increase of median elevation towards the interior as an indicator for decreasing precipitation is questioned, as explained in Section 7.1.1. Marine-terminating glaciers would have to be excluded to see whether this pattern of increasing median elevation is still existent, allowing statements about the precipitation pattern based on inventory data. The glaciers on Svalbard reveal a dependency on mean aspect showing a tendency of glacier numbers towards the north (Nuth *et al.* 2013), which is interpreted as an evidence of solar radiation incidence as the dominant influence for this region (Evans and Cox 2010).

Region	Count	Area [km <sup>2</sup> ]	Marine-terminating glaciers [km <sup>2</sup> ]	Marine-terminating glaciers of the total area [%]	Minimum-area threshold [km <sup>2</sup> ]	References
Alaska/northwest Canada	27 109	86 723	10 372	19	0.025	Kienholz <i>et al.</i> (2015)
Greenland	19 323	89 720	31 106	31	0.05	Rastner <i>et al.</i> (2012); Pfeffer <i>et al.</i> (2014)
Svalbard	1668	33 775	22 967	68	0.05	Nuth <i>et al.</i> (2013)
AP	1588	94 743	59 406	63	0.05	

Table 7.1. Summary of selected inventory parameters of different regions.

What really strikes the eye is the exceptionally shaped hypsometric curve of the AP (Figure 7.1), comparing the glacier hypsometry of the entire AP with those of glaciers in Alaska/northwest Canada (Kienholz *et al.* 2015), Greenland (Rastner *et al.* 2012) and Svalbard. The AP has a distinctly different hypsometric curve compared to the parabolic-shaped hypsometries of the other regions, with increasing area percentages towards their mid-elevation. Hence, the AP has most of its glacierized area at lower elevations and has a secondary peak at higher elevations. Whereas the other regions have most of their area in the middle of their

elevation ranges, confirming the findings of Pfeffer *et al.* (2014). As the hypsometry of a glacier controls the sensitivity on a rising ELA (Jiskoot *et al.* 2009) this comparison identifies the regions of high sensitivities on an equal rise in ELA. Higher sensitivities are expected for the AP, compared to the regions such as Alaska/northwest Canada, Greenland and Svalbard because depending on the current location of the ELA on the AP, at some point a rising ELA causes huge additional glacierized areas to be in the ablation zone. Regarding the sensitivity on changes in ocean temperatures, the sensitivity of glaciers in Svalbard and on the AP is highest due to the high areal fraction of marine-terminating glaciers.

#### 7.1.4 Comparison of the sea level equivalent with that of other studies and regions

As the volume and the potential SLE at individual glacier level has not been assessed so far, the comparison of the results presented here with those of other studies is limited. The volume per sector, the total volume and the volume grounded below sea level has been calculated for cross-validation and confirm the values presented by Huss and Farinotti (2014). The SLE was also calculated by Huss and Farinotti (2014) based on their, and hence the same bedrock and ice thickness dataset. However, their approach was more sophisticated. For instance, they used a modelled mean ice density of  $852 \text{ km m}^{-3}$  and for the ice grounded below sea level they also considered the SLR contributing mass between the ice equivalent surface and the floatation level (Fretwell *et al.* 2013). The SLE calculations introduced here are more elementary and straightforward. Hence, the SLE values differ: Their total SLE value (68.8 mm) is slightly lower than the SLE calculated here (83.2 mm), but they are still in a very similar range. However, Huss and Farinotti (2014) do not provide thickness, volume and SLE information per individual glacier. Hence, compared to the data of Huss and Farinotti (2014), the dataset provided here has two advantages:

1. Warranty of simple reproducibility
2. Availability of thickness, volume and SLE information per individual glacier

An updated estimate of distributed glacier SLE has recently been calculated by Huss and Hock (2015) based on RGIv4.0 outlines. Compared to these values, the AP has a much higher contribution potential than the glaciers of Alaska (45 mm), Central Asia (10 mm), Greenland periphery (38 mm), Russian Arctic (31 mm), Svalbard (20 mm) and is about equal to Arctic Canada North (67 mm) and South (20 mm) together. All in all, the global glaciers and ice caps sum up to a potential SLR of about 374 mm (Huss and Hock 2015) to 500 mm (Paul 2011; Huss and Farinotti 2012; Vaughan *et al.* 2013), which is still significant for low-laying coastal regions (Paul 2011). Compared to the Antarctic ice sheet with a SLE of 58.3 m (Vaughan *et al.* 2013), the SLE of the AP seems negligible. However, regarding the high sensitivity and short response times of these glaciers on climate change, they are expected to be major contributors to SLR in the next decades. Moreover, the contribution of the AP's glaciers has not yet been fully considered in most of the studies.

### 7.1.5 Representativeness of the mass balance glaciers of the World Glacier Monitoring Service

Benchmark glaciers have often been used in the past to estimate glacier change in a specific region (Fountain *et al.* 2009). The WGMS provides mass balance measurements for a small number of glaciers on and in the proximity of the AP, such as the Anvers Ice Cap and the glaciers Bahia del Diabolo, Hurd and Johnson (WGMS 2015). These glaciers and their mass balances might be used for upscaling and as representatives for this region to assess glacier changes. Østrem and Brugman (1991) list different criteria, which a benchmark glacier should meet to represent a geographical area. Thus, how well do the WGMS mass balance glaciers mirror the 1588 glaciers of the AP?

The inventory presented here only includes two of the WGMS glaciers, which are located on two different islands around the AP as shown in Figure 7.3.: The Montiel Glacier, alias Anvers Ice Cap (WGMS name), is located in the north-western sector, whereas the Glaciar Smit, alias Bahia del Diabolo (WGMS name), is located in the north-eastern sector. The two glaciers Hurd and Johnson are located further north on Livingston Island (South Shetland Islands). Table 7.2 compares a selection of the attribute values of these two glaciers as found in the present inventory and as provided by the WGMS. Due to different delineations of the glaciers and methodologies applied to determine the attributes, some values differ a bit more, some a bit less. However, they are in the same order of magnitude and reflect the general pattern similarly. For consistency, the values of the present inventory here are used in the following discussion. The Montiel Glacier is far larger than the mean glacier area of all glaciers (59.7 km<sup>2</sup>) of the AP but is thinner than the mean thickness of all glaciers (237 m). The Glaciar Smit is somewhat smaller than the mean area, but thicker and corresponds with the mean thickness of all glaciers. The attribute combinations area versus mean slope (Figure 7.4a) and mean aspect versus mean elevation (Figure 7.4b), reveal that the two glaciers are not outliers and do not belong to boundary values. Nevertheless, as the range in area, slope, aspect and mean elevation of the AP's glaciers is rather large, trends and dependencies are not that strong, their fitting is not very surprising. However, considering the glacier hypsometry with normalized area, the curves of the two glaciers do not represent the general shape of the hypsometry of the entire AP (Figure 7.5). Whereas the Glaciar Smit only represents about 20% of the elevation range, the Montiel Glacier represents about 80%. The glacierized area of the Glaciar Smit is restricted to the lowest 500 m. Most of the glacierized area of the Montiel Glacier is found below 1000 m a.s.l. with three peaks, which are reducing towards lower elevations. And above all, this glacier does not have a secondary peak at higher elevations, representing a glacierized plateau region. Østrem and Brugman (1991: 9) state that a representative glacier should cover at least "*the main [elevation] range of other glaciers in the area*". This is obviously not given by these two WGMS glaciers. And hence based on the hypsometry, the sensitivities of these two glaciers on climate change associated with a rising ELA differ from those of the entire AP. On the other hand, both glaciers seem to be marine-terminating glaciers as almost all other glaciers on the AP. Therefore, they do reproduce the high sensitivity on changes in ocean temperature. But the sensitivity on climate change might be overestimated as, firstly, these two glaciers are located in very low elevations. And secondly, the WGMS glaciers, especially Glaciar Smit and the

glaciers Hurd and Johnson on Livingston Island, are located at the very north and hence in warmer regions.

All in all, these two glaciers might represent the glaciers regarding parameters such as size, aspect, slope and mean thickness. But they might not be adequate for crucial hypsometry-based assumptions and statements (i.e. sensitivities) of the entire glacier sample to assess glacier changes and estimate SLR. Whether these two glaciers are well representing area changes, annual mass balance variations and (cumulative) mass changes cannot be stated as this information is not provided here for the individual glaciers. However, as already elaborated by Fountain *et al.* (2009) and aptly expressed by Pritchard and Vaughan (2007: 2): “[T]here is strong evidence that the behavior of individual glaciers may be quite different from the mean (see Cook *et al.* 2005) and so the use of a few benchmark glaciers could be misleading.” Even though Pritchard and Vaughan (2007) stated this in the context of the regional glacier flow, Fountain *et al.* (2009) show that SLR estimates based on benchmark glaciers might cause a lot of uncertainty. Hence, being aware of the extensive effort and limitations, the mass balance measurement network should be extended all over the AP for an appropriate representation of the true range of conditions.

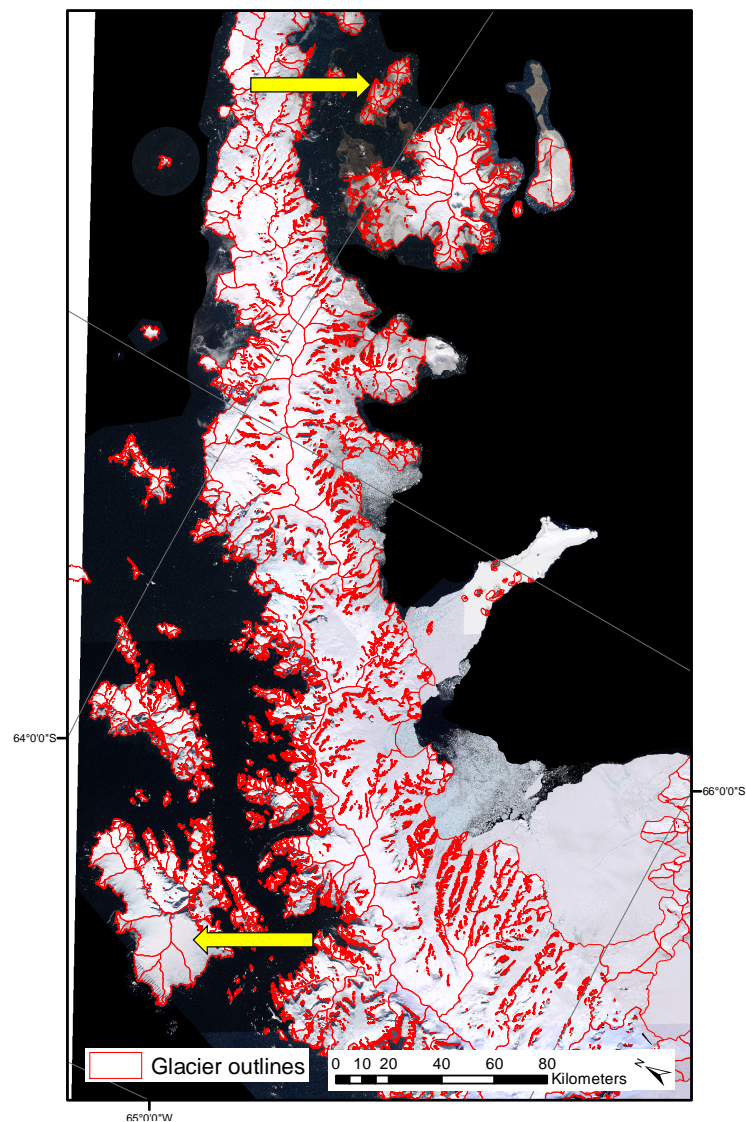


Figure 7.3. Location of the two WGMS mass balance glaciers indicated by the two yellow arrows.

Attribute	Inventory of the AP		WGMS	
Name	Montiel Glacier	Glaciar Smit	Anvers Ice Cap	Bahia del Diabolo
Year of investigation	2001	2000	unknown	2004, 2008, 2010, 2014
Number of Observations in the registered dataset	1	1	2	14
Area [km <sup>2</sup> ]	280.6	35.5	230	12.9 (2014)
Class	Ice-cap	Mountain glacier	-	Outlet glacier
Form	Uncertain/Misc	Uncertain/Misc	-	Simple basin
Front	Calving/Piedmont	Calving, tidewater	-	Single lobe, mainly clean ice
Minimum elevation [m]	2.2	4.4	0	50
Maximum elevation [m]	2507.2	593.4	1600	630
Mean elevation [m]	590.3	284.1	-	-
Median elevation [m]	595.7	281.8	-	390
Mean Slope [°]	5.6	5.5	-	-
Mean Aspect	SE	N	-	Accumulation area: NE Ablation area: E
Mean thickness [m]	141.8	235.3	-	-
Volume [km <sup>3</sup> ]	112.8	7.6	-	-

Table 7.2. Selection of glacier attributes as provided by the present inventory (left) and as provided by the WGMS (2015; right). The Montiel glacier and the Anvers Ice Cap refer to the same glacier (red). Same is true for the Glaciar Smit and the Bahia del Diabolo (green).

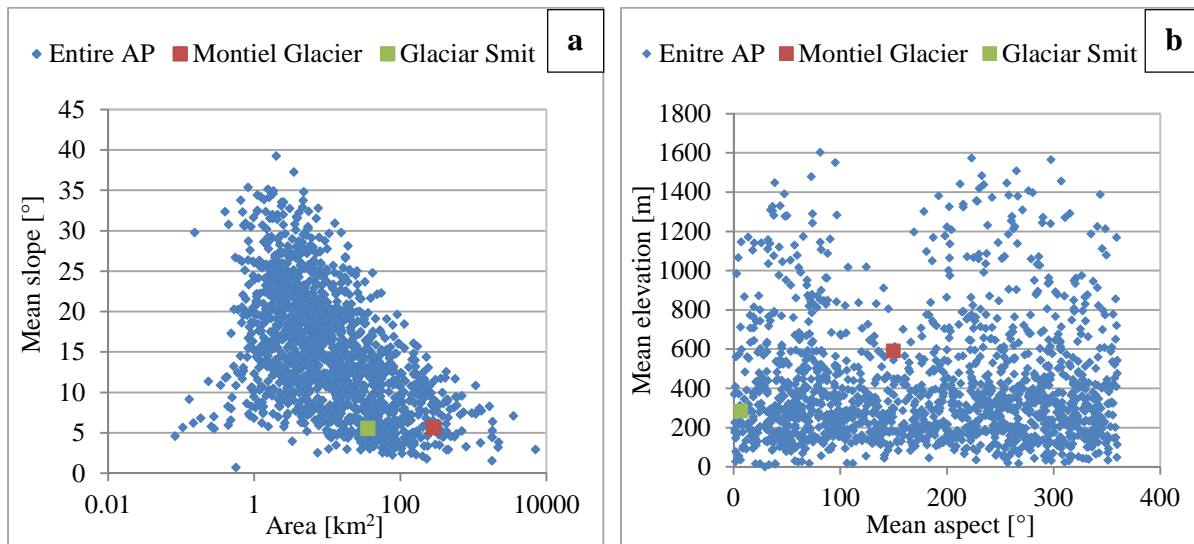


Figure 7.4. Localization of the WGMS mass balance glaciers Montiel Glacier (red) and Glaciar Smit (green) in the scatterplots area vs. mean slope (a) and mean aspect vs. mean elevation (b), based on values of the introduced inventory.



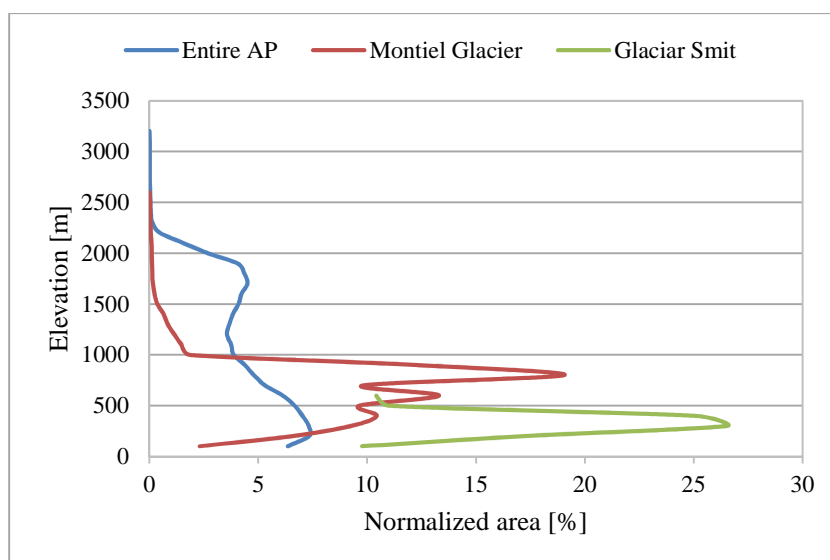


Figure 7.5. Glacier hypsometries with normalized area for the entire AP (blue), the Montiel Glacier (red) and the Glaciar Smit (green). The calculations are based on the here provided outlines.

## 7.2 Challenges and restrictions

### 7.2.1 Challenges of the inventory compilation based on existing datasets

The collection of existing datasets to compile a glacier inventory, in this case of the AP, is associated with difficulties, which have to be surmounted. Not only the searching of data, but also the accessibility and the inconsistency of the data themselves, as well as the methods the data are generated with, bear different challenges. Web-based research platforms, advanced search engines as well as a wide range of databases provide possibilities for extensive research in an enormous pool of scientific studies and data. To find and consider all the publications and data dealing with the glaciers and glacier related topics of the AP is almost impossible and goes beyond the scope of a Master's thesis. Besides the challenges of finding appropriate published work, the knowledge about the existence of unpublished material requires insider information, which still does not guarantee the accessibility of unpublished data. Generally, it is of interest to the scientific community to progress in such topics dealing with the current state of glaciers to assess ongoing and future changes. Therefore, this work about the glacier inventory of the AP was met with great approval among the researchers contacted in the framework of this thesis. The will to help and support was abundant. However, the dependency on the willingness and finding time to provide the data requested of scientists, which are in possession of relevant data, exists with no doubt. Also the available and provided data themselves caused difficulties, as they are, for instance, of different formats, crucial meta-data were partially missing making reproducibility impossible or the method they were generated with did not meet the requirements. All of these challenges have been faced in all conscience to achieve the best result possible in the framework of this thesis. However, limitations of an inventory dataset based on existing data (cf. Section 7.2.2) are inevitable. Hence, this thesis and the results are largely influenced by these challenges and how these challenges have been surmounted.

### 7.2.2 Restrictions of the inventory: origins, impacts and suggestions for improvements

The restrictions arising from the compilation of a glacier inventory based on existing data are similar to the limitations of a satellite-derived inventory as described by Paul (2003): The data availability, the data quality and data (pre-)processing. In case of the inventory provided here, besides the challenge of receiving the data needed as described in Section 7.2.1, the following is seen to account for most of the restrictions:

1. The quality of the rock outcrops dataset, which has been used for processing the inventory of Cook *et al.* (2014)
2. The quality of the DEM, which has been used to determine the glacier parameters
3. The assignment of the connectivity levels and, coupled with this, the delineation and separation of the AP from the Antarctic ice sheet

#### Rock outcrops

As mentioned in Section 5.1, the rock outcrops dataset provided by the ADD (ADD Consortium, 2012) originates from different sources, has partially been updated and is therefore of varying accuracy and detail. The accuracy is qualitatively assessed by overlaying the Landsat Image Mosaic of Antarctica (LIMA; Bindschadler *et al.* 2008) with the rock outcrops layer. Figure 7.6a, b and c visualize three major problems. Firstly, some areas (mainly islands) are detected which are entirely or for the most part classified as rock outcrops, even though they obviously seem to be glacierized (Figure 7.6a and b). Secondly, the dataset has locally considerable georeferencing inaccuracies. Thirdly, by intersecting this dataset with the catchment outlines, some glacier outlines became highly fragmented as exemplified in Figure 7.6c. Before the intersection, the glacier shown was made up of one complete polygon. Now the glacier consists of several smaller polygons. This raises the question whether this is still one glacier, more than one glacier or not a glacier at all. Hence, extensive time-consuming manual corrections for the entire AP would be needed. Regarding the time management of this thesis and as these manual corrections would further introduce subjectivity and reduce transparency and reproducibility, this has not been done here. In addition, there are ongoing efforts to improve the underlying data for the ADD (Fox, written communication). In this context, a study about a new rock outcrops dataset is currently in review and will probably be published soon. This new dataset has been generated by automatic extraction of outcrops for the entire continent from Landsat images using a combined methodology that takes into account sunlit rock, shaded rock, water, cloud and snow. The new dataset is more detailed and suggests that the actual amount of outcrop is only around half the area of that in the ADD at present (Peter Fretwell, British Antarctic Survey, written communication, 5.1.2016). Thus, once this new rock outcrop dataset is available, it should be used to improve the inventory derived here.

Furthermore, other limitations might arise in relation to the rock outcrops dataset, such as the assumption of all area not classified as rock being glacierized. This assumption seems appropriate for the almost entirely glacierized AP. However, as snowfields might look like glacierized areas, it is advisable to validate the entire region, for instance, with velocity field data, to identify possible snowfields. The study of Nagler *et al.* (2015) demonstrates the

potential of the Sentinel-1 mission for mapping and monitoring the surface velocity of glaciers and ice sheets. These might ultimately help to distinguish the both and also verify the DEM derived drainage divides over flat terrain.

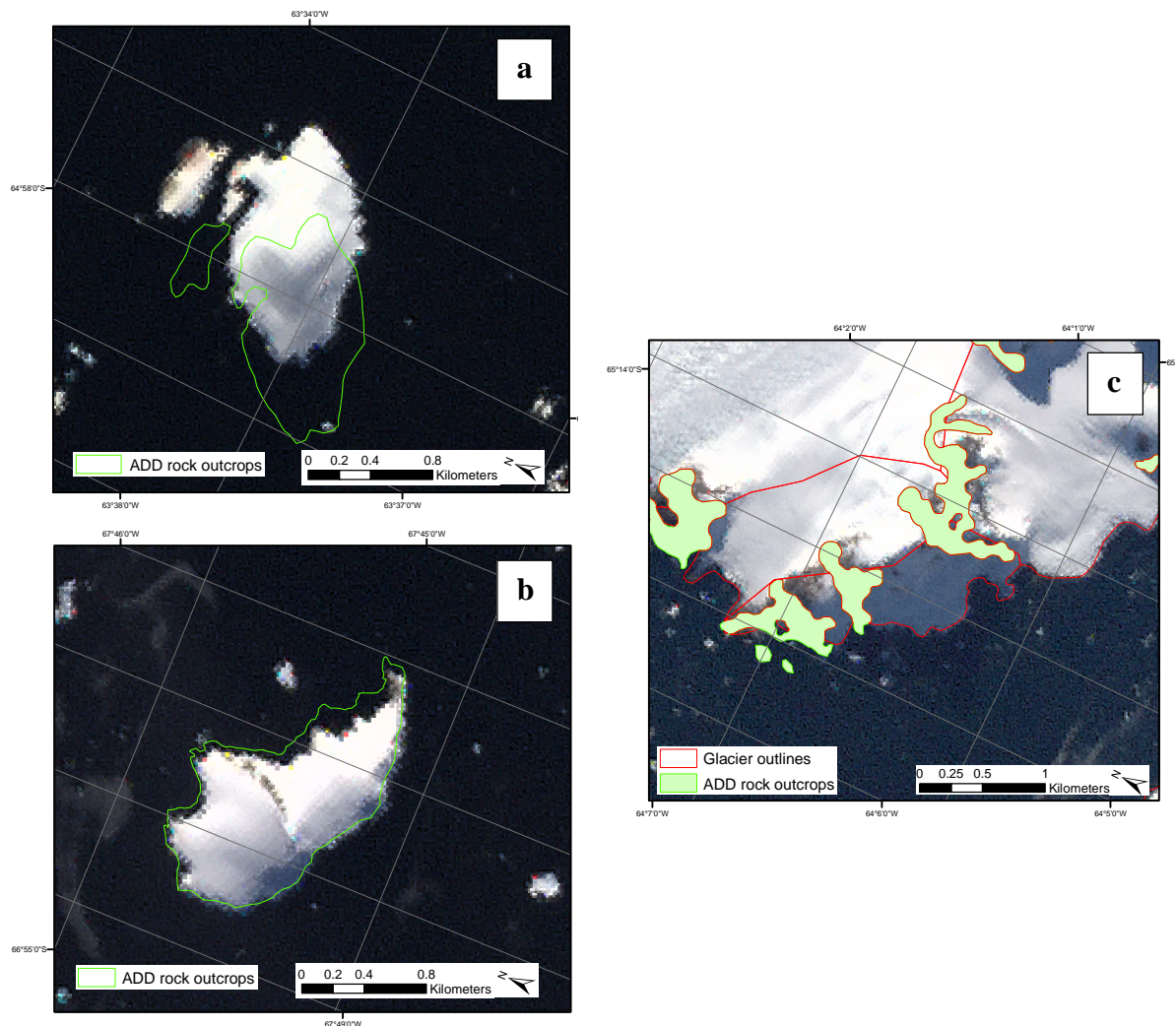


**Figure 7.6.** Examples of glacierized islands incorrectly classified as rock outcrops (a and b) and an example of a highly fragmented glacier outline after intersecting with the rock outcrops layer (c). In addition, georeferencing inaccuracies are detectible.

### Digital elevation model

As mentioned in Section 5.3.1, the DEM of Cook *et al.* (2012) provides currently the best quality and covers the area of the AP most accurately. However, the DEM only covers 93 250 km<sup>2</sup> and hence 98.4% of the total glacierized area. Therefore, the calculation of the topographic parameters (mean, median, min., max. elevation, slope, aspect) was not possible for 48 glaciers, which are entirely excluded by the DEM, representing an area of 1044 km<sup>2</sup>, about 3% of the total number and 1.1% of the total area. As some glaciers are only partially covered by the DEM, for instance one glacier is only covered by one pixel of the DEM, the values of their 3D parameters are based only on a restricted area and are not representative for the entire glacier. Even though only about 1.6% of the total glacierized area is not covered by the DEM and mainly a few islands are affected, their values of the 3D parameters are expected

to have inaccuracies. In addition, as the glacier hypsometry is calculated based on the DEM, the curves represent only the area covered by the DEM. Therefore, these curves might also be slightly altered by including the missing areas. Furthermore, as the ice thickness and bedrock dataset of Huss and Farinotti (2014) is based on the DEM of Cook *et al.* (2012), the mean thickness, the volume and the SLE could not be calculated for 49 glaciers<sup>2</sup>. Accordingly, the values of mean thickness, the total volume and SLE for the glaciers on the islands which are not completely covered by the ice thickness and bedrock dataset are not representative for the entire glaciers. Hence, the total SLE of the AP should be somewhat higher than calculated here, as the SLE of 49 glaciers is missing.

As a fast and result-oriented solution, a new DEM could be generated by completing the incomplete outlined areas based on statistics of the part of the area including elevation information. For instance, a glacier with missing values at the coast the DEM would be filled with the lowest occurring elevation value. This would counteract the problem of glaciers with incomplete elevation information. However, the accuracy and hence adequacy of this method would have to be further assessed. In addition, it does not solve the problem for areas where no elevation information is available at all. Hence, another DEM should be used or a new DEM should be generated to provide elevation information for the remaining 48 glaciers. Cook *et al.* (2012) gives an overview on high resolution elevation datasets for the AP and how existing DEMs can be improved. Accordingly, the bedrock and thickness dataset should be completed for the areas of missing information, for instance, based on the procedures of Huss and Farinotti (2014).

### **Delineation and separation from the ice sheet**

The decision about what still belongs to the AP and what is not part of it anymore has a major influence on the results. As the generation of the inventory is mainly based on the existing dataset of Cook *et al.* (2014), the glacierized islands further north of the mainland and nearby islands of the AP are not included. These islands are in some cases seen as Subantarctic Islands and, are already existent in the RGI (Arendt *et al.* 2015). The assignment of the connectivity levels and, connected with this, the separation from ice sheet (cf. Section 5.2) is based on the Antarctic ice sheet drainage divides dataset provided by the Cryosphere Science Laboratory of NASA's Earth Sciences Divisions (Zwally *et al.* 2012), which is shown in Figure 5.2. As a result, the ice masses south of 70°S are assigned CL2 and therefore seen as being part of the Antarctic ice sheet. However, these glaciers assigned with CL2 might still reveal behaviors, dynamics, sensitivities and time scales similar to the glaciers further north (CL0 and CL1), even though their drainage divide is connected to the ice sheet. Hence, depending on the scientific research question, it might be more accurate to treat CL2 ice masses as glaciers. The separation from the ice sheet presented here mainly counteracts the problem of double-counting of the ice masses on the AP. But it might not correspond and reflect the boundary between glacier and ice sheet regarding individual internal dynamics.

---

<sup>2</sup> One glacier was only covered by one 100x100 m pixel of the DEM. This pixel does not have any bedrock/thickness information in the dataset of Huss and Farinotti (2014). Hence, 48 glaciers do not have any topographic information and 49 glaciers do not have any thickness, volume and SLE information at all.

## 8 Conclusions and perspectives

### 8.1 Compilation of the glacier inventory

In the framework of this thesis, it was possible to compile a complete glacier inventory of the AP north of 70°S based on several already existing but not fully complementary geo-spatial datasets (Section 5.1), including the separation of the glaciers from the ice sheet (Section 5.2), the derivation of glacier-specific parameters (Section 5.3) and the analysis of these parameters to identify the characteristics of the glaciers in this region (Section 6). In addition, this work demonstrates the potential of inventory data for improving the knowledge about the glaciers on the AP (Section 7.1). Furthermore, as neither GLIMS (GLIMS and NSIDC 2005, updated 2015), the RGI (Arendt *et al.* 2015) nor any other database currently provides a complete glacier outlines dataset of the AP, a significant gap in global glacier inventory can be closed. Hence, this dataset makes an important contribution to global SL change estimations as most studies did not fully consider the glaciers of the AP.

The compilation was achieved by combining already existing data and GIS techniques. The reassessment revealed that the dataset of Cook *et al.* (2014), consisting of glacier catchment outlines, provides the most appropriate basis for this inventory. The exclusion of rock outcrops by the use of the corresponding dataset of the ADD (ADD Consortium, 2012) resulted in 1588 glacier outlines (excluding ice shelves and islands <0.05 km<sup>2</sup>), covering an area of 94 743 km<sup>2</sup>. Based on the recommendations for the compilation of a glacier inventory (Paul *et al.* 2009), combining the outlines with the DEM of Cook *et al.* (2012) enabled to derive topographic parameters per individual glacier (i.e. area, aspect, slope, minimum, maximum, mean and median elevation). By the application of the ice thickness and bedrock dataset of Huss and Farinotti (2014), volume, mean thickness and SLE information is provided for each glacier.

By applying the concept of connectivity levels with the ice sheet as introduced by Rastner *et al.* (2012) for the glaciers around Greenland, the problem of the missing separation of the glaciers from the ice sheet is approached. All glaciers on islands are assigned CL0 (no connection) and the glaciers on the mainland are assigned CL1 (weak connection). Based on the Antarctic drainage systems of Zwally *et al.* (2012) ice masses south of 70°S are connected with the ice sheet. Therefore, glaciers in these areas (Palmer Land) are assigned CL2 (strong connection) and are regarded as being part of the ice sheet and not included in the present inventory. Nevertheless, depending on the research objective (e.g. single glacier modelling), it might be more appropriate to consider these ice masses also as glaciers. In such cases this separation might have to be reconsidered.

The resulting inventory as well as its quality is largely influenced by the availability and accessibility of accurate data. Two facts about the data used account for limitations of the inventory: First, the quality of the applied rock outcrops dataset is reduced. Second, the DEM does not entirely cover the glacierized area, but 98.4%. Hence, for less than 50 glaciers the topographic glacier parameters as well as thickness, volume and SLE information are missing. For some other glaciers these values are not representative for the entire glacier extent. However, prospective improved rock outcrops and DEMs can solve this problem.

## 8.2 Major findings of the glacier inventory analysis

The analysis of the glacier inventory reveals the following major findings with respect to the research questions (2) – (5) (Section 1.2):

### (2) Topographic characteristics of the glaciers

- The glacier size distribution reflects the areal dominance of the rather few large glaciers, but most of the glaciers can be found in the size classes 4 – 6 (1.0 – 50 km<sup>2</sup>).
- The glacier aspect distribution is balanced and does not reveal any aspect tendencies.
- The median elevation increases from the islands and coast towards the interior, but this is influenced by the variability in maximum elevation.
- Mean slope is dependent on glacier size: the larger the glacier, the smaller the mean slope (with increasing variability towards smaller glaciers).
- The modelled ice thickness is unsurprisingly dependent on area and slope: The steeper/smaller the glacier, the thinner the ice. But mean ice thicknesses are higher in the very south towards the ice sheet.
- The total ice volume is 34 650 km<sup>3</sup>. According to the ice thickness distribution, 70% of the total volume is found in two southern sectors, which are also largest in terms of area. But also the highest volumes per individual glacier are found in the south towards the ice sheet. About one third of the total volume is grounded below sea level.
- In terms of *glacier type*, outlet glaciers account for most of the glacierized area (71%), whereas numerically, mountain glaciers are most prevalent (n = 550).
- In terms of *glacier frontal type*, marine-terminating glaciers are numerically most prevalent (n = 872) as well as accounting for most of the area (68%). About 35% of the area is covered by ice shelf nourishing glaciers. They are exclusively located on the south-eastern sector.
- The hypsometric curve has a bimodal shape: The maximum of glacierized areas is located at about 200 – 500 m a.s.l. and a secondary maximum is found at about 1500 – 1900 m a.s.l..

The glacier number, size and aspect distribution are highly dependent on the quality of the DEM and the automated drainage basin delineation algorithm. The mean, median, maximum and minimum elevation, mean thickness, volume distribution, the glacier hypsometry as well as the glacier (frontal) types are determined by the topography of the AP and no dependence on aspect or precipitation patterns is detectable.

### (3) Sensitivity of the glaciers on changes in air or water temperature

As most of the glaciers are both, marine-terminating glaciers and extending into higher elevations, they reveal large areal fractions at lower as well as at higher elevations. At some point, rising ELAs due to rising air temperatures exposes enormous additional area to enhanced ablation. Rising ocean temperatures increase melting and calving of the glaciers with water contact. Hence, both, changes in atmospheric, associated with ELA changes, as well as changes in ocean temperatures are expected to cause high sensitivities of these glaciers. Which sector

will be affected most and first from one or the other climate induced change depends on the warming pattern of the region as well as on the hypsometry of each sector. Ice shelf tributary glaciers reveal additional high sensitivities on changes of their frontal characteristics (i.e. collapsing of the ice shelf). Due to the buttressing effect of a stable ice shelf, glaciers of the south-eastern sector nourishing the Larsen C ice shelf are currently expected to show lower sensitivities on climatic changes. However, a collapsing of the ice shelf would result in a devastating effect.

#### **(4) Potential sea level contribution:**

Based on the proposed simple calculations assuming a mean ice density of  $900 \text{ kg m}^{-3}$  and an ocean surface of  $3.62 \times 10^8 \text{ km}^2$  the AP has a SLE of 83.2 mm. Due to the expectedly high sensitivity and short response times on climate change compared to the ice sheet, these glaciers are expected to be major contributors to SLR in the next decades.

#### **(5) Comparison with the glaciers of Greenland, Alaska/northwest Canada and Svalbard:**

- The AP has the largest glacier cover.
- In all regions, the few larger glaciers make up for most of the area.
- The number of glaciers is distinctively higher for smaller glaciers in all regions compared to the AP.
- AP has the largest absolute and the second largest relative area covered by marine-terminating glaciers.
- The bimodal-shaped hypsometry of the AP is distinctly different from the parabolic-shaped hypsometries of the other regions, with highest area percentages towards their mid-elevation. This results in a different sensitivity of the AP on rising temperatures.
- Regarding the sensitivity on changes in ocean temperatures, the sensitivity of glaciers in Svalbard and on the AP is highest due to the high areal fraction of marine-terminating glaciers.

## **8.3 Outlook**

As mentioned above, there is still room for improvement and also considerable potential of this dataset to be trapped. Therefore, a number of further suggested improvements of the dataset itself as well as a selection of possible further analysis and applications of the dataset are presented in the following.

### **8.3.1 Suggested improvements**

**Rock outcrops:** The application of a revised rock outcrops dataset will improve the quality of the outlines and the inventory in general. There are ongoing efforts revising the ADD rock outcrops dataset (Fretwell *et al.* 2015).

**DEM:** Through the application of a DEM of at least the same resolution and quality as well as of a thickness dataset covering the entire glacierized area, the topographic glacier parameters, thickness, volume and SLE can be calculated for all 1588 glaciers based on their outlined area.

**Glacier (frontal) types:** The distinction between glacier types and frontal characteristics should be completed as this is missing for some glaciers. This information is needed to identify and model glacier sensitivity and response time to climate change (Rastner 2014).

**Surface velocity data:** The application of ice surface velocity data from the Sentinel-1 mission allows identifying possible snow fields as well as to review the accuracy of the lateral boundaries of a glacier outline.

### 8.3.2 Possible further analysis and applications

**Statistics:** Further (multivariate) statistical analysis and visualizations are suggested to identify primary influences on glacier parameters.

**Glacier parameters:** The inventory could be extended with further glacier parameters for different practical purposes as described by Paul *et al.* (2009). For instance, the glacier length or the glacier-specific hypsometry in 100 m bins. The former would allow deriving length changes. The latter provides information for improved calculation of the glacier response on a changing climate (Paul *et al.* 2009).

**Areal change:** The dataset could be extended with the dataset of Cook *et al.* (2014), which provides ice front positions of 860 marine-terminating glaciers of the AP since the 1940s. Hence, studies about future areal changes through continued monitoring and repeated surveys as well as about past areal changes, as already induced by Cook *et al.* (2014), could be added.

**Volume change:** The generation of new and high-quality DEMs in the future does not only allow improving the quality of the drainage divides and topographic parameters but, also generating new thickness and volume datasets of the AP which makes it possible to determine volume changes.

This thesis, presenting and analyzing the first complete glacier inventory of the AP, consisting of glacier outlines accompanied with parameters for the individual glaciers, is a major contribution for forthcoming regional and global glaciological investigations. To approach data availability and consistency, this dataset will be provided to the GLIMS database. This enables to apply and add additional and/or new arising data and approaches to improve, extend and further investigate the glaciers of the AP. This will be needed to further improve the knowledge about the glaciers of the AP and their behavior with respect to a changing climate.



## 9 References

- ADD Consortium, 2000. *Antarctic Digital Database, Version 3.0.*, Scientific Committee on Antarctic Research, Cambridge.
- ADD Consortium, 2012. *Antarctic Digital Database, Version 6.0*, Scientific Committee on Antarctic Research, Cambridge, <http://add.scar.org/home/add6>, accessed 4 May 2015.
- Arendt, A., Bolch, T., Cogley, J.G., Gardner, A., Hagen, J.-O., Hock, R., Kaser, G., Pfeffer, W.T., Moholdt, G., Paul, F., Radić, V., Andreassen, M., Bajracharya, S., Beedle, M.J., Berthier, E., Bhambri, R., Bliss, A., Brown, I., Burgess, D.O., Burgess, E.W., Cawkwell, F., Chinn, T., Copland, L., Davies, B., Angelis, H. de, Dolgova, H., Filbert, K., Forester, R., Fountain, A., Frey, H., Giffen, B., Glasser, N., Gurney, S., Hagg, W., Hall, D., Haritashya, U.K., Hartmann, G., Helm, C., Herreid, S., Howat, I.M., Kapustin, G., Khromova, T., Kienholz, C., Koenig, M., Kohler, J., Kriegel, D., Kutuzov, S., Lavrentiev, I., Le Bris, R., Lund, J., Manley, W.F., Mayer, C., Miles, E.S., Li, X., Menounos, B., Mercer, A., Mölg, N., Mool, P., Nosenko, G., Negrete, A., Nuth, C., Pettersson, R., Racoviteanu, A., Ranzi, R., Rastner, P., Rau, F., Raup, B.H., Rich, J., Rott, H., Schneider, C., Seliverstov, Y., Sharp, M.J., Sigurosson, O., Stokes, C.R., Wheate, R., Wolken, G.J., Wyatt, F. and Zheltyhina, N., 2012. *Randolph Glacier Inventory – A Dataset of Global Glacier Outlines: Version 2.0*. Global Land Ice Measurements from Space, Boulder CO, USA., Global Land Ice Measurements from Space, Boulder CO, USA.
- Arendt, A., Bolch, T., Cogley, J.G., Gardner, A., Hagen, J.-O., Hock, R., Kaser, G., Pfeffer, W.T., Moholdt, G., Paul, F., Radić, V., Andreassen, M., Bajracharya, S., Beedle, M.J., Berthier, E., Bhambri, R., Bliss, A., Brown, I., Burgess, D.O., Burgess, E.W., Cawkwell, F., Chinn, T., Copland, L., Davies, B., Angelis, H. de, Dolgova, H., Filbert, K., Forester, R., Fountain, A., Frey, H., Giffen, B., Glasser, N., Gurney, S., Hagg, W., Hall, D., Haritashya, U.K., Hartmann, G., Helm, C., Herreid, S., Howat, I.M., Kapustin, G., Khromova, T., Kienholz, C., Koenig, M., Kohler, J., Kriegel, D., Kutuzov, S., Lavrentiev, I., Le Bris, R., Lund, J., Manley, W.F., Mayer, C., Miles, E.S., Li, X., Menounos, B., Mercer, A., Mölg, N., Mool, P., Nosenko, G., Negrete, A., Nuth, C., Pettersson, R., Racoviteanu, A., Ranzi, R., Rastner, P., Rau, F., Raup, B.H., Rich, J., Rott, H., Schneider, C., Seliverstov, Y., Sharp, M.J., Sigurosson, O., Stokes, C.R., Wheate, R., Wolken, G.J., Wyatt, F. and Zheltyhina, N., 2015. *Randolph Glacier Inventory – A Dataset of Global Glacier Outlines: Version 5.0*. Global Land Ice Measurements from Space, Boulder CO, USA., Global Land Ice Measurements from Space, Boulder CO, USA.
- Arigony-Neto, J., Skvarca, P., Marinsek, S., Braun, M., Humbert, A., Júnior, C.W.M. and Jaña, R., 2014. Monitoring Glacier Changes on the Antarctic Peninsula. In: Kargel, J.S., Leonard, G.J., Bishop, M.P., Käab, A. and Raup, B.H. (eds), *Global Land Ice Measurements from Space*. Springer Berlin Heidelberg, Berlin, Heidelberg. 717–741.
- Bahr, D.B., Meier, M.F. and Peckham, S.D., 1997. The physical basis of glacier volume-area scaling. *Journal of Geophysical Research*, 102 (B9), 20355. doi: 10.1029/97JB01696
- Bentley, M.J., Hodgson, D.A., Smith, J.A., Cofaigh, C., Domack, E.W., Larter, R.D., Roberts, S.J., Brachfeld, S., Leventer, A., Hjort, C., Hillenbrand, C.-D. and Evans, J., 2009. Mechanisms of Holocene palaeoenvironmental change in the Antarctic Peninsula region. *The Holocene*, 19 (1), 51–69. doi: 10.1177/0959683608096603

- Berthier, E., Scambos, T.A. and Shuman, C.A., 2012. Mass loss of Larsen B tributary glaciers (Antarctic Peninsula) unabated since 2002. *Geophysical Research Letters*, 39 (13), n/a-n/a. doi: 10.1029/2012GL051755
- Bindschadler, R., Vornberger, P., Fleming, A.H., Fox, A.J., Mullins, J., Binnie, D., Paulsen, S.J., Granneman, B. and Gorodetzky, D., 2008. The Landsat Image Mosaic of Antarctica. *Remote Sensing of Environment*, 112, 4214–4226.
- Bliss, A., Hock, R. and Cogley, J.G., 2013. A new inventory of mountain glaciers and ice caps for the Antarctic periphery. *Annals of Glaciology*, 54 (63), 191–199. doi: 10.3189/2013AoG63A377
- Bolch, T., Menounos, B. and Wheate, R., 2010. Landsat-based inventory of glaciers in western Canada, 1985–2005. *Remote Sensing of Environment*, 114 (1), 127–137. doi: 10.1016/j.rse.2009.08.015
- Braithwaite, R.J. and Raper, S., 2009. Estimating equilibrium-line altitude (ELA) from glacier inventory data. *Annals of Glaciology*, 50 (53), 127–132. doi: 10.3189/172756410790595930
- Braun, M., Rau, F. and Simões, J., 2001. A GIS-based glacier inventory for the Antarctic Peninsula and the South Shetland Islands —A first case study on King George Island. *Geo-spatial Information Science*, 4 (2), 15–24. doi: 10.1007/BF02826973
- Cogley, J.G., Berthier, E. and Donoghue, S., 2010. Glaciers of the Subantarctic islands. *Global Land Ice Measurements from Space*.
- Cogley, J.G., Hock, R., Rasmussen, L.A., Arendt, A.A., Bauder, A., Braithwaite, R.J., Jansson, P., Kaser, G., Möller, M., Nicholson, L. and Zemp, M., 2011. *Glossary of glacier mass balance and related terms*. Technical documents in hydrology, IHP-VII, no. 86. Unesco, Paris, France. vi, 114.
- Cook, A.J., Fox, A.J., Vaughan, D.G. and Ferrigno, J.G., 2005. Retreating Glacier Fronts on the Antarctic Peninsula over the Past Half-Century. *Science*, 308 (5721), 541–544. doi: 10.1126/science.1104235
- Cook, A.J., Murray, T., Luckman, A., Vaughan, D.G. and Barrand, N.E., 2012. A new 100-m Digital Elevation Model of the Antarctic Peninsula derived from ASTER Global DEM: methods and accuracy assessment. *Earth System Science Data*, 4 (1), 129–142. doi: 10.5194/essd-4-129-2012
- Cook, A.J., Vaughan, D.G., Luckman, A.J. and Murray, T., 2014. A new Antarctic Peninsula glacier basin inventory and observed area changes since the 1940s. *Antarctic Science*, 26 (06), 614–624. doi: 10.1017/S0954102014000200
- Davies, B.J., 2014. *Glacier response time*, <http://www.antarcticglaciers.org/modern-glaciers/glacier-response-time/>, accessed 12 December 2015.
- Davies, B.J., Carrivick, J.L., Glasser, N.F., Hambrey, M.J. and Smellie, J.L., 2011. A new glacier inventory for 2009 reveals spatial and temporal variability in glacier response to atmospheric warming in the Northern Antarctic Peninsula, 1988–2009. *The Cryosphere Discussions*, 5 (6), 3541–3595. doi: 10.5194/tcd-5-3541-2011
- Davies, B.J., Hambrey, M.J., Smellie, J.L., Carrivick, J.L. and Glasser, N.F., 2012. Antarctic Peninsula Ice Sheet evolution during the Cenozoic Era. *Quaternary Science Reviews*, 31, 30–66. doi: 10.1016/j.quascirev.2011.10.012

- Dueker, K.J. and Kjerne, D., 1989. *Multipurpose cadastre: Terms and definitions*. American Soc. for Photogrammetry and Remote Sensing, Falls Church Va.
- Erasov, N.V., 1968. Metod opredelenija ob'ema gornych lednikov [Method for determining glacier volume]. *Mater. Glyatsiol. Issled. Kazakhstan*, 14, 307–308. [In Russian]
- Evans, I.S., 2006. Local aspect asymmetry of mountain glaciation: A global survey of consistency of favoured directions for glacier numbers and altitudes. *Geomorphology*, 73 (1-2), 166–184. doi: 10.1016/j.geomorph.2005.07.009
- Evans, I.S., 2007. Glacier distribution and direction in the Arctic: The unusual nature of Svalbard. *Landform Analysis*, 5, 21–24.
- Evans, I.S. and Cox, N.J., 2005. Global variations of local asymmetry in glacier altitude: Separation of north–south and east–west components. *Journal of Glaciology*, 51 (174), 469–482. doi: 10.3189/172756505781829205
- Evans, I.S. and Cox, N.J., 2010. Climatogenic north–south asymmetry of local glaciers in Spitsbergen and other parts of the Arctic. *Annals of Glaciology*, 51 (55), 16–22. doi: 10.3189/172756410791392682
- Fountain, A.G., Hoffman, M.J., Granshaw, F. and Riedel, J., 2009. The 'benchmark glacier' concept – does it work?: Lessons from the North Cascade Range, USA. *Annals of Glaciology*, 50 (50), 163–168. doi: 10.3189/172756409787769690
- Fretwell, P., Burton-Johnson, A. and Black, M., 2015. *Extracting Outcrop Extents in Antarctica: Current problems, new solutions and a complete dataset for the Antarctic continent*. AGU Fall Meeting, San Francisco.
- Fretwell, P., Pritchard, H.D., Vaughan, D.G., Bamber, J.L., Barrand, N.E., Bell, R., Bianchi, C., Bingham, R.G., Blankenship, D.D., Casassa, G., Catania, G., Callens, D., Conway, H., Cook, A.J., Corr, H. F. J., Damaske, D., Damm, V., Ferraccioli, F., Forsberg, R., Fujita, S., Gogineni, P., Griggs, J.A., Hindmarsh, R. C. A., Holmlund, P., Holt, J.W., Jacobel, R.W., Jenkins, A., Jokat, W., Jordan, T., King, E.C., Kohler, J., Krabill, W., Riger-Kusk, M., Langley, K.A., Leitchenkov, G., Leuschen, C., Luyendyk, B.P., Matsuoka, K., Nogi, Y., Nost, O.A., Popov, S.V., Rignot, E., Rippin, D.M., Riviera, A., Roberts, J., Ross, N., Siegert, M.J., Smith, A.M., Steinhage, D., Studinger, M., Sun, B., Tinto, B.K., Welch, B.C., Young, D.A., Xiangbin, C. and Zirizzotti, A., 2013. Bedmap2: improved ice bed, surface and thickness datasets for Antarctica. *The Cryosphere Discussions*, 6 (5), 4305–4361. doi: 10.5194/tcd-6-4305-2012
- Frey, H. and Paul, F., 2012. On the suitability of the SRTM DEM and ASTER GDEM for the compilation of topographic parameters in glacier inventories. *International Journal of Applied Earth Observation and Geoinformation*, 18, 480–490. doi: 10.1016/j.jag.2011.09.020
- Fund, W. and Hogan, C., 2013. *Antarctic Peninsula*, <http://www.eoearth.org/view/article/150106>, accessed 10 January 2016.
- Glasser, N.F., Kulesa, B., Luckman, A., Jansen, D., King, E.C., Sammonds, P.R., Scambos, T.A. and Jezek, K.C., 2009. Surface structure and stability of the Larsen C ice shelf, Antarctic Peninsula. *Journal of Glaciology*, 55 (191), 400–410.
- Glasser, N.F. and Scambos, T.A., 2008. A structural glaciological analysis of the 2002 Larsen B ice-shelf collapse. *Journal of Glaciology*, 54 (184), 3–16. doi: 10.3189/002214308784409017

- GLIMS and NSIDC, 2005, updated 2015. Global Land Ice Measurements from Space glacier database, Compiled and made available by the international GLIMS community and the National Snow and Ice Data Center, Boulder CO, USA. doi: 10.7265/N5V98602
- Haerberli, W., 2005. Mountain Glaciers in Global Climate-related Observing Systems. In: Beniston, M., Huber, U.M., Bugmann, H.K.M. and Reasoner, M.A. (eds), *Global Change and Mountain Regions*. Advances in Global Change Research. Springer Netherlands, Dordrecht. 169–175.
- Haerberli, W. and Beniston, M., 1998. Climate change and its impacts on glaciers and permafrost in the Alps. *Ambio*, 27 (4), 258–265.
- Haerberli, W. and Hoelzle, M., 1995. Application of inventory data for estimating characteristics of and regional climate-change effects on mountain glaciers: a pilot study with the European Alps. *Annals of Glaciology*, 21, 206–212.
- Helm, V., Humbert, A. and Miller, H., 2014. Elevation and elevation change of Greenland and Antarctica derived from CryoSat-2. *The Cryosphere*, 8 (4), 1539–1559. doi: 10.5194/tc-8-1539-2014
- Hock, R., Woul, M. de, Radić, V. and Dyurgerov, M., 2009. Mountain glaciers and ice caps around Antarctica make a large sea-level rise contribution. *Geophysical Research Letters*, 36 (L07501). doi: 10.1029/2008GL037020
- Huss, M. and Farinotti, D., 2012. Distributed ice thickness and volume of all glaciers around the globe. *Journal of Geophysical Research*, 117 (F4). doi: 10.1029/2012JF002523
- Huss, M. and Farinotti, D., 2014. A high-resolution bedrock map for the Antarctic Peninsula. *The Cryosphere*, 8 (4), 1261–1273. doi: 10.5194/tc-8-1261-2014
- Huss, M. and Hock, R., 2015. A new model for global glacier change and sea-level rise. *Frontiers in Earth Science*, 3, 382. doi: 10.3389/feart.2015.00054
- Jansen, D., Kulesa, B., Sammonds, P.R., Luckman, A., King, E.C. and Glasser, N.F., 2010. Present stability of the Larsen C ice shelf, Antarctic Peninsula. *Journal of Glaciology*, 56 (198), 593–600.
- Jenkins, A. and Holland, D., 2007. Melting of floating ice and sea level rise. *Geophysical Research Letters*, 34 (16), n/a-n/a. doi: 10.1029/2007GL030784
- Jiskoot, H., Curran, C.J., Tessler, D.L. and Shenton, L.R., 2009. Changes in Clemenceau Icefield and Chaba Group glaciers, Canada, related to hypsometry, tributary detachment, length–slope and area–aspect relations. *Annals of Glaciology*, 50 (53), 133–143. doi: 10.3189/172756410790595796
- Kieffer, H., Kargel, J.S., Barry, R., Bindschadler, R., Bishop, M., MacKinnon, D., Ohmura, A., Raup, B., Antoninetti, M., Bamber, J., Braun, M., Brown, I., Cohen, D., Copland, L., DueHagen, J., Engeset, R.V., Fitzharris, B., Fujita, K., Haerberli, W., Hagen, J.O., Hall, D., Hoelzle, M., Johansson, M., Kaab, A., Koenig, M., Konovalov, V., Maisch, M., Paul, F., Rau, F., Reeh, N., Rignot, E., Rivera, A., De Ruyter de Wildt, Martiyn, Scambos, T., Schaper, J., Scharfen, G., Shroder, J., Solomina, O., Thompson, D., van der Veen, Kees, Wohlleben, T. and Young, N., 2000. New eyes in the sky measure glaciers and ice sheets. *Eos, Transactions American Geophysical Union*, 81 (24), 265. doi: 10.1029/00EO00187
- Kienholz, C., Herreid, S., Rich, J.L., Arendt, A.A., Hock, R. and Burgess, E.W., 2015. Derivation and analysis of a complete modern-date glacier inventory for Alaska and northwest Canada. *Journal of Glaciology*, 61 (227), 403–420. doi: 10.3189/2015JoG14J230

- Kienholz, C., Hock, R. and Arendt, A.A., 2013. A new semi-automatic approach for dividing glacier complexes into individual glaciers. *Journal of Glaciology*, 59 (217), 925–937.
- King, J.C., Turner, J., Marshall, G.J., Connolley, W.M. and Lachlan-Cope, T.A., 2003. Antarctic Peninsula climate variability and its causes as revealed by analysis of instrumental records, 79, 17–30. doi: 10.1029/AR079p0017
- Le Bris, R., Paul, F., Frey, H. and Bolch, T., 2011. A new satellite-derived glacier inventory for western Alaska. *Annals of Glaciology*, 52 (59), 135–143. doi: 10.3189/172756411799096303
- Lillesand, T.M., Kiefer, R.W. and Chipman, J.W., 2015. *Remote sensing and image interpretation*. John Wiley & Sons, Inc, Hoboken, N.J. 768 p.
- Nagler, T., Rott, H., Hetzenecker, M., Wuite, J. and Potin, P., 2015. The Sentinel-1 Mission: New Opportunities for Ice Sheet Observations. *Remote Sensing*, 7 (7), 9371–9389. doi: 10.3390/rs70709371
- Nuth, C., Kohler, J., König, M., Deschwanden, A. von, Hagen, J.O., Köhler, J., Moholdt, G. and Pettersson, R., 2013. Decadal changes from a multi-temporal glacier inventory of Svalbard. *The Cryosphere Discussions*, 7 (3), 2489–2532. doi: 10.5194/tcd-7-2489-2013
- Oerlemans, J., 2007. Estimating response times of Vadret da Morteratsch, Vadret da Palü, Briksdalsbreen and Nigardsbreen from their length records. *Journal of Glaciology*, 53 (182), 357–362. doi: 10.3189/002214307783258387
- Ohmura, A., 2010. Completing the World Glacier Inventory. *Annals of Glaciology*, 50 (53), 144–148. doi: 10.3189/172756410790595840
- Østrem, G. and Brugman, M., 1991. *Glacier mass-balance measurements: A manual for field and office work*. NHRI science report, 4, Ottawa. IX, 224.
- Paterson, W.S.B., 1994. *The Physics of Glaciers*. Pergamon, Frankfurt, Oxford. 480 p.
- Paul, F., 2003. *The new Swiss glacier inventory 2000 - Application of remote sensing and GIS*, PhD Thesis, Department of Geography, University of Zurich.
- Paul, F., 2011. Sea-level rise: Melting glaciers and ice caps. *Nature Geoscience*, 4 (2), 71–72. doi: 10.1038/ngeo1074
- Paul, F., Andreassen, L.M. and Winsvold, S.H., 2011. A new glacier inventory for the Jostedalbreen region, Norway, from Landsat TM scenes of 2006 and changes since 1966. *Annals of Glaciology*, 52 (59), 153–162. doi: 10.3189/172756411799096169
- Paul, F., Barry, R.G., Cogley, J.G., Frey, H., Haeberli, W., Ohmura, A., Ommanney, C., Raup, B., Rivera, A. and Zemp, M., 2009. Recommendations for the compilation of glacier inventory data from digital sources. *Annals of Glaciology*, 50 (53), 119–126. doi: 10.3189/172756410790595778
- Pfeffer, W.T., 2003. Tidewater glaciers move at their own pace. *Nature*, 426 (6967), 602. doi: 10.1038/426602b
- Pfeffer, W.T., Arendt, A.A., Bliss, A., Bolch, T., Cogley, J.G., Gardner, A.S., Hagen, J.-O., Hock, R., Kaser, G., Kienholz, C., Miles, E.S., Moholdt, G., Mölg, N., Paul, F., Radić, V., Rastner, P., Raup, B.H., Rich, J. and Sharp, M.J., 2014. The Randolph Glacier Inventory: a globally complete inventory of glaciers. *Journal of Glaciology*, 60 (221), 537–552. doi: 10.3189/2014JoG13J176

- Pritchard, H.D. and Vaughan, D.G., 2007. Widespread acceleration of tidewater glaciers on the Antarctic Peninsula. *Journal of Geophysical Research*, 112 (F3). doi: 10.1029/2006JF000597
- Rabassa, J., Skvarca, P., Bertani, L. and Mazzoni, E., 1982. Glacier Inventory of James Ross and Vega Islands, Antarctic Peninsula. *Annals of Glaciology* (3), 260–264.
- Racoviteanu, A.E., Paul, F., Raup, B., Khalsa, Siri Jodha Singh and Armstrong, R., 2009. Challenges and recommendations in mapping of glacier parameters from space: results of the 2008 Global Land Ice Measurements from Space (GLIMS) workshop, Boulder, Colorado, USA. *Annals of Glaciology*, 50 (53), 53–69. doi: 10.3189/172756410790595804
- Radić, V. and Hock, R., 2010. Regional and global volumes of glaciers derived from statistical upscaling of glacier inventory data. *Journal of Geophysical Research*, 115 (F01010). doi: 10.1029/2009JF001373
- Radić, V., Hock, R. and Oerlemans, J., 2007. Volume–area scaling vs flowline modelling in glacier volume projections. *Annals of Glaciology*, 46 (1), 234–240. doi: 10.3189/172756407782871288
- Radić, V., Hock, R. and Oerlemans, J., 2008. Analysis of scaling methods in deriving future volume evolutions of valley glaciers. *Journal of Glaciology*, 54 (187), 601–612. doi: 10.3189/002214308786570809
- Rastner, P., 2014. *The Local Glaciers and Ice Caps on Greenland: Their Mapping, Separation from the Ice Sheet and their Climate Sensitivity*, PhD Thesis, Department of Geography, University of Zurich.
- Rastner, P., Bolch, T., Mölg, N., Machguth, H., Le Bris, R. and Paul, F., 2012. The first complete inventory of the local \newline glaciers and ice caps on Greenland. *The Cryosphere*, 6 (6), 1483–1495. doi: 10.5194/tc-6-1483-2012
- Rau, F., Kargel, J. and Raup, B.H., 2006. The GLIMS Glacier Inventory of the Antarctic Peninsula. *Earth Observer* (18), 9–11.
- Rau, F., Mauz, F., Vogt, S., Khalsa, S.J.S. and Raup, B., 2005. *Illustrated GLIMS glacier classification manual: glacier classification guidance for the GLIMS inventory. Version 1.*, Freiburg, Albert-Ludwigs-Universität. Institut für Physische Geographie. GLIMS Regional Center "Antarctic Peninsula", [www.glims.org/MapsAndDocs/guides.html](http://www.glims.org/MapsAndDocs/guides.html).
- Raup, B., Arendt, A., Armstrong, R., Barrett, A., Khalsa, S.J.S. and Racoviteanu, A., 2013. *GLIMS and the RGI: relationships present and future: Geophysical Research Abstracts*. 15. EGU2013-11831.
- Raup, B. and Khalsa, S.J.S., 2010. *GLIMS Analysis Tutorial*, Boulder, Colorado USA: National Snow and Ice Data Center, [www.glims.org/MapsAndDocs/guides.html](http://www.glims.org/MapsAndDocs/guides.html).
- Raup, B., Racoviteanu, A., Khalsa, Siri Jodha Singh, Helm, C., Armstrong, R. and Arnaud, Y., 2007. The GLIMS geospatial glacier database: A new tool for studying glacier change. *Global and Planetary Change*, 56 (1-2), 101–110. doi: 10.1016/j.gloplacha.2006.07.018
- Rignot, E., Mouginot, J. and Scheuchl, B., 2011. Ice flow of the antarctic ice sheet. *Science*, 333, 1427–1430. [In english]
- Rignot, E. and Thomas, R.H., 2002. Mass balance of polar ice sheets. *Science (New York, N.Y.)*, 297 (5586), 1502–1506. doi: 10.1126/science.1073888

- Rott, H., Müller, F., Nagler, T. and Floricioiu, D., 2011. The imbalance of glaciers after disintegration of Larsen-B ice shelf, Antarctic Peninsula. *The Cryosphere*, 5 (1), 125–134. doi: 10.5194/tc-5-125-2011
- Rott, H., Rack, W., Nagler, T. and Skvarca, P., 1998. Climatically Induced Retreat and Collapse of Northern Larsen Ice Shelf, Antarctic Peninsula. *Annals of Glaciology*, 27, 86–92.
- Rott, H., Skvarca, P. and Nagler, T., 1996. Rapid Collapse of Northern Larsen Ice Shelf, Antarctica. *Science*, 271 (5250), 788–792. doi: 10.1126/science.271.5250.788
- Royal Holloway University of London, 2014. *Glaciers in northern Antarctic Peninsula melting faster than ever - despite increased snowfall*, <https://www.royalholloway.ac.uk/aboutus/newsandevents/news/newsarticles/glaciersinnorthernantarcticpeninsulameltingfasterthanever-despiteincreasedsnowfall.aspx>, accessed 7 January 2016.
- Scambos, T.A., 2004. Glacier acceleration and thinning after ice shelf collapse in the Larsen B embayment, Antarctica. *Geophysical Research Letters*, 31 (18). doi: 10.1029/2004GL020670
- Scambos, T.A., Hulbe, C., Fahnestock, M. and Bohlander, J., 2000. The link between climate warming and break-up of ice shelves in the Antarctic Peninsula. *Journal of Glaciology*, 46 (154), 516–530. doi: 10.3189/172756500781833043
- Shepherd, A., Ivins, E.R., A, G., Barletta, V.R., Bentley, M.J., Bettadpur, S., Briggs, K.H., Bromwich, D.H., Forsberg, R., Galin, N., Horwath, M., Jacobs, S., Joughin, I., King, M.A., Lenaerts, J.T.M., Li, J., Ligtenberg, S.R.M., Luckman, A., Luthcke, S.B., McMillan, M., Meister, R., Milne, G., Mouginot, J., Muir, A., Nicolas, J.P., Paden, J., Payne, A.J., Pritchard, H., Rignot, E., Rott, H., Sorensen, L.S., Scambos, T.A., Scheuchl, B., Schrama, E.J.O., Smith, B., Sundal, A.V., van Angelen, J.H., van de Berg, W.J., van den Broeke, M.R., Vaughan, D.G., Velicogna, I., Wahr, J., Whitehouse, P.L., Wingham, D.J., Yi, D., Young, D. and Zwally, H.J., 2012. A Reconciled Estimate of Ice-Sheet Mass Balance. *Science*, 338 (6111), 1183–1189. doi: 10.1126/science.1228102
- Shepherd, A., Wingham, D., Payne, T. and Skvarca, P., 2003. Larsen ice shelf has progressively thinned. *Science (New York, N.Y.)*, 302 (5646), 856–859. doi: 10.1126/science.1089768
- Turner, J., Bindschadler, R., Convey, P., DiPrisco, G., Fahrbach, E., Gutt, J., Hodgson, D., Mayewski, P. and Summerhayes, C., 2009. *Antarctic climate change and the environment: A contribution to the International Polar Year 2007 - 2008*. Scientific Committee on Antarctic Research, Cambridge. 20 p.
- van Lipzig, N.P.M., 2004. Precipitation, sublimation, and snow drift in the Antarctic Peninsula region from a regional atmospheric model. *Journal of Geophysical Research*, 109 (D24). doi: 10.1029/2004JD004701
- Vaughan, D.G., J.C. Comiso, I. Allison, J. Carrasco, Kaser, G., R. Kwok, P. Mote, T. Murray, F. Paul, J. Ren, E. Rignot, O. Solomina and K. Steffen and T. Zhang, 2013. Observations: Cryosphere. In: *Climate Change 2013*.
- Vieli, A., Jania, J. and Kolondra, L., 2002. The retreat of a tidewater glacier: Observations and model calculations on Hansbreen, Spitsbergen. *Journal of Glaciology*, 48 (163), 592–600. doi: 10.3189/172756502781831089

- Wendt, J., Rivera, A., Wendt, A., Bown, F., Zamora, R., Casassa, G. and Bravo, C., 2010. Recent ice-surface-elevation changes of Fleming Glacier in response to the removal of the Wordie Ice Shelf, Antarctic Peninsula. *Annals of Glaciology*, 51 (55), 97–102. doi: 10.3189/172756410791392727
- WGMS, 1989. *World glacier inventory: Status 1988; a contribution to the Global Environment Monitoring System (GEMS) and the International Hydrological Programme*. IAHS [u.a.], Wallingford.
- WGMS, 2015. Global Glacier Change Bulletin No. 1 (2012-2013). Zemp, M., Gärtner-Roer, I., Nussbaumer, S. U., Hüsler, F., Machguth, H., Mölg, N., Paul, F., and Hoelzle (eds.), M.ICSU(WDS)/IUGG(IACS)/UNEP/UNESCO/WMO, World Glacier Monitoring Service., Zurich, Switzerland. 230 p. doi: 10.5904/wgms-fog-2015-11
- WGMS and NSIDC, 1999, updated 2012. *World Glacier Inventory*. Compiled and made available by the World Glacier Monitoring Service, Zurich, Switzerland, and the National Snow and Ice Data Center, Boulder CO, USA., 10.7265/N5/NSIDC-WGI-2012-02.
- Wouters, B., Martin-Español, A., Helm, V., Flament, T., van Wessem, J.M., Ligtenberg, S.R.M., van den Broeke, M R and Bamber, J.L., 2015. Dynamic thinning of glaciers on the Southern Antarctic Peninsula. *Science (New York, N.Y.)*, 348 (6237), 899–903. doi: 10.1126/science.aaa5727
- Zwally, H.J., Giovinetto, M.B., Beckley, M.A. and Saba, J.L., 2012. *Antarctic and Greenland Drainage Systems*, [http://icesat4.gsfc.nasa.gov/cryo\\_data/ant\\_grn\\_drainage\\_systems.php](http://icesat4.gsfc.nasa.gov/cryo_data/ant_grn_drainage_systems.php), accessed 7 January 2016.



# 10 Appendix

## Definitions of Nominal classifications as applied by Cook *et al.* (2014)

Definitions of nominal parameters obtained from the Global Land Ice Measurements from Space (GLIMS) Classification Manual (Rau *et al.*, 2005) and the Glossary of Glacier Mass Balance (Cogley *et al.* 2011). The category numbers conform to those in GLIMS classification system.

### *Primary classification (Class):*

- 2 - Ice-field: ice covering mountainous terrain, not thick enough to overwhelm surrounding topography, and where flow is not radial or dome shaped. This may include low-lying areas where ice divides are not clearly detectable. Flow is influenced by underlying topography. It can include an ice mass that has flow features visible but does not qualify as an outlet glacier or an ice cap.
- 3 - Ice-cap: dome shaped ice mass with approximately radial flow, which largely obscures bedrock and where the profile is even/regular. The ice mass is unconstrained by topography. It can include a low-relief, radial ice mass with little flow that originates from mountains. Large islands that are covered in ice are defined as an ice-cap, even if topography may imply ice-field.
- 4 - Outlet glacier: glacier (usually of valley glacier form) that drains an ice sheet, ice field or ice cap. It follows local topographic depressions. The catchment area may not be clearly delineated. These are larger than mountain glaciers, flow features are clearly visible and the ice velocity tends to be greater than the surrounding ice mass. Includes ice draining from icefield/ice caps that have had floating tongues in the past.
- 6 - Mountain glacier: the glacier adheres to mountain sides and is any shape, often located in a cirque/niche. The terminus is often constrained within a bay, has clear ‘pinning points’ at the edge of the drainage basin and has flow features visible. The accumulation region is not on a broad plateau and has clearly definable catchment.
- 10 - Small ice-covered island: the island is between 1 – 5 km long/wide, and the majority is ice-covered. This is not a GLIMS glacier type, but was added as such features are prevalent close to the Antarctic Peninsula.
- 0 - Uncertain/Misc

### *Form:*

- 1 - Compound basins: more than one compound basin that merge together.
- 2 - Compound basin: more than one accumulation basin feeding one glacier system. In many cases on the AP separate glacier entities coalesce to form a single glacier at the terminus.
- 3 - Simple basin: glacier is fed from one single accumulation area.
- 0 - Uncertain/Misc

*Front:*

- 4 - Calving: tidewater, sufficiently extending into sea to produce icebergs.
- 10 - Calving/Piedmont: occurs in unconstrained topographic areas, with expanding glacier fronts or from an ice field. These have steeper-sloped calving fronts than lobed glacier fronts and flow is not radial.
- 12 - Calving/lobed: initial stage of tongue formation, part of an ice cap or ice field with a radial margin, and is grounded. The front has a lower slope angle than a piedmont front.
- 13 - Ice-shelf nourishing: tributaries of an ice shelf.
- 14 – Floating: the terminus is floating in the sea and an approximate grounding line may be detectable. The grounding line is not clearly identifiable for many marine-terminating glaciers on the AP so the term ‘floating’ was only assigned in cases where it was considered to be unambiguous. These decisions were based on the positions of the AS Aid grounding line, combined with interpretation from surface features visible on the LIMA.
- 20 - Land-terminating: the terminus is behind the LIMA coastline.
- 0 - Uncertain/Misc

*Confidence:*

Due to the subjective nature of nominal categorisation, a degree of confidence in decisions made was assigned to each glacier. One value was assigned to summarise the overall confidence in allocation of *Class*, *Form* and *Front* attributes:

- 1 – Confident about all (*Class*, *Form* and *Front*) classification types
- 2 – Confident about some aspects of classification but not others
- 3 – Unsure/guess as to all aspects of classification

*Mainland/Island:*

- 1 – Situated on mainland
- 2 – Situated on large island
- 3 – Situated on medium island

# 11 Personal Declaration

“I hereby declare that the submitted thesis is the result of my own, independent, work. All external sources are explicitly acknowledged in the thesis.”

City, Date:

Signature:

---